



**UNIVERSITY OF NAIROBI
FACULTY OF ENGINEERING**

DEPARTMENT OF ELECTRICAL AND INFORMATION ENGINEERING

**INVESTIGATION OF CONSTRAINED VSC-HVDC TIE LINES FOR TRANSIENT
STABILITY IMPROVEMENT OF INTERCONNECTED POWER SYSTEMS**

Thesis Report submitted in Partial fulfilment of the requirements for the Degree of Master of
Science in Electrical and Electronic Engineering, in the Department of Electrical and
Information Engineering of the University of Nairobi

BY

MWASAHA NYEMI MWANGUDZA


F56/38456/2020

October 2023

DECLARATION OF ORIGINALITY

<p><u>NAME OF STUDENT:</u> MWASAHA NYEMI MWANGUDZA</p> <p><u>REGISTRATION NUMBER:</u> F56/38456/2020 <u>FACULTY:</u> ENGINEERING</p> <p><u>DEPARTMENT:</u> ELECTRICAL & INFORMATION ENGINEERING</p> <p><u>COURSE NAME:</u> MASTER OF SCIENCE IN ELECTRICAL & ELECTRONIC ENGINEERING</p> <p><u>TITLE OF WORK:</u> INVESTIGATION OF CONSTRAINED VSC-HVDC TIE LINES FOR TRANSIENT STABILITY IMPROVEMENT OF INTERCONNECTED POWER SYSTEMS</p>

- 1) I understand what plagiarism is and I am aware of the university policy in this regard.
- 2) I declare that this thesis report is my original work and has not been submitted elsewhere for examination, award of a degree or publication. Where other people’s work or my own work has been used, this has properly been acknowledged and referenced in accordance with the University of Nairobi’s requirements.
- 3) I have not sought or used the services of any professional agencies to produce this work.
- 4) I have not allowed, and shall not allow anyone to copy my work with the intention of passing it off as his/her own work.
- 5) I understand that any false claim in respect of this work shall result in disciplinary action, in accordance with University anti- plagiarism policy.

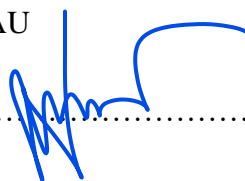
Signature: 

Date:..... 14/10/2023

This Thesis Report is submitted to the Faculty of Engineering with our approval as University supervisors:

SUPERVISORS:

1. Dr. A. NYETE  17/10/2023
SIGNATURE.....DATE.....

2. Dr. PETER MUSAU  15-10-23
SIGNATURE.....DATE.....

ACKNOWLEDGEMENT

My acknowledgment goes to THE ALMIGHTY GOD for granting me the gift of salvation and the gift of life to carry out this thesis research. Having good health, a sober mind and the strength to carry out this research can not be taken for granted. Glory be to GOD.

I will not forget my employer KETRACO who throughout the entire research and thesis duration accorded me the required support to make this successful.

Finally, I will also not forget Dr. Abraham Nyete, Dr. George Kamucha, and Dr. Peter Musau who throughout my research and thesis have given me the required knowledge, training, advice, and motivation to work hard toward its completion. My sincere thanks to you all.

ABSTRACT

Mwasaha Nyemi Mwangudza, F56/38456/2020

Investigation of Constrained VSC-HVDC Tie Lines for Transient Stability Improvement of Interconnected Power Systems.

Voltage Source Converter (VSC) – High Voltage Direct Current (HVDC) tie lines have become popular for the interconnection of power systems owing to their ability to independently control active and reactive powers. This attribute has been harnessed for transient stability improvement through the control of active or reactive powers. The supporting control area in interconnected power systems through the VSC-HVDC tie lines can modulate the DC power to support a faulted control area to recover stable conditions. However, it has been traditionally assumed that the supporting control area is an infinite system able to support the faulted control area without compromising its stable operating conditions. On the contrary, power systems have operational limits which must be respected. Violation of stable conditions compromises the system's integrity and at worst can cause a total system collapse. Providing the required regulating power beyond the ability of the supporting control area should be prevented to avoid unstable conditions. It is on this gap that this thesis has studied and simulated two cases of a Kundur two-area power system interconnected through a VSC-HVDC tie line. The first case has the traditional unconstrained VSC-HVDC tie line assuming an infinite system for the supporting control area. The second case has a constrained VSC-HVDC tie line that monitors the amount of the required regulating power and compares it with the system strength of the supporting area to avoid violating its stable conditions. The transient stability response of the two cases of a Kundur two-area system connected through a VSC-HVDC tie line was simulated in MATLAB/SIMULINK software. Transient faults were performed on the two systems and their transient responses were plotted under different fault scenarios. The first fault scenario resulted in the required regulating power within the ability of the supporting control area and the second fault scenario resulted in the required regulating power above the ability of the supporting control area. The simulation results showed that the unconstrained VSC-HVDC system exhibits unstable conditions with its frequency response and rotor speed deviation deteriorating significantly without recovering stable conditions. With the incorporation of the Inter-Area Frequency Supplementary Controller (IAFSC), the modulated link power is reset to assist in recovering stable conditions once the stability threshold limit is violated. The IAFSC monitors the frequency of the control areas in real-time to mitigate violation of stable conditions. It is armed with a modulation release signal logic dependent on the

frequency operating condition of the supporting control area. When the stability threshold limit is violated, the controller blocks the power ramp-up and resets the power modulation to the initial power order. In severe fault conditions, the IAFSC controller achieved transient stability improvement in the supporting control area thus mitigating unstable conditions that could jeopardize its stability.

Key Words — *VSC-HVDC, Transient Stability, Infinite System, IAFSC, Regulating Power, Active Power, Reactive Power, Kundur Two-Area System.*

TABLE OF CONTENTS

CHAPTER 1 INTRODUCTION	1
1.1 Background.....	1
1.2 Problem Statement	2
1.3 Objectives.....	3
1.3.1 Main objective	3
1.3.2 Specific objectives.....	3
1.3.2 Research Questions.....	3
1.4 Justification for the Study.....	3
1.5 Scope of work.....	4
1.6 Thesis Organization.....	4
CHAPTER 2 LITERATURE REVIEW	5
2.1 Basic Concepts.....	5
2.1.1 Power system Interconnection.....	5
2.1.2 Power system stability.....	6
2.1.3 Steady State Stability.....	6
2.1.4 Transient Stability.....	6
2.1.5 Transient Stability Analysis Methods.....	7
2.1.6 VSC-HVDC System.....	9
2.2 Review of Previous Work.....	11
2.3 Summary of previous work done.....	13
2.4 Research Gap.....	18
2.5 Chapter Conclusion.....	18
CHAPTER 3 MATERIALS AND METHODS	19
3.1 Introduction.....	19
3.2 The Kundur Two-Area Test System.....	20
3.3 The VSC-HVDC System Description.....	21
3.3.1. The Converter Transformer.....	22
3.3.2. The Phase Reactor.....	22
3.3.3. AC Filters.....	23

3.4 VSC-HVDC Control Scheme.....	24
3.4.1 The IAFSC Controller.....	25
3.4.2 The IAFSC Controller Parameter Selection and Tuning.....	29
3.4.3 IAFSC Controller Circuit in MATLAB/SIMULINK.....	31
3.4.4 Calculation of Regulating Power.....	33
3.4.4 IAFSC Controller Algorithm Flow Chart.....	34
3.5 Simulation of Steady-state Condition.....	37
3.6 Simulation of Transient Faults.....	37
3.6.1 Simulation Case I.....	37
3.6.2 Simulation Case II.....	38
3.7 Chapter Conclusion.....	38
CHAPTER 4 RESULTS AND ANALYSIS.....	39
4.1 Introduction.....	39
4.2 Simulation of Steady State Condition.....	39
4.3 Case I Fault Condition	43
4.3.1 Case I without IAFSC Controller.....	43
4.3.2 Case I with IAFSC Controller.....	48
4.4 Case II Fault Condition.....	52
4.4.1 Case II without IAFSC Controller.....	52
4.4.2 Case II with IAFSC Controller.....	57
4.5 Validation of Results.....	61
4.6 Chapter Conclusion.....	71
CHAPTER 5 CONCLUSIONS AND RECOMMENDATIONS.....	72
5.1 Conclusion.....	72
5.2 Recommendations.....	73
5.2.1 Recommendations for Further Works.....	73
5.2.1 Adoption of the Results.....	73
5.3 Research Contribution.....	73
REFERENCES.....	74
APPENDICES.....	79
TURNIT IN REPORT.....	86

LIST OF TABLES

Table 2.1: Summary of the Literature Review.....	14
Table 3.1: The Kundur Two-Area Test System Data	21
Table 4.1: Control Area 1 Response under Fault Scenario II without The IAFSC Controller.....	63
Table 4.2: Control Area 1 Response under Fault Scenario II with The Proposed IAFSC Controller.....	64
Table 4.3: Control Area 1 Response under Fault Scenario II with The Proposed IAFSC Controller.....	65
Table 4.4: Control Area 1 Response under Fault Scenario II with The Proposed.....	66
Table 4.5: Validation of the IAFSC Controller with Control Area 1 Frequency Response.....	67
Table 4.6: Validation of the IAFSC Controller with Control Area 1 Rotor Angle Response.....	69

LIST OF FIGURES

Figure 2.1: Types of Interconnection Tie Lines.....	5
Figure 2.2: VSC-HVDC Interconnection.....	6
Figure 2.3: Power Angle Characteristic Curve.....	8
Figure 2.4: Basic Structure of a VSC-HVDC System	9
Figure 2.5: VSC-HVDC terminal.....	10
Figure 3.1: The Conventional VSC-HVDC System.....	19
Figure 3.2: The Proposed VSC-HVDC System.....	20
Figure 3.3: Two-Area Kundur Test System with a VSC-HVDC Tie Line.....	22
Figure 3.4: VSC-HVDC Inner Controller.....	23
Figure 3.5: VSC-HVDC Vector Control Scheme.....	24
Figure 3.6: VSC-HVDC Inner Controller.....	25
Figure 3.7: The IAFSC Controller Circuit [Proposed].....	26
Figure 3.8: The IAFSC Controller Block Diagram.....	27
Figure 3.9: PI Controller Block Diagram.....	27
Figure 3.10: Block diagram representation of the IAFSC controller system.....	28
Figure 3.11: Step Response of the PI Controller.....	29
Figure 3.12: Step Response of the PI Controller.....	30
Figure 3.13: Step Response of the PI Controller.....	30
Figure 3.14: Step Response of the PI Controller.....	31
Figure 3.15: The IAFSC Control Circuit for the Rectifier Side.....	32
Figure 3.16: The IAFSC Control Circuit for the Inverter Side.....	33
Figure 3.17: The IAFSC Controller Algorithm Flowchart.....	35
Figure 3.18: The Proposed VSC-HVDC System Design in MATLAB/SIMULINK Software.....	36
Figure 4.1: Area 1 Frequency Response.....	39
Figure 4.2: Area 2 Frequency Response.....	40
Figure 4.3: Area 1 Rotor Speed Deviation Response.....	40
Figure 4.4: Area 2 Rotor Speed Deviation Response.....	41
Figure 4.5: HVDC Tie Order Power from Area 1.....	41
Figure 4.6: Area 1 Generation.....	42
Figure 4.7: Area 2 Generation.....	42

Figure 4.8: Area 1 Frequency Response.....	43
Figure 4.9: Area 2 Frequency Response.....	44
Figure 4.10: Area 1 Rotor Speed Deviation Response.....	45
Figure 4.11: Area 2 Rotor Speed Deviation Response.....	46
Figure 4.12: HVDC Tie Power Order from Area 1.....	46
Figure 4.13: Area 1 Generation.....	47
Figure 4.14: Area 2 Generation.....	47
Figure 4.15: Area 1 Frequency Response.....	48
Figure 4.16: Area 2 Frequency Response.....	49
Figure 4.17: Area 1 Rotor Speed Deviation Response.....	50
Figure 4.18: Area 2 Rotor Speed Deviation Response.....	50
Figure 4.19: HVDC Tie Power Order from Area 1.....	51
Figure 4.20: Area 1 Generation.....	52
Figure 4.21: Area 2 Generation.....	52
Figure 4.22: Area 1 Frequency Response.....	54
Figure 4.23: Area 2 Frequency Response.....	54
Figure 4.24: Area 1 Rotor Speed Deviation Response.....	55
Figure 4.25: Area 2 Rotor Speed Deviation Response.....	56
Figure 4.26: HVDC Tie Power Order from Area 1.....	56
Figure 4.27: Area 2 Generation.....	57
Figure 4.28: Case II Fault Area 1 Frequency Response with IAFSC Controller.....	58
Figure 4.29: Case II Fault Area 2 Frequency Response with IAFSC Controller.....	59
Figure 4.30: Case II Fault Area 1 Rotor Speed Deviation Response with IAFSC Controller.....	59
Figure 4.31: Case II Fault Area 2 Rotor Speed Deviation Response with IAFSC Controller.....	59
Figure 4.32: Case II Fault HVDC Tie Power Order from Area 1 with IAFSC Controller.....	60
Figure 4.33: Case II Fault Area 1 Generation with IAFSC Controller.....	60
Figure 4.34: Case II Fault Area 2 Generation with IAFSC Controller.....	61

GLOSSARY

AC	Alternating Current
ACEC	Africa Clean Energy Corridor
APC	Active Power Controller
DC	Direct Current
EAC	Equal Area Criterion
EAPP	East Africa Power Pool
HVAC	High Voltage Alternating Current
HVDC	High Voltage Direct Current
IAFSC	Inter Area Frequency Supplementary Controller
IGBT	Insulated Gate Bipolar Transistors
KETRACO	Kenya Electricity Transmission Company Ltd.
LCC	Line Commutated Converter
PI	Proportional and Integral
Pu	Per Unit
PWM	Pulse With Modulation
VSC	Voltage Source Converter

CHAPTER 1

INTRODUCTION

1.1 Background

Power system interconnection has become a means of accessing secured and reliable power from member states. Many countries including the East Africa Power Pool (EAPP) have pursued the establishment of regional power pools owing to its benefits [1]. Nevertheless, power system interconnection comes with its challenges. High Voltage Alternating Current (HVAC) interconnection for example has the limitation of inter-area system disturbance propagation where severe system disturbances can threaten the security and integrity of the interconnected power systems [2],[45]. To mitigate inter-area system disturbance propagation, High Voltage Direct Current (HVDC) tie lines have been proposed [3], [25]. Moreover, HVDC technology specifically the Voltage Source Converter (VSC) has the advantage of independent control of active and reactive power flow. The active and reactive power can independently be modulated as and when required, unlike the synchronously connected tie lines where the power flow is solely dependent on the power system operating conditions. For this reason, the Voltage Source Converter (VSC) has a competitive advantage that accounts for its wide application in connecting offshore renewable generation, interconnection of asynchronous grids, and bulk power transfer over long distances [4], [26], [31]. With the increasing need for interconnected grid security and reliability [5], it is paramount that the HVDC fast control response is harnessed to improve the transient stability of interconnected power systems during transient disturbances. HVDC power modulation capability has thus been utilized to support stressed power systems during transient system disturbance [6]. The control of active power flow to support the stressed system is fundamental to achieving its stability. On the other hand, the supporting system must have the ability to provide the required regulating power without compromising its stability. Therefore, the amount of active power modulation from the supporting control area must be restrained to maintain its grid stability, security, and reliability. Because power systems have operational limits, this thesis has proposed and investigated the constrained VSC-HVDC tie lines for the interconnection of power systems as a means of transient stability improvement during severe transient disturbances by utilizing its Active Power Modulation (APM) capability. This has been achieved by implementing a supplementary controller that is connected to the control area through Phasor Measurement Units (PMU). PMUs have been used owing to their fast data acquisition and high accuracy [46].

1.2 Problem Statement

Power system coupling is necessitated by the need to establish secured and reliable grids. Many regions including Europe, America, Asia, and Africa have interconnected their grids through synchronous links. With synchronous links, studies have shown that severe system disturbance in one control area results in the generation and propagation of low-frequency power oscillations that could compromise the survivability of the interconnected large power grids. To enhance grid stability and security there is a need to decouple the dynamic interactions between the coupled systems which have now compelled the increased research and deployment of HVDC tie lines and more so the VSC-HVDC tie lines as a means of interconnecting power systems including integrating offshore renewable energy resources which in their nature exhibit intermittent frequency variation. VSC-HVDC links have handily been harnessed to ramp up power to support faulted interconnected systems during transient faults or disturbances. Research in VSC-HVDC systems for transient stability improvement of interconnected power systems has been advanced and recommended as a solution to realize a robust grid. However, a serious assumption is made, that the supporting control area is an infinite system. This assumption means therefore the VSC-HVDC link can draw any amount of power from the supporting area without causing deviations of system parameters no matter how severe the system disturbance is. This is not the case. On the contrary, power systems have operational limits, and especially in Africa electricity grids operate close to their stability limits owing to the exponential growth in load attributed to modernization and industrialization that has been accompanied by little or no expansion in the generation and transmission infrastructure. Given this scenario, the unconstrained VSC-HVDC link in trying to support the stressed power system will cause severe system disturbance in the supporting control area. To mitigate such catastrophic events, this research utilizes constrained VSC-HVDC links that modulate the active power based on real-time system conditions to improve the transient stability of the interconnected power system.

1.3 Objectives

1.3.1 Main Objective

To investigate the transient stability response of interconnected power systems with unconstrained and constrained VSC-HVDC tie lines.

1.3.2 Specific Objectives

- i) To develop and incorporate a supplementary controller in the proposed constrained VSC-HVDC tie line.
- ii) To simulate transient faults on the existing unconstrained VSC-HVDC tie line to investigate its transient response.
- iii) To simulate transient faults on the proposed constrained VSC-HVDC tie line to investigate its transient response.
- iv) Validation of results.

1.3.3 Research Questions

- i) How is the transient system response of the supporting control area when providing regulating power beyond its support capacity?
- ii) How is the transient system response of the faulted control area during severe transient system disturbance?
- iii) How can the two-area operating system parameters be monitored in real-time to provide system input parameters to the proposed supplementary IAFSC controller?
- iv) What inputs of the VSC-HVDC system shall be used by the IAFSC controller to develop an algorithm to adjust and provide the modulating power input to the supporting control area to improve its transient stability response?

1.4 Justification for Study

The Africa Clean Energy Corridor (ACEC) initiative is advocating for the interconnection of power systems to promote regional electricity trade in Africa [8]. Therefore, African countries like their counterparts in America and Europe, are implementing power systems interconnection projects to establish cross-border power trade to achieve a secure and reliable grid. Recent trends have seen the growth of VSC-HVDC tie lines for transient stability improvement of interconnected power systems. However, the VSC-HVDC links have been implemented without considering the

strength of the interconnected power systems. It has been assumed that the interconnected grids are infinite systems and thus the VSC-HVDC tie line can ramp up any amount of power to support the stressed system. On the contrary, power systems have operational limits. This study therefore proposes a VSC-HVDC tie line that considers the support capacities of the interconnected power systems in real-time. With the proposed system, the transient stability of the interconnected power systems is ensured during large power system disturbances while maintaining the security and integrity of the interconnected systems. This solution can thus be aptly utilized in the proposed East Africa Power Pool (EAPP) to guarantee its integrity and security.

1.5 Scope of Work

The proposed research studies a Kundur two-area interconnected power system to perform transient stability analysis. The first case has an unconstrained VSC-HVDC tie line and the second case has the proposed constrained VSC-HVDC tie line. The transient stability analysis was done in MATLAB/SIMULINK programming software. The second proposed case considered power system operational limits.

1.6 Thesis Organization

This thesis is organized into five Chapters with chapter 1 describing the background, objectives, justification, and scope of work undertaken. Chapter 2 provides the literature review which includes the basic concepts of HVDC systems, a review of previous works, the research gap, and the problem formulation of the proposed solution. Chapter 3 gives the methodology of the proposed solution giving a review of the previous methods used, the proposed method for this research proposal, and the expected results. Chapter 4 gives the results and analysis of the system with the unconstrained and constrained VSC-HVDC link. Chapter 5 gives the conclusions drawn and the recommendations. The Thesis report has also provided the reference and appendices sections after the last chapter of the report.

1.7 Published Works

This research has been published in Heliyon Journal with authors as Mwashia Mwangudza, Dr. Abraham Nyete and Dr. Peter Musau. The research paper was accepted, comments addressed and resubmitted and is currently under review.

CHAPTER 2

LITERATURE REVIEW

2.1 Basic Concepts

2.1.1 Power System Interconnection

Power system interconnection is the integration of isolated power systems into one grid through tie lines to operate as one system with the system operational quantities i.e. frequency, voltage, and phase angle maintained at an optimum limit. Over time, many nations have interconnected their power systems owing to the benefits that come along with system interconnection [9]. Isolated power systems can be connected through synchronous or asynchronous links. Recent trends have seen HVDC links gaining popularity owing to their ability to interconnect power systems with different operating system frequencies, interconnecting systems over long distances including integration of offshore renewable energy resources, and the ability to modulate power [10]. A summary of the comparison of the types of tie lines that can be used is shown in Figure 2.1.

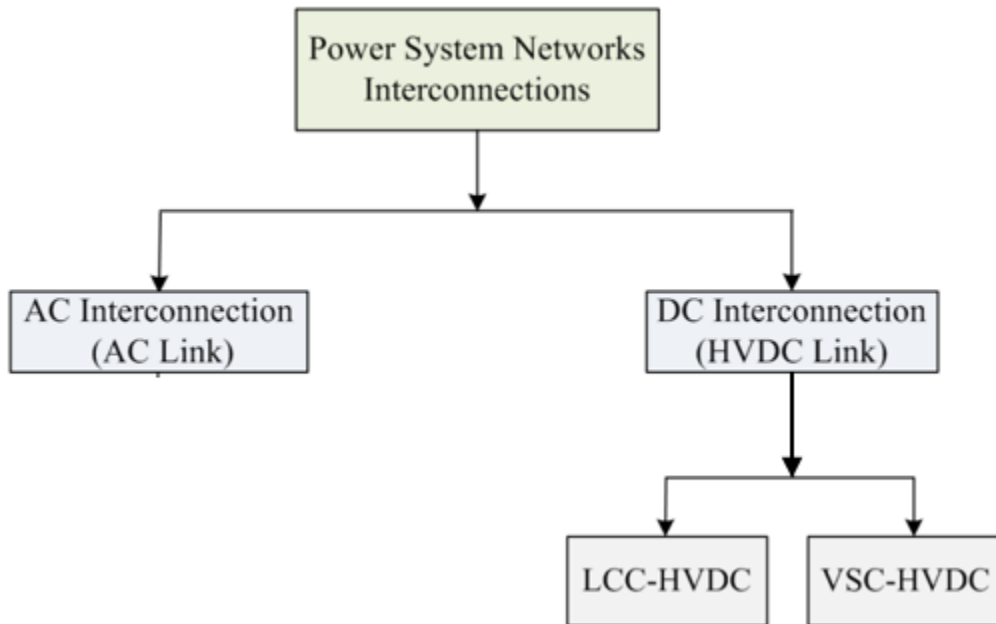


Figure 2.1: Types of Interconnection Tie Lines [6]

HVDC transmission tie lines can further be subdivided into Line Commutated Converters (LCC) and Voltage Source Converters (VSC). VSC-HVDC links offer better performance in terms of active and reactive power flow control [10]. Therefore this thesis employs VSC-HVDC tie lines to interconnect a Kunder two-area system. Figure 2.2 shows a simple structure of a VSC-HVDC tie line with U_1 as the A.C voltage on the rectifier side, U_2 and U_{dc} as the D.C voltage of the rectifier converter and the D.C line respectively.

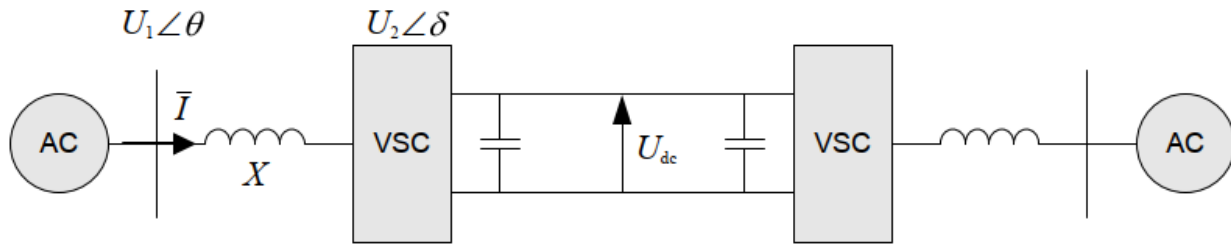


Figure 2.2: VSC-HVDC interconnection [13].

2.1.2 Power System Stability

Despite the benefits of a reliable and secured power system, power system interconnection comes with the challenge of stability problems. The stability problems inherent in interconnected power systems can be classified into steady-state stability and transient stability [11].

2.1.3 Steady-State Stability

As stated in [11], steady-state stability is the ability of the power system to maintain synchronism when subjected to small disturbances. This is true when the equations describing the system rotor angle response can be linearized.

2.1.4 Transient Stability

In [11],[33] transient stability is defined as the ability of the power system to maintain synchronism when subjected to a severe transient fault such as transmission faults, loss of generation, or loss of a large load. The system response is usually followed by the oscillation of the generator rotor angles that become unstable.

To study power system stability the swing equation is used.

The swing equation is expressed as [12], [20];

$$\frac{d^2\delta}{dt^2} = \frac{1}{M}(P_m - P_{\max} \sin \delta) = P_a / M \quad (2.1)$$

Where δ is the generator rotor angle in degrees, M is the moment of inertia given by;

$$M = \frac{GH}{\pi} \text{ or in pu system } M = \frac{H}{\pi f} \quad (2.2)$$

Where G is the MVA machine rating, H is the inertia constant in MJ/MVA, f is the system frequency in hertz, P_m is the mechanical power in per unit, P_{\max} is the maximum mechanical power in pu, and P_a is the per-unit accelerating power.

2.1.5 Transient Stability Analysis Methods

Transient stability analysis can be carried out using numerical (direct) methods or the indirect method by Equal Area Criterion (EAC) [12]. The numerical methods include the point-by-point method, the digital technique (Runge Kutta method), Liapunov's direct method, and the Rate of Change of Kinetic Energy (RACKE). The most utilized and popular methods used in transient stability analysis are the EAC and point-by-point methods which are discussed in this proposal [12].

2.1.5.1 The Equal Area Criterion

Transient analysis by Equal Area Criterion states that for stability conditions the rate of change of the generator rotor angle should be zero. This is expressed as;

$$\frac{d\delta}{dt} = 0 \quad (2.3)$$

Equation 2.3 implies that;

$$\int_{\delta_0}^{\delta} P_{ad\delta} = 0 \quad (2.4)$$

The Equal Area Criterion is described by the power-angle curve as illustrated in Figure 2.3 where P_{i0} is the generator mechanical input power at initial stable condition, P_i is the generator input mechanical power following system disturbance, P_e is the electrical output power, P_{max} is the maximum generator mechanical input power.

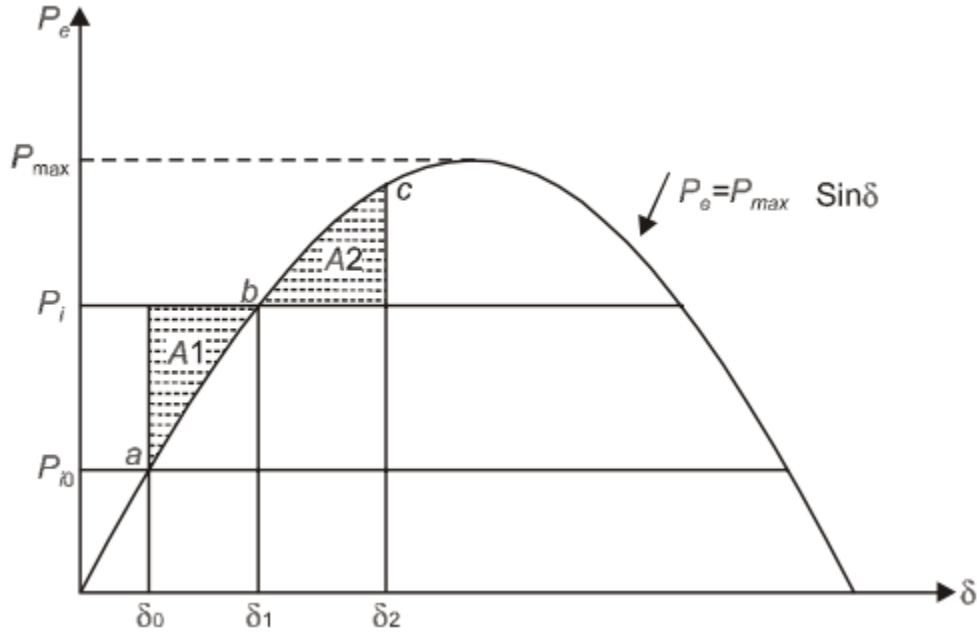


Figure 2.3: Power angle Characteristic Curve. [11]

The EAC requires that for stable conditions to be achieved after a system disturbance, area A1 should equal area A2. This condition is mathematically described and achieved when;

$$(\delta_2 - \delta_0) \sin \delta_1 + \cos \delta_2 - \cos \delta_0 = 0 \quad (2.5)$$

2.1.5.2 Point-by-Point Method

The point-by-point method is a numerical method of transient stability analysis [8]. The change in rotor angle is expressed as;

$$\Delta \delta_n = \Delta \delta_{(n-1)} + \{(\Delta t)^2 / M\} * P a_{(n-1)} \quad (2.6)$$

And the rotor angle at time t_n (sec) can now be expressed as;

$$\delta_n = \delta_{(n-1)} + \Delta \delta_n \quad (2.7)$$

This thesis has used the point-by-point method to perform the transient stability analysis of the interconnected systems normally used for multi-machine systems [8]. The EAC is only applicable in a single machine swinging with respect to an infinite bus. The point-by-point method is a well-proven analysis numerical method applicable to a multi-machine system where more than one generating unit is interconnected as is the case in this research thesis.

2.1.6 VSC-HVDC System.

2.1.6.1 Introduction

VSC-HVDC switching devices are made of IGBTs that switch on and off at a speed of 20 kHz as compared to thyristors that switch on and off at a frequency of 50 hertz. Through Pulse Width Modulation (PWM) the VSC system independently controls active and reactive power [13]. The control of active and reactive power is achieved by varying the phase angle and amplitude of the converter output voltage with respect to the AC line voltage.

2.1.6.2 Basic Structure of a VSC-HVDC System

The VSC-HVDC system consists of the following major components;

- i) The VSC Rectifier Converter and the Inverter Converter where voltage conversion from AC to DC and DC to AC is done respectively.
- ii) The Converter Transformer for voltage transformation.
- iii) The DC capacitors that form the voltage source of the Converters.

The major components of a VSC-HVDC system are shown in Figure 2.4.

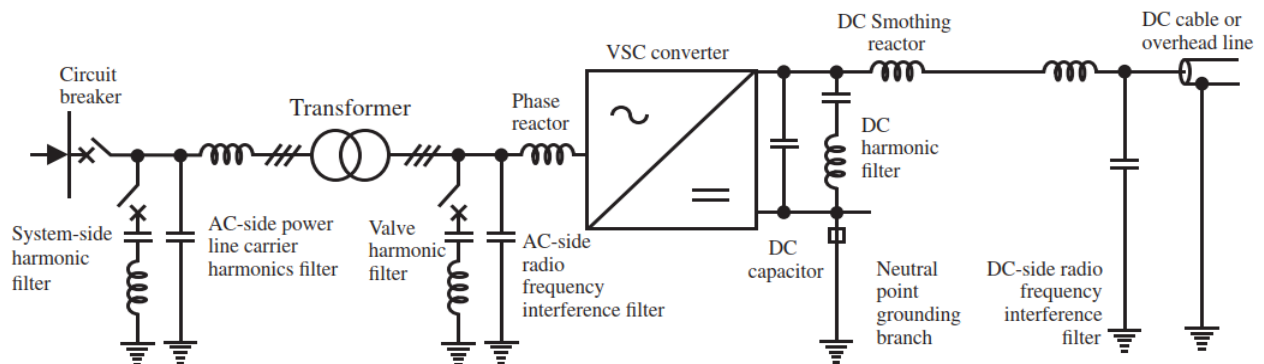


Figure 2.4: Basic Structure of a VSC-HVDC System [13]

The VSC-HVDC system can operate as a rectifier or an inverter. It operates as a rectifier when active power flows from the AC side to the DC side. It operates as an inverter when the active power flows from the DC side to the AC side.

2.1.6.3 Active and Reactive Power Modulation.

The active and reactive powers P_{conv} and Q_{conv} flowing between the converter and the AC system can be expressed by equations 2.5 and 2.6 [13],[34].

$$P_{conv} = \frac{U_{conv} \cdot U_L}{X_{conv}} \sin \delta \quad (2.5)$$

$$Q_{conv} = \frac{U_L^2}{X_{conv}} - \frac{U_L U_{conv}}{X_{conv}} \cos \delta \quad (2.6)$$

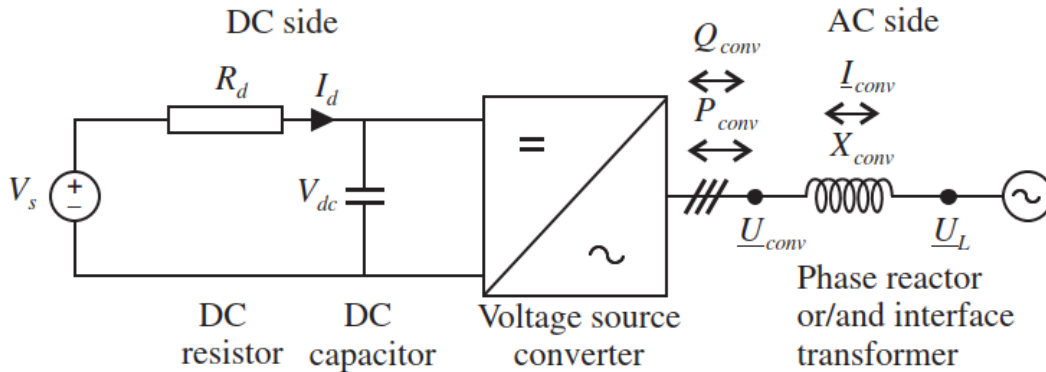


Figure 2.5: VSC-HVDC Terminal [13]

From equation (2.5), the active power can be controlled by varying the phase angle δ between voltages U_{conv} and U_L . No active power flows in the system when the phase difference is zero. To change the direction of power flow the sign of the phase angle must be changed. From equation (2.6), when U_L is greater than U_{conv} the AC system supplies reactive power to the DC side. When U_L is lower than U_{conv} the DC side supplies reactive power to the AC side. The reactive power can be controlled by controlling the converter and AC line voltages. The power magnitude and

direction can be modulated by varying the direction and magnitude current. The direct current can be expressed as;

$$I_d = \frac{\sqrt{6}}{\pi} \frac{U_L}{X} \sin \delta \quad (2.7)$$

The converter can operate in rectifier mode or inverter mode. When U_{conv} lags U_L , the HVDC system absorbs active AC power and hence works as a rectifier. The direct voltage V_{dc} will be expressed as equation 2.8.

$$V_{dc} = V_s + R_d I_d \quad (2.8)$$

When U_{conv} leads the voltage U_L , the HVDC system supplies active power to the AC side. The then operates as an inverter. The direct voltage V_{dc} will be expressed as equation 2.9;

$$V_{dc} = V_s - R_d I_d \quad (2.9)$$

2.2 Review of Previous Works

Research has been advanced in VSC-HVDC tie lines used for power systems interconnection and as a means of transient stability improvement with the VSC-HVDC highly proposed and recommended to be used for regional power system interconnections. This section discusses the previous works done on this subject.

Teja Bandaru et al (2018) [6] in their research, Improving the Transient Stability by Modifying the Power Exchange by the HVDC Transmission used a test system that assumes the supporting area is large and has the inertia to absorb any large variations in the dc link power. The HVDC controls are thus not constrained to mitigate the loss of synchronism in the supporting area in case of severe system disturbance that requires large regulating power beyond the capacity of the supporting control area.

Issarachai Ngamroo et al (2002) [14] proposed the stabilization of frequency oscillations using a power modulation control of HVDC link in parallel AC-DC interconnected systems. This study has assumed that the supporting area is an infinite bus. The stability limit of the supporting control area is not considered.

Mao Xiao-ming et al (2007) [15] in the application of HVDC modulation in damping electromechanical oscillations, proposed the use of wide-area information signals in the AC-DC parallel interconnected systems to provide power modulation on the HVDC link. The wide-area signals provide better power modulation signals as opposed to the local signals. Despite providing better power modulation in damping frequency oscillations, this research did not address the system constraints of the interconnected power systems in terms of their support capability.

R. Leelaruji et al (2010) [16] in their study, coordination of protection systems for mitigating cascading failures proposed using protection relays in providing power modulation signals to the VSC-HVDC system. The protection relays as proposed in their research use an overcurrent element as a modulating signal to the HVDC system. The overcurrent protection in nature is a slow-acting protection function and cannot be effectively used for the fast operation of the HVDC power modulation. The system model used in this research assumes an infinite system which does not reflect a real-case scenario since power systems have operational limits.

Sharlene M Builu (2016) [17] in his thesis proposed a parallel AC-DC tie line using the first-generation HVDC systems i.e. the LCC HVDC technology. He never studied the dynamic response for transient system disturbances. The proposed LCC HVDC system has the disadvantage of poor control of reactive power flow [14]. On the contrary, the VSC-HVDC system has the capability of independent control of active and reactive power and is used in this proposal.

AN Fuchs et al (2010) [19] in their study proposed a VSC-HVDC system to improve the stability of the interconnected systems. In their study, a parallel AC-DC network model was used which assumed an infinite system of the supporting area. The system model does not reflect the real case scenario as power systems have their operational limits.

Omid Borazjani et al (2015) [22] in their study Stability Improvement of AC System by Controllability of the HVDC used a Single Machine Infinite Bus (SMIB) for transient stability improvement during system disturbance. The SMIB assumes an infinite system and does not consider operational limits.

P. Bapaiah (2013) [37] in his study, Improvement of Power System Stability using HVDC Controls utilized a single machine test system connected to an infinite bus. The infinite bus will always provide the regulating power required for any amount of power step change regardless of the magnitude of the transient fault. This does not reflect a true case scenario of power systems that often operate with defined stability limits.

Muhammad Abdul Basit et al (2018) [38] in their publication, Intelligent Damping Control for Transient Stability Enhancement using HVDC used a Single Machine Infinite Bus (SMIB) system which forms the basis of this thesis problem statement. The HVDC link as applied in their multi-machine test system has its controller not restrained to consider the capacity of the supporting area. It is assumed that the supporting area will always provide the synchronizing torque to the stressed control area.

Lakshmi Sundaresh et al (2020) [39] in their publication, Improving Power Grid Transient Stability and Transfer Capability using HVDC Emergency Power Controls studied two control schemes i.e. frequency and voltage phase angle where the HVDC control scheme continuously changes the modulated power until the critical swing is mitigated. The control scheme does not incorporate checks on the strength of the supporting control area whenever the required modulated power is beyond its capability.

2.3 Summary of the Previous Works

Transient stability improvement utilizing VSC-HVDC tie lines has gained popularity and interest among researchers. A summary of the previous works is given in Table 2.3 which describes the work done and the areas that are unexplored forming the basis of this study

Table 2.1: A summary of the Literature Review.

Reference	Authors	Work done	Gaps to be addressed
[6]	Teja Bandaru et al (2018)	Improving the Transient Stability by Modifying the Power Exchange by the HVDC Transmission	<ul style="list-style-type: none"> Utilized a test system that assumes the supporting area is large and has the inertia to absorb any large variations in the DC link power. The HVDC controls are thus not constrained to mitigate the loss of synchronism in the supporting area in case of severe system disturbance that requires large regulating power beyond the capacity of the supporting control area.
[14]	Issarachai Ngamroo et al (2002)	Stabilization of frequency oscillations using a power modulation control of HVDC link in parallel AC-DC interconnected systems.	<ul style="list-style-type: none"> The stability limit of the supporting area is not considered. The HVDC controller is not restrained in terms of active power modulation which is catastrophic for large power system disturbances beyond the capacity of the supporting area.
[15]	Mao Xiao-ming, Zhang Yao et al (2007) [16]	Application of HVDC modulation in damping electromechanical oscillations. A theoretical analysis has been done on the modulation of DC power in an AC/DC power system.	<ul style="list-style-type: none"> The stability limit of the supporting area is not considered. The HVDC controller is not restrained in terms of active power modulation which is catastrophic for large power system disturbances beyond the capacity of the supporting area.

[16]	R. Leelaruji et al (2010)	Coordination of protection systems for mitigating cascading failures.	<ul style="list-style-type: none"> • The system model utilized assumes infinite power systems. Power systems have operational limits a factor that needs to be considered to reflect a real-case scenario. The HVDC controller is not restrained in terms of active power modulation which is catastrophic for large power system disturbances beyond the capacity of the supporting area.
[17]	Sharlene M Builu (2016)	Parallel AC-DC tie line using the first-generation HVDC systems.	<ul style="list-style-type: none"> • Utilized LCC-VSC HVDC technology which has poor reactive power control. The stability limit of the supporting area is not considered. The HVDC controller is not restrained in terms of active power modulation which is catastrophic for large power system disturbances beyond the capacity of the supporting area.
[24]	J. Hazra et al (2009)	HVDC Control Strategies to Improve Transient Stability in Interconnected Power Systems. Three HVDC control strategies on frequency, phase angle, and power difference between the sending and receiving end were studied.	<ul style="list-style-type: none"> • The stability limit of the supporting area is not considered. The HVDC controller is not restrained in terms of active power modulation which is catastrophic for large power system disturbances beyond the capacity of the supporting area.

[37]	P. Bapaiah (2013)	Improvement of Power System Stability using HVDC Controls	<ul style="list-style-type: none"> • Used a single-machine test system connected to an infinite bus. The infinite bus will always provide the regulating power required for any amount of power step change regardless of the magnitude of the transient fault. This does not reflect a true case scenario of power systems that often operate with defined stability limits.
[38]	Muhammad Abdul(2018)	Intelligent Damping Control for Transient Stability Enhancement using HVDC	<ul style="list-style-type: none"> • Used a Single Machine Infinite Bus (SMIB) system which forms the basis of this thesis problem statement. The HVDC link as applied in their multi-machine test system has its controller not restrained to consider the capacity of the supporting area. It is assumed that the supporting area will always provide the synchronizing torque to the stressed control area.
[39]	Lakshmi Sundaresh et al (2020)	Improving power grid transient stability and transfer capability using HVDC emergency power controls	<ul style="list-style-type: none"> • Studied two control schemes for frequency and voltage phase angle where the HVDC control scheme continuously changes the modulated power until the critical swing is mitigated. The control scheme does not incorporate checks on the strength of the supporting control area whenever the required modulated power is beyond its capability.

Proposed Work	Investigation of Constrained VSC-HVDC Tie Lines for Transient Stability Improvement of Interconnected Power Systems	<ul style="list-style-type: none"> The proposed work addresses the gap of transient stability loss in the supporting control area when the regulating power required by the faulted control area is beyond its capacity. It incorporates an IAFSC controller which monitors in real-time the system frequency of the control areas and mitigates unstable conditions by controlling the HVDC controls during severe fault conditions. This supplementary controller does not assume the power systems to be infinite hence maintains its operational limits to prevent catastrophic unstable conditions.
---------------	---	---

2.4 Research Gap

Researchers have put forward the concept of VSC-HVDC tie lines as a means of transient stability improvement of interconnected power systems [28]. However, in their proposals a serious assumption is made, i.e. the supporting area is an infinite system able to support any amount of power to the stressed area without causing deviations in system parameters irrespective of how severe the system disturbance is. On the contrary, power systems have operational limits and these limits must be respected. With the conventional system, the unconstrained HVDC link will cause instability issues in the supporting area if this control area's supporting strength is limited. Given the limitation of the conventional system controllers, this thesis has studied the transient stability response of an interconnected power system while considering the support capacity of the supporting area using real-time data to mitigate unstable conditions during severe disturbances where its support capacity is limited. Therefore, an IAFSC (Inter Area Frequency System Controller) that is capable of restraining the active power modulation using real-time power system data has been proposed in this thesis. Two system models have been used to simulate the dynamic behavior of the interconnected systems, the first case with an unconstrained VSC-HVDC link and the second case with constrained VSC-HVDC links that utilize the proposed controller.

2.5 Chapter Conclusion

Based on the review of the previous work done and the research gap described in this chapter, this thesis studied a constrained VSC-HVDC tie line with a controller receiving real-time control area data for transient stability improvement of the interconnected systems during severe system disturbances. A Kundur two-area interconnected system is used to simulate the dynamic behaviour of the interconnected systems with the first case using a constrained VSC-HVDC link and the second case using an unconstrained VSC-HVDC link.

CHAPTER 3

MATERIALS AND METHODS

3.1 Introduction

This chapter provides the research approaches and methods used to enhance the transient stability of interconnected power systems by utilizing the active power control capability of the VSC-HVDC system [23], [29]. Unlike the traditional systems, the addition of the IAFSC in the VSC-HVDC control strategy is done to mitigate unstable conditions in the supporting control area whenever the system disturbance is severe beyond its support capacity. The Kundur two-area system [40],[44] has been used as a test system for the simulation of transient faults, where modifications have been done to include a VSC-HVDC tie line and the proposed control method in this thesis. The test systems representing the traditional and the proposed systems are shown in Figures 3.1 and 3.2 respectively. Two fault scenarios were simulated, with the first case leading to the loss of 10% of generation in control area 2 for which control area 1 can effectively support, and the second case leading to the loss of 25% of generation in control area 2 for which control area 1 is incapable of providing the required regulating power to effectively restore system stability in control area 2. The system responses are studied for the test system with and without the proposed IAFSC and validation of the proposed control method is done by comparing the two case scenario responses.

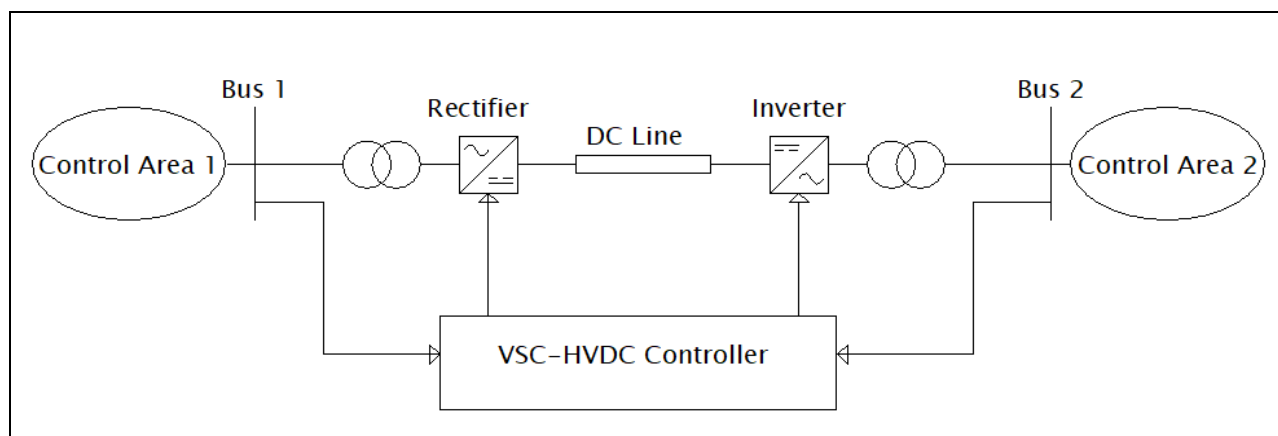


Figure 3.1: The Conventional VSC-HVDC System

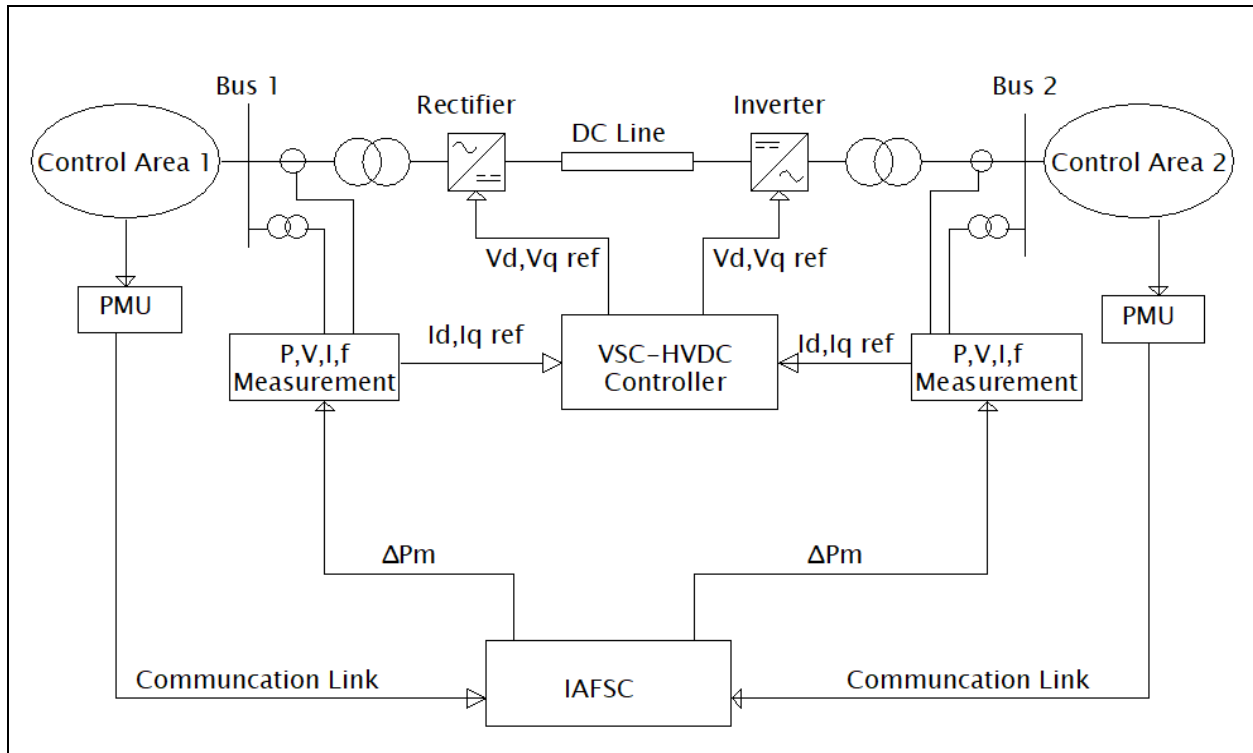


Figure 3.2: The Proposed VSC-HVDC System

3.2 The Kundur Two-Area Test System

The Kundur two-area test system consists of four generators with each pair forming a control area connected via a tie line. Originally proposed by Kundur, this test system has become popular for the simulation of interconnected power systems [43], [47]. In this thesis, modifications were done to connect the two areas with a VSC-HVDC tie line. The traditional HVDC controls were improved to include the proposed IAFSC controller in this thesis. Figure 3.2 shows the improved test system whose system design in MATLAB/SIMULINK is shown in Figure 3.17. The system data for the Kundur two-area test system is given in Table 3.1.

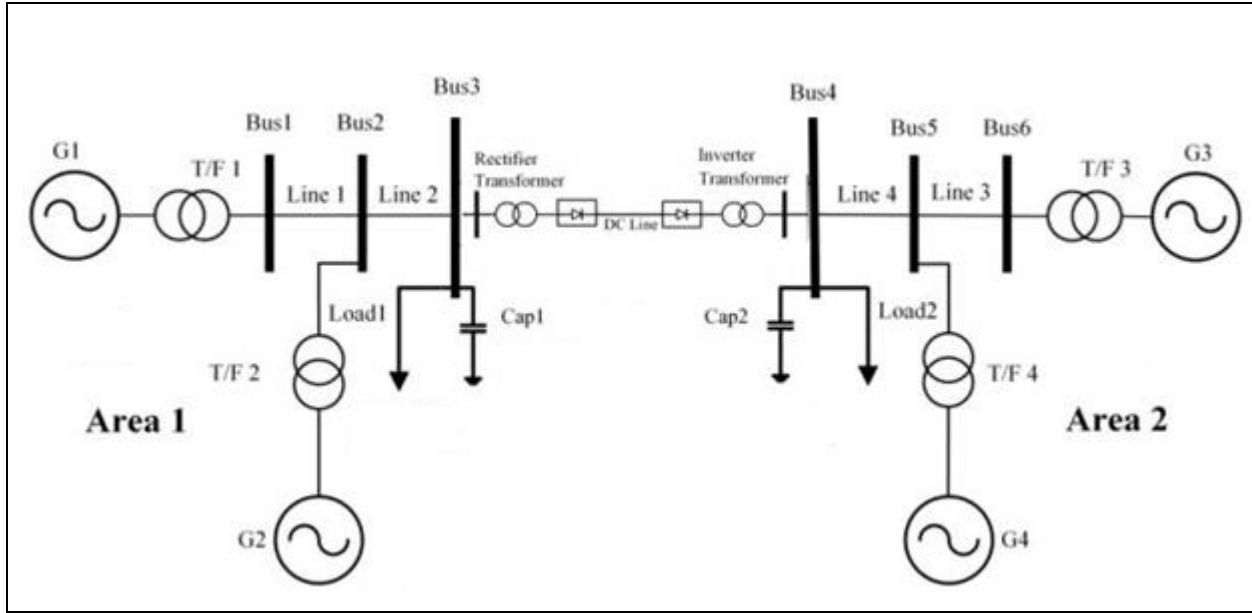


Figure 3.3: Two-Area Kundur Test System with a VSC-HVDC Tie Line [11]

Table 3.1: The Kundur Two-Area Test System Data [11]

Generator	Rating (MVA)	X_d (pu)	X'_d (pu)	X''_d (pu)	T'_{do} (s)	T''_{do} (s)	X'_q (pu)	X''_q (pu)	T'_{qo} (s)	T''_{qo} (s)	H (s)	R (pu)
G1	900	1.8	0.3	0.25	8	0.03	1.7	0.25	0.4	0.05	6.5	0.05
G2	900	1.8	0.3	0.25	8	0.03	1.7	0.25	0.4	0.05	6.5	0.05
G3	900	1.8	0.3	0.25	8	0.03	1.7	0.25	0.4	0.05	6.175	0.05
G4	900	1.8	0.3	0.25	8	0.03	1.7	0.25	0.4	0.05	6.175	0.05

3.3 The VSC-HVDC System Description

The VSC-HVDC system used in this thesis is a 200MVA, 230kV AC, and +/- 100kV DC side system with 230/100kV converter transformers on the rectifier and the inverter sides. The VSC-HVDC system has AC filters, phase reactors, and DC capacitors connected to it as shown in Figure 3.4 which is described in detail in the subsequent sections.

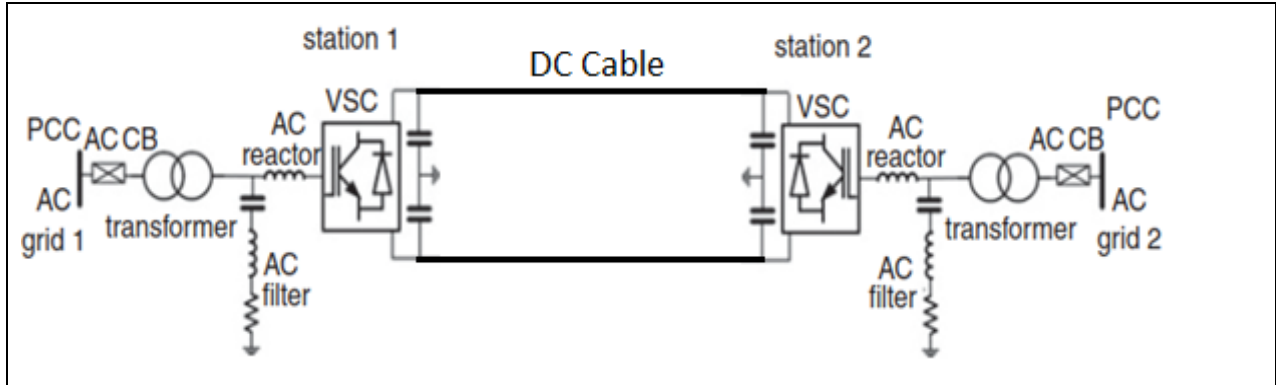


Figure 3.4: VSC-HVDC System Architecture [41]

3.3.1 The Converter Transformer

The 230/100kV converter transformers transform the AC voltage to DC voltage and vice versa on the rectifier and inverter side respectively. The converter transformer leakage reactance permits the converter output voltage to shift in phase and amplitude with respect to the AC system Point of Common Coupling (PCC) and allows independent control of the converter's active and reactive power outputs [42].

3.3.2 The Phase Reactor

The phase reactor is a fundamental component of the VSC-HVDC system whose leakage impedance being 15% is essential for independent control of active and reactive power. It functions as a low-pass filter blocking harmonic current components related to high-frequency switching thus reducing harmonic losses in the converter coupling transformers. The phase reactor leakage reactance (X_p) should be large enough to minimize sudden variation current caused by high-frequency switching, but at the same time, it should be small enough so that the voltage drop across the inductances can be considered negligible. Therefore its value is normally between 0.15pu to 0.2pu [42]. In this thesis, a value of 0.15pu is used [21].

Given the 0.15pu value of the leakage reactance, its corresponding inductance can be calculated in equation 3.1.

$$\begin{aligned}
 X_f &= X_p * (V^2/MVA) \\
 &= 0.15 \cdot \frac{100^2}{200} = 7.5 \Omega
 \end{aligned}
 \tag{3.1}$$

Where V is the rated voltage, X_p is the leakage reactance per unit and X_f is the leakage reactance in ohms and its associated inductance L_p is calculated as;

$$\begin{aligned} L_p &= X_f / 2\pi f \\ &= \frac{7.5}{2\pi \cdot 50} = 23.87mH \end{aligned} \quad (3.2)$$

3.3.3 AC Filters

The AC filters are fundamentally used to suppress high-frequency harmonic currents. Unlike the LCC-HVDC filters, they are not required for reactive power compensation in VSC-HVDC applications and therefore are permanently connected to the HVDC system. The dominant harmonic voltages are generated at and around multiples of the frequency index p , which is the carrier frequency per modulator frequency. The switching frequency (1350Hz) with a sampling time T_s of 7.406e-6 seconds gives the frequency index p as 27. The dominant harmonic components are thus exhibited at the 27th and 54th harmonics. The AC filters must filter these harmonics and hence are tuned at the 27th and 54th harmonic frequencies. The selection of the filter parameters is thus highly dependent on the switching frequency f_s and the VSC base impedance Z_f value. The filter parameter values are calculated as [42], [48];

$$\begin{aligned} Z_f &= X_p * (V^2/MVA) \\ Z_f &= 0.15 \cdot \frac{100^2}{(200)} = 7.5\Omega \end{aligned} \quad (3.3)$$

The filter inductance L_f and capacitance C_f as calculated in this thesis are;

$$\begin{aligned} L_f &= Z_f / 2\pi f_s \\ &= \frac{7.5}{(2\pi \cdot 1350)} = 0.8842mH \end{aligned} \quad (3.4)$$

$$\begin{aligned} C_f &= L_f / (Z_f^2) \\ &= \frac{8.8842e-4}{(7.5^2)} = 15.72\mu F \end{aligned} \quad (3.5)$$

3.4 VSC-HVDC Control Scheme

The VSC-HVDC control scheme uses the vector control scheme to achieve a decoupled control of active and reactive power [30]. The vector control principle has been used in this thesis to control the active and reactive power on the rectifier side and the voltage and reactive power on the inverter side. Figure 3.5 shows the vector control scheme used to control the modulation index of the converter.

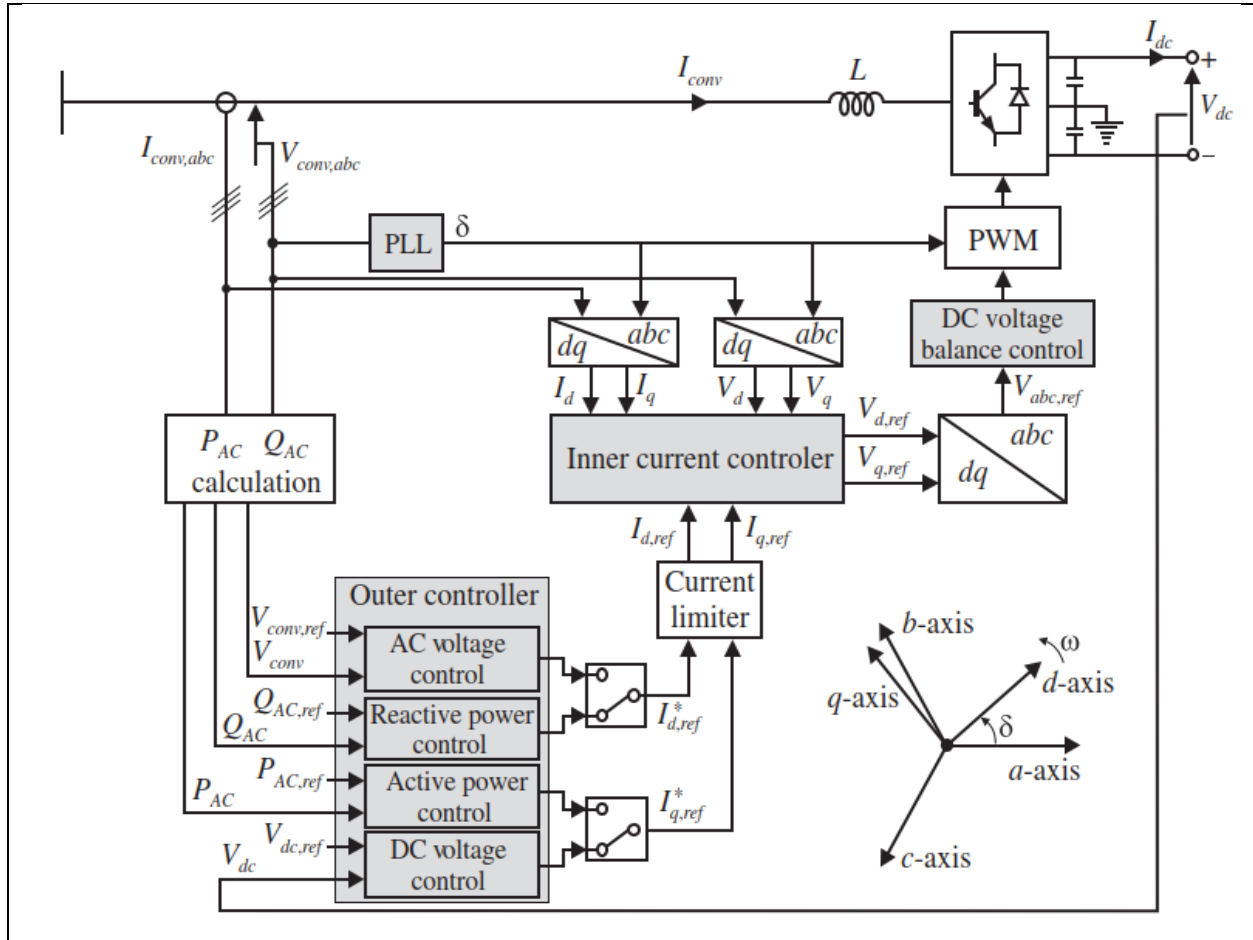


Figure 3.5: VSC-HVDC Vector Control Scheme [13], [30]

In the vector control strategy, the abc stationary coordinates system is transformed to the equivalent dq coordinates system which provides an effective way of independent control of active and reactive powers [35]. The outer controller in the vector control scheme provides the reference currents $I_{d.ref}$ and $I_{q.ref}$ to the inner controller. For the active and reactive power control, the instantaneous powers are calculated in equations [3.6] and [3.7].

$$P = \frac{3}{2} (V_d I_d + V_q I_q) \quad (3.6)$$

$$Q = \frac{3}{2} (V_q I_d - V_d I_q) \quad (3.7)$$

In the vector control strategy, the q -axis of the dq -frame is aligned with the AC voltage phasor such that the q -axis voltage becomes zero i.e. $V_q = 0$. This reduces equations 3.6 and 3.7 to equations 3.8 and 3.9 respectively.

$$P = \frac{3}{2} * V_d I_d \quad (3.8)$$

$$Q = -\frac{3}{2} * V_d I_q \quad (3.9)$$

The inner controller shown in Figure 3.6 controls the modulated voltages V_d and V_q that generate the required PWM switching sequence. To decouple the dq -axis, a feed-forward technique is used to compensate for cross-coupling terms [27], [44].

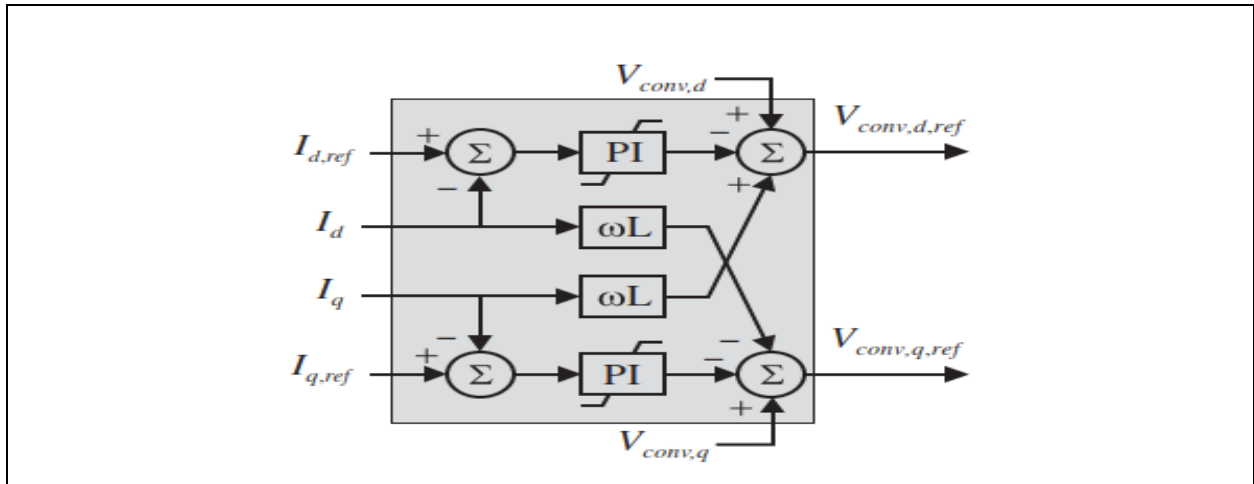


Figure 3.6: VSC-HVDC Inner Controller [13]

3.4.1 The IAFSC Controller

The IAFSC controller proposed in this thesis is a supplementary controller that determines the amount of modulated power depending on the system support capacity of the supporting control area. It is implemented as an additional controller to the existing VSC-HVDC controller to improve the transient stability of the supporting area during severe system disturbances that require regulating power beyond its ability. The IAFSC controller as implemented in this thesis is shown in Figure 3.7. It is connected to the rectifier and inverter Phasor Measurement Units (PMU) to

monitor the frequency changes of the two control areas. The IAFSC controller is composed of a frequency summation circuit, a conditioning circuit, a Proportional and Integral (PI) controller, and a modulation release logic circuit as shown in Figure 3.8. The PI controller achieves the desired controller response through the selection of proper proportional and integral gains K_p and K_i respectively. The PI controller was selected owing to its inherent reduction of steady-state errors, faster response time, and reduced settling time.

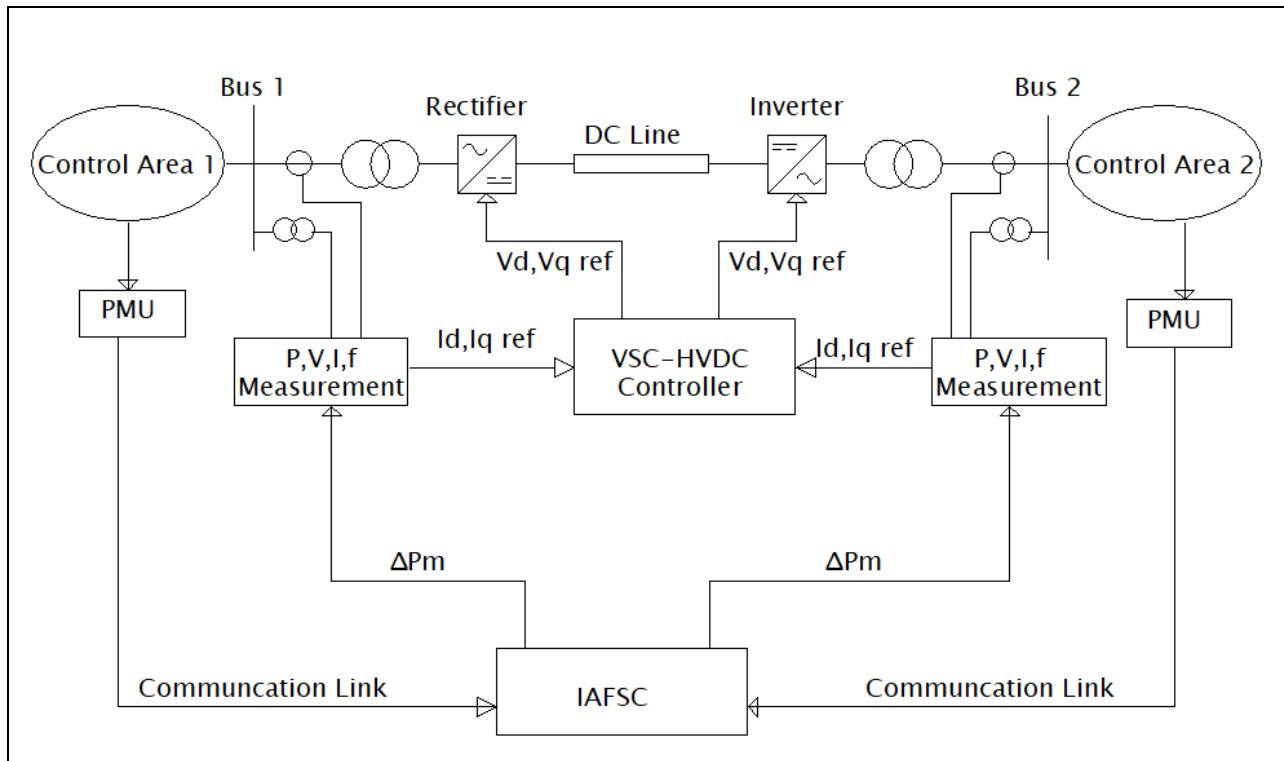


Figure 3.7: The IAFSC Controller Circuit [Proposed]

During fault conditions, the frequency deviation of the faulted control region is calculated to give the required modulated power ramp order to the primary VSC-HVDC controller to assist the faulted control area in recovering stable conditions. At the same time, the supporting control area frequency is monitored to avoid violation of the stable limit. When the stability limit is exceeded the IAFSC controller resets the power to assist in recovering stable conditions.

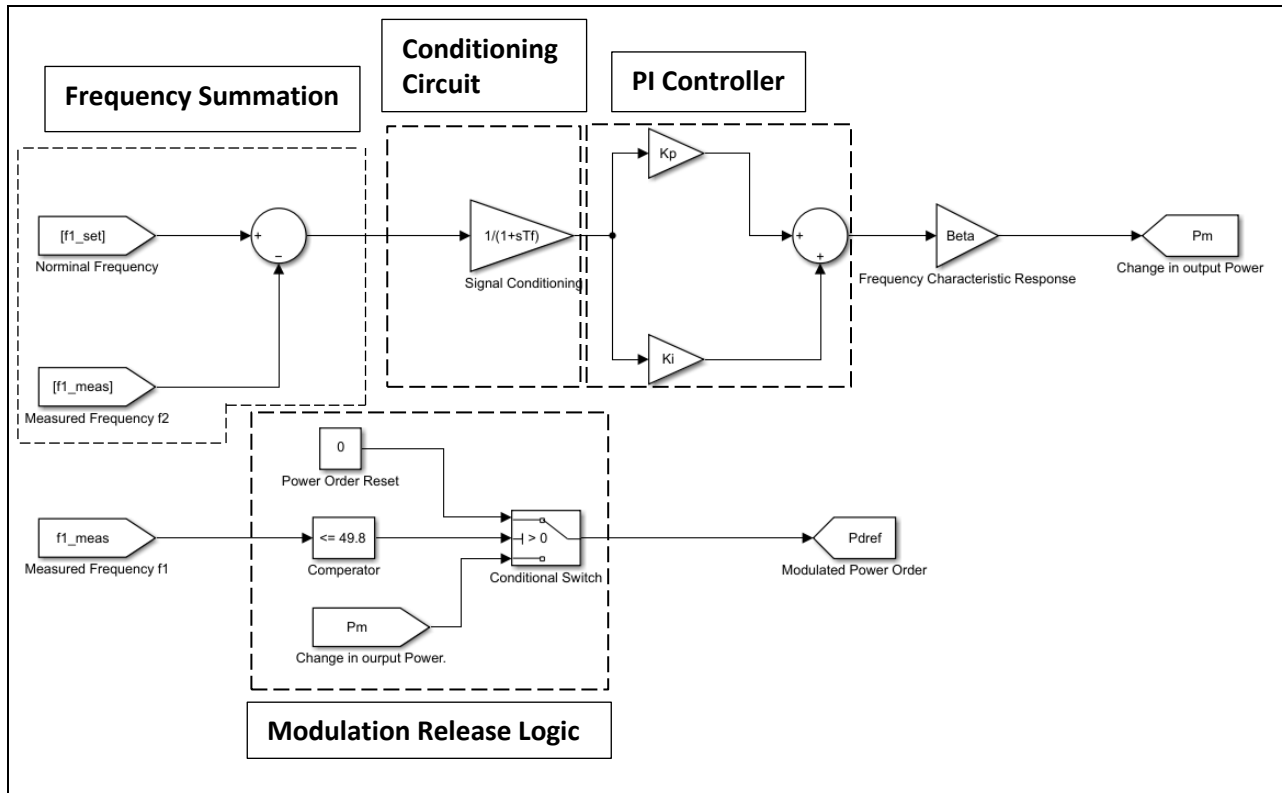


Figure 3.8: The IAFSC Controller Block Diagram

The PI controller block diagram is shown in Figure 3.9 [32]. From this figure, the controller equation can be described by equation 3.10.

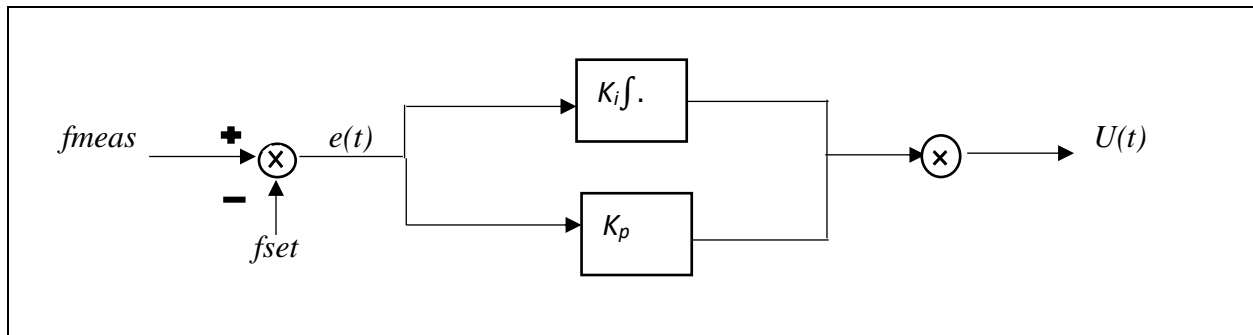


Figure 3.9: PI Controller Block Diagram

$$U(t) = K_p e(t) + K_i \int e(t) dt \quad (3.10)$$

Where $U(t)$ is the output of the PI controller, $e(t)$ is the error signal, K_p and K_i are proportional and integral gains respectively, f_{meas} and f_{set} are the measured and threshold frequencies respectively.

The transfer function of the PI controller is obtained by taking the Laplace transform of equation 3.10 and is described in equations 3.11 and 3.12.

$$U(s) = (K_p + \frac{K_i}{s})E(s) \quad (3.11)$$

$$\frac{U(s)}{E(s)} = (K_p + \frac{K_i}{s}) \quad (3.12)$$

Where $U(s)$ is the output of the controller, $E(s)$ is the error input signal and $(K_p + \frac{K_i}{s})$ is the controller Transfer Function (TF).

Figure 3.10 shows the block diagram of the IAFSC controller system used to determine the system transfer function. It consists of signal conditioning, and PI controller block diagrams respectively.

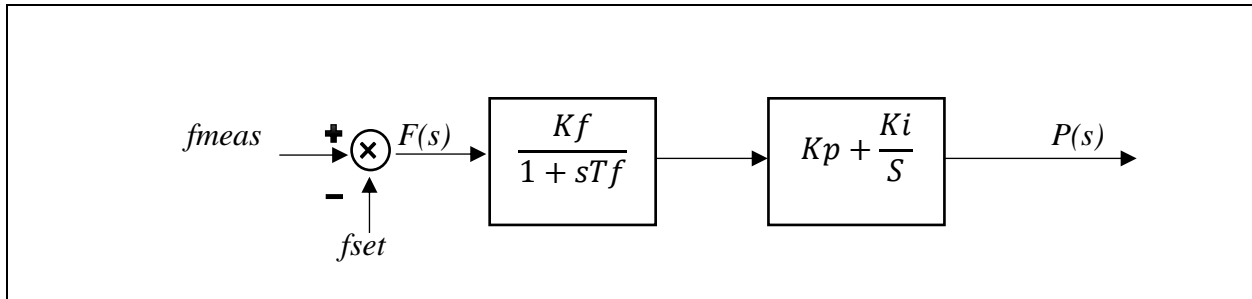


Figure 3.10: Block diagram representation of the IAFSC controller system

The system equation of Figure 3.9 is described in equation 3.13 as;

$$P(s) = F(s) * (\frac{K_f}{1+sT_f}) * (K_p + \frac{K_i}{s}) \quad (3.13)$$

Therefore, the IAFSC system transfer function $T(s)$ is given by equation 3.14.

$$\frac{P(s)}{F(s)} = T(s) = (\frac{K_f}{1+sT_f}) * (K_p + \frac{K_i}{s}) \quad (3.14)$$

Where $P(s)$ and $F(s)$ are the system output and input signals respectively, $T(s)$ is the system transfer function, K_p , K_i , and K_f are the controller proportional and integral and regulator gains respectively, and T_f is the sampling time.

3.4.2 The IAFSC Controller Parameter Selection and Tuning.

From the knowledge of the characteristics of the proportional and integral gains, their advantages are exploited while taking careful consideration of their disadvantages. Since the proportional gain reduces steady-state error and achieves stable control whereas the integral gain eliminates steady-state error but increases the settling time, let the initial proportional and integral values of the controller be $K_p = 10.0$, and $K_i = 20.0$, $K_f = 1.0$ and a sampling time of $T_f = 7.4074e^{-4}$. The step response of the transfer function was plotted in MATLAB/SIMULINK as shown in Figure 3.11.

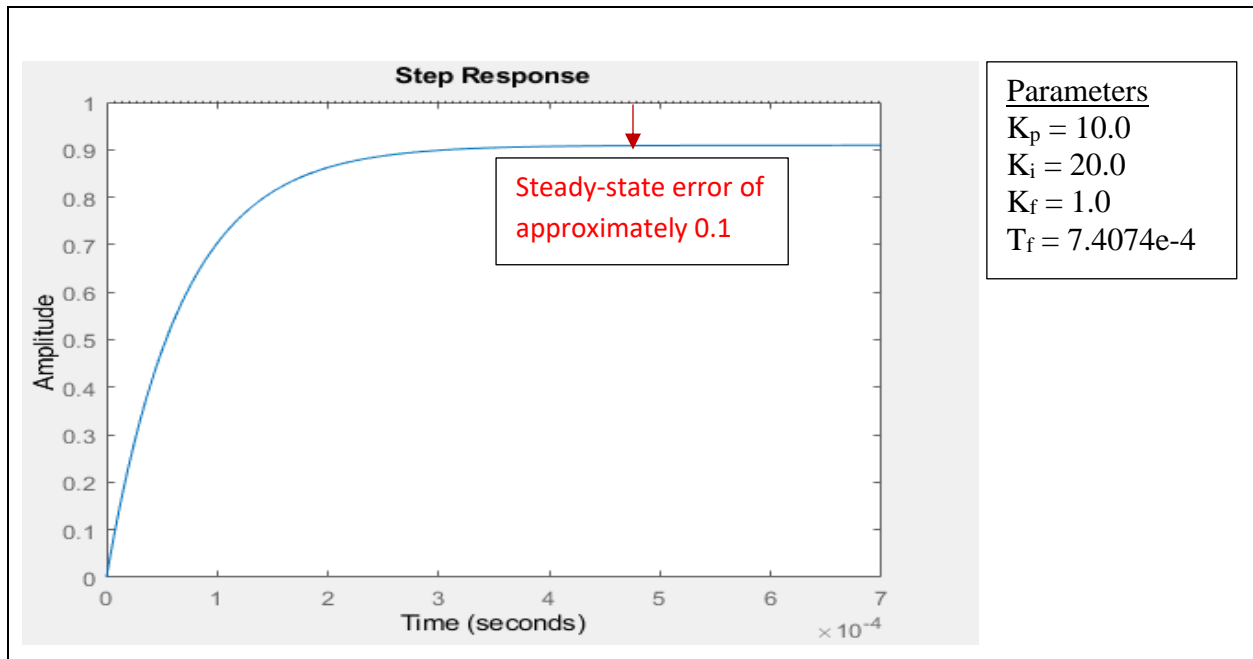


Figure 3.11: Step Response of the PI Controller

It is noted that the step response has a steady-state error of approximately 0.1 as per the graph in Figure 3.11. To further reduce the steady state error and the rise time, the proportional and the integral gains are increased to a value of $K_p = 20.0$ $K_i = 50.0$, and the step response was plotted in MATLAB/SIMULINK. From the graph in Figure 3.12 it can be shown that the steady-state error reduces by approximately 0.05.

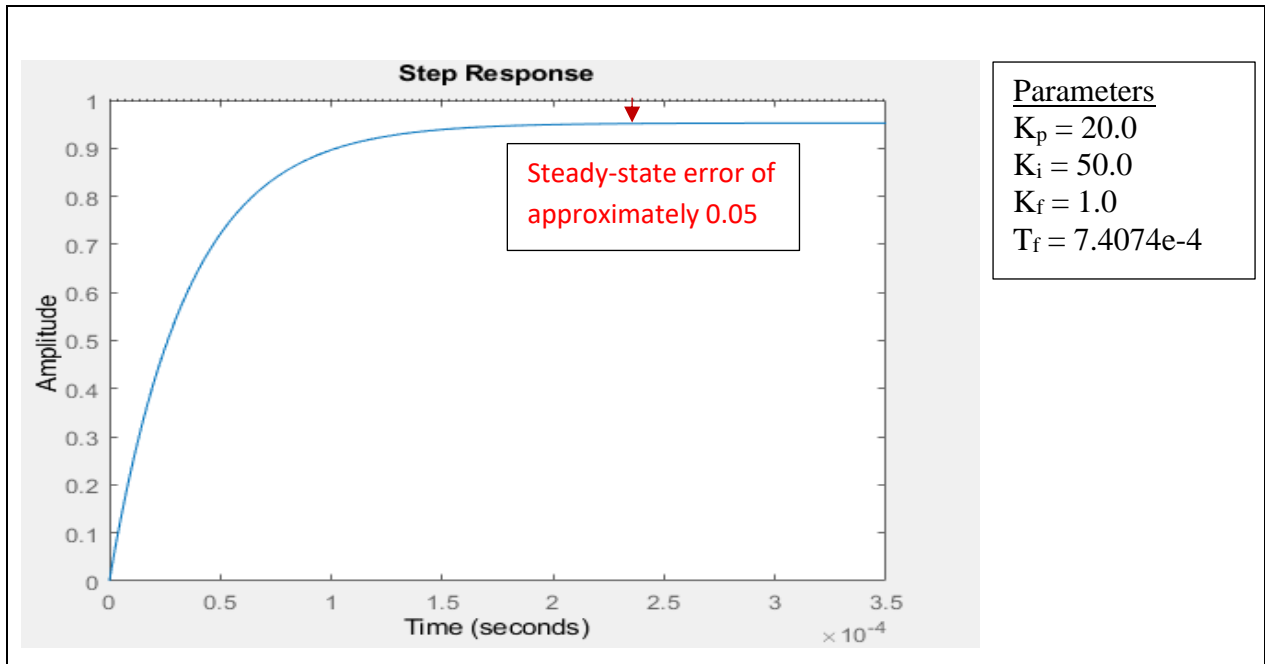


Figure 3.12: Step Response of the PI Controller

To eliminate the steady-state error, the proportional, integral, and conditioning gains are further increased iteratively until the desired response is obtained as shown in Figure 3.14.

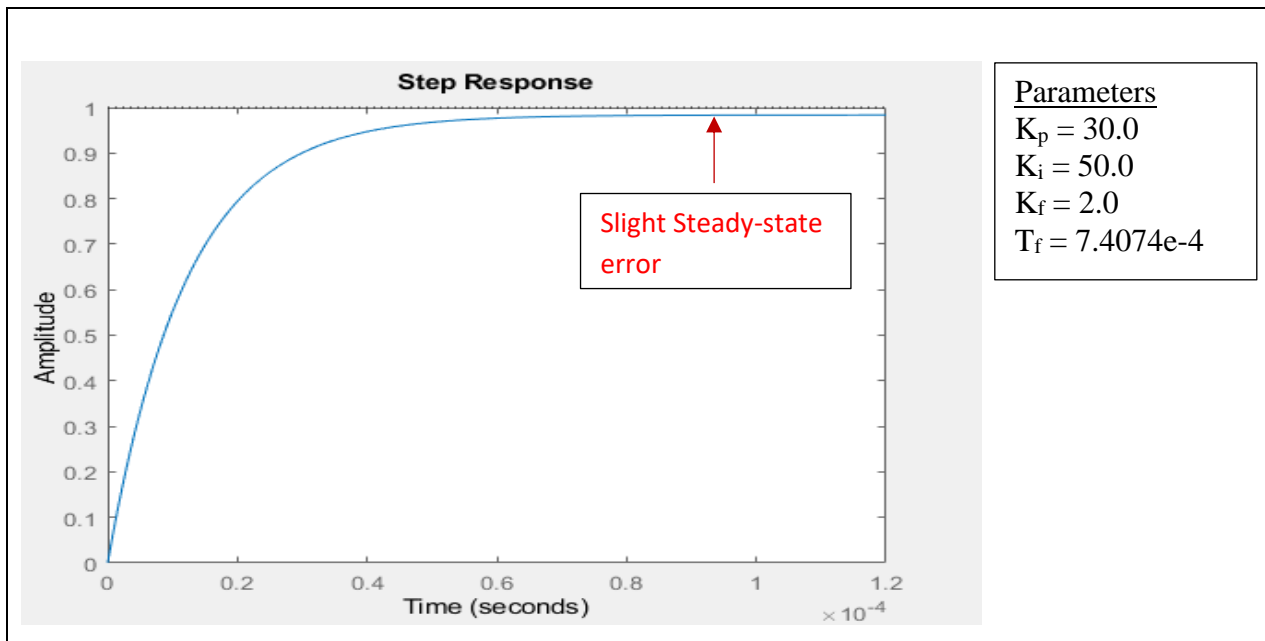


Figure 3.13: Step Response of the PI Controller

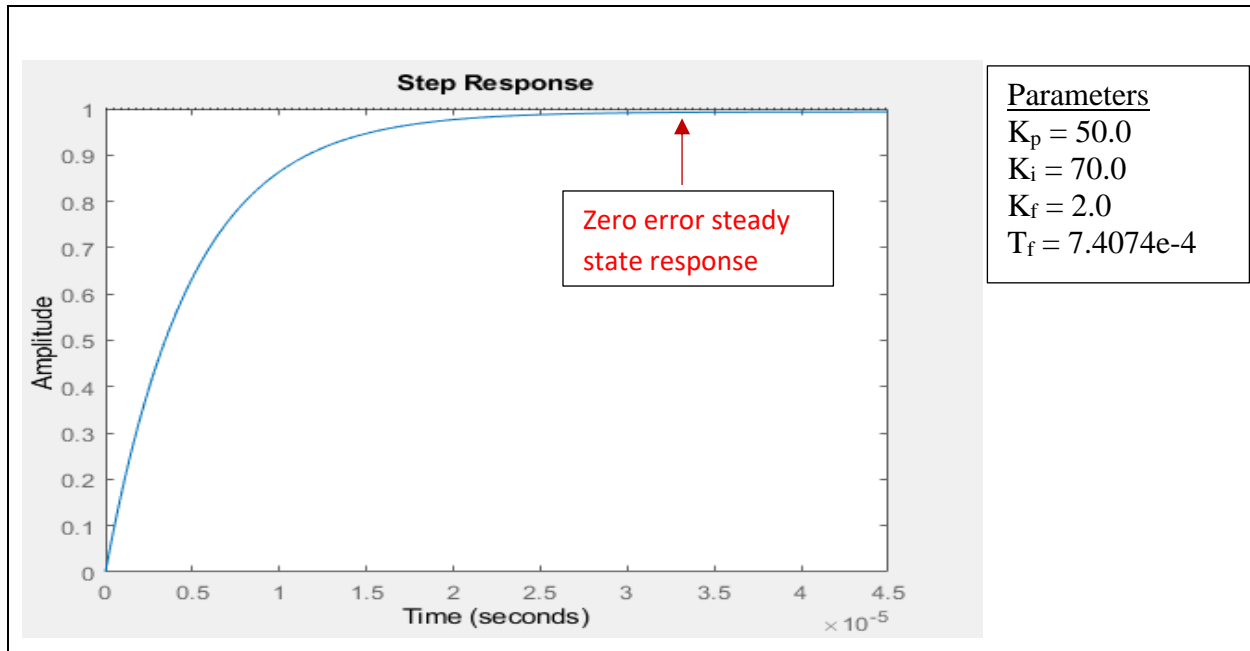


Figure 3.14: Step Response of the PI Controller

The IAFSC controller parameters were thus set to $K_p=50.0$, $K_i=70.0$, $K_f=2.0$, and $T_f= 7.4074e-4$ to achieve the desired system response.

3.4.3 The IAFSC Controller Circuit in MATLAB/SIMULINK.

Figure 3.15 shows the IAFSC controller as implemented on the rectifier side. It measures the real-time frequency of the control area 1. A settable cut-off frequency for the system stability limit is continuously monitored below which the modulated power is reset. The control circuit is comprised of a PMU measurement system that measures the area frequency, the frequency comparator that compares the area frequency and the threshold stability limit, the PI controller, the power modulation logic circuit for release or block signal depending on the area stability, and an oscillography measurement circuit for signal plotting.

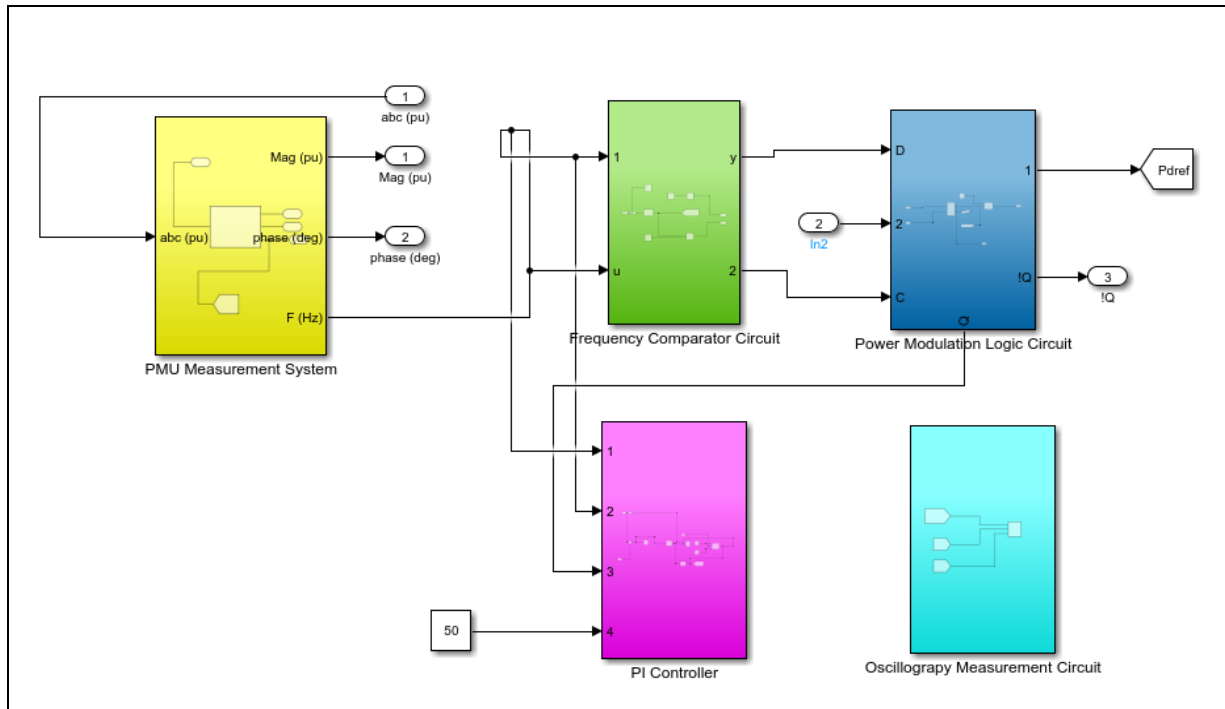


Figure 3.15: The IAFSC Control Circuit for the Rectifier Side

On the inverter AC side, the IAFSC controller equally monitors the real-time frequency of the system and calculates the required regulating power to restore stability during system disturbances. This regulating power is then compared with the system strength on the rectifier side to establish whether it is capable of providing it before the release of the active power ramp-up signal to the rectifier converter. The inverter side supplementary controller is shown in Figure 3.16. It comprises a PMU measurement system, a regulating power calculation circuit, a PI controller, and a power order ramping circuit.

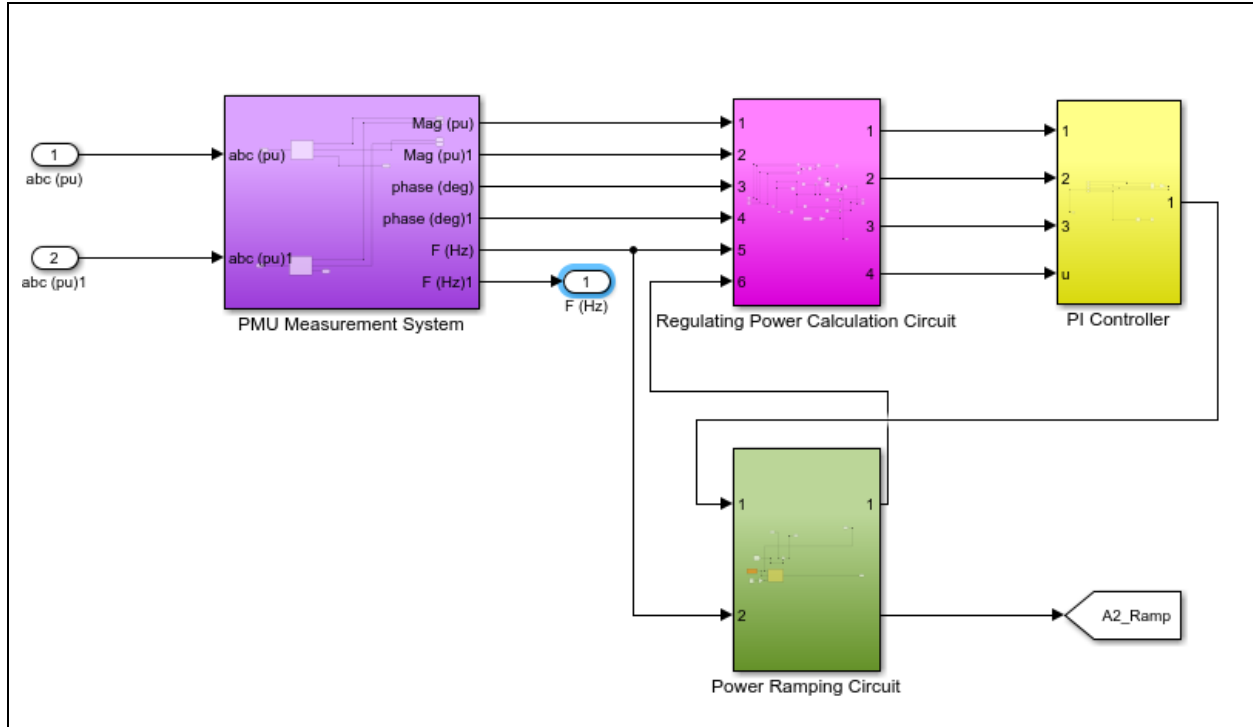


Figure 3.16: The IAFSC Control Circuit for The Inverter Side

3.4.4 Calculation of Regulating Power

To modulate the active power during transient disturbances the VSC-HVDC system achieves this through the IAFSC controller that monitors the system support capability. The change in frequency following the system disturbance is translated to an equivalent step change in power. This is expressed as [36];

$$\Delta P_m = \Delta P_{ref} - \left(\frac{1}{R}\right) * \Delta f \quad (3.15)$$

Where ΔP_m is the step change in power, ΔP_{ref} is the change in generator power reference setting, Δf is the change in system frequency and R is the generator regulating constant. For a fixed generator speed changer setting then $\Delta P_{ref} = 0$. Therefore, equation 3.15 reduces to;

$$\Delta P_m = - \left(\frac{1}{R}\right) * \Delta f \quad (3.16)$$

In an interconnected power system containing n generating units, the step change in power is given by;

$$\Delta P_m = - \left(\frac{1}{R_1} + \frac{1}{R_2} + \frac{1}{R_3} + \dots + \frac{1}{R_n}\right) * \Delta f \quad (3.17)$$

Where R_n is the regulating constant of the n^{th} generating unit. The summation of the reciprocal of the generator regulating constant is known as the Frequency Response Characteristic defined as;

$$\beta = \sum \frac{1}{R_n}; n = 1, 2, 3, \dots n. \quad (3.18)$$

For an interconnected system with n generator units, the change in the output power equation is expressed as;

$$\Delta P_m = -\beta \Delta f \quad (3.19)$$

The generator regulation constants for the Kundur test system are $R1 = 0.05$, $R2 = 0.05$, $R3 = 0.05$, and $R4 = 0.05$. Therefore the step change in power for the test system is expressed as;

$$\Delta P_m = -\left(\frac{1}{0.05} + \frac{1}{0.05}\right) * \Delta f \quad (3.20)$$

$$\Delta P_m = -40.0 \Delta f \quad (3.21)$$

3.4.5 IAFSC Controller Algorithm Flowchart

The IAFSC controller output ensures the stability of the supporting control area whenever the regulating power required to support the faulted control area is beyond its capacity. The algorithm flowchart of the IAFSC controller is shown in Figure 3.17. Through the PMUs on the rectifier and inverter sides, the system frequencies are measured and compared to a settable frequency threshold. On the inverter side, the controller calculates the regulating power required to restore system stability. This is sent as a modulated active power order to the rectifier controls which start to ramp up/down power while monitoring the rectifier system frequency against the threshold setting.

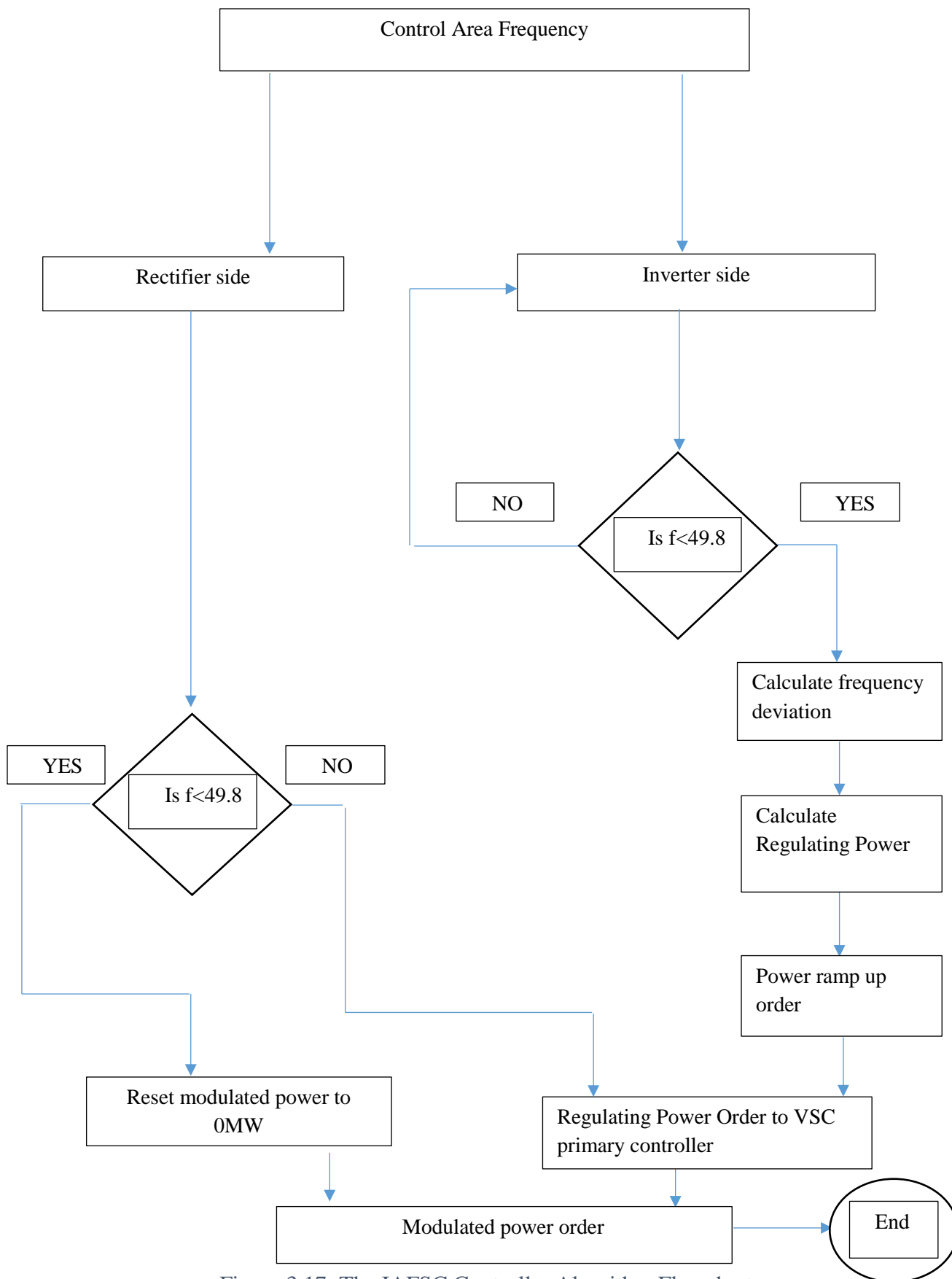


Figure 3.17: The IAFSC Controller Algorithm Flowchart

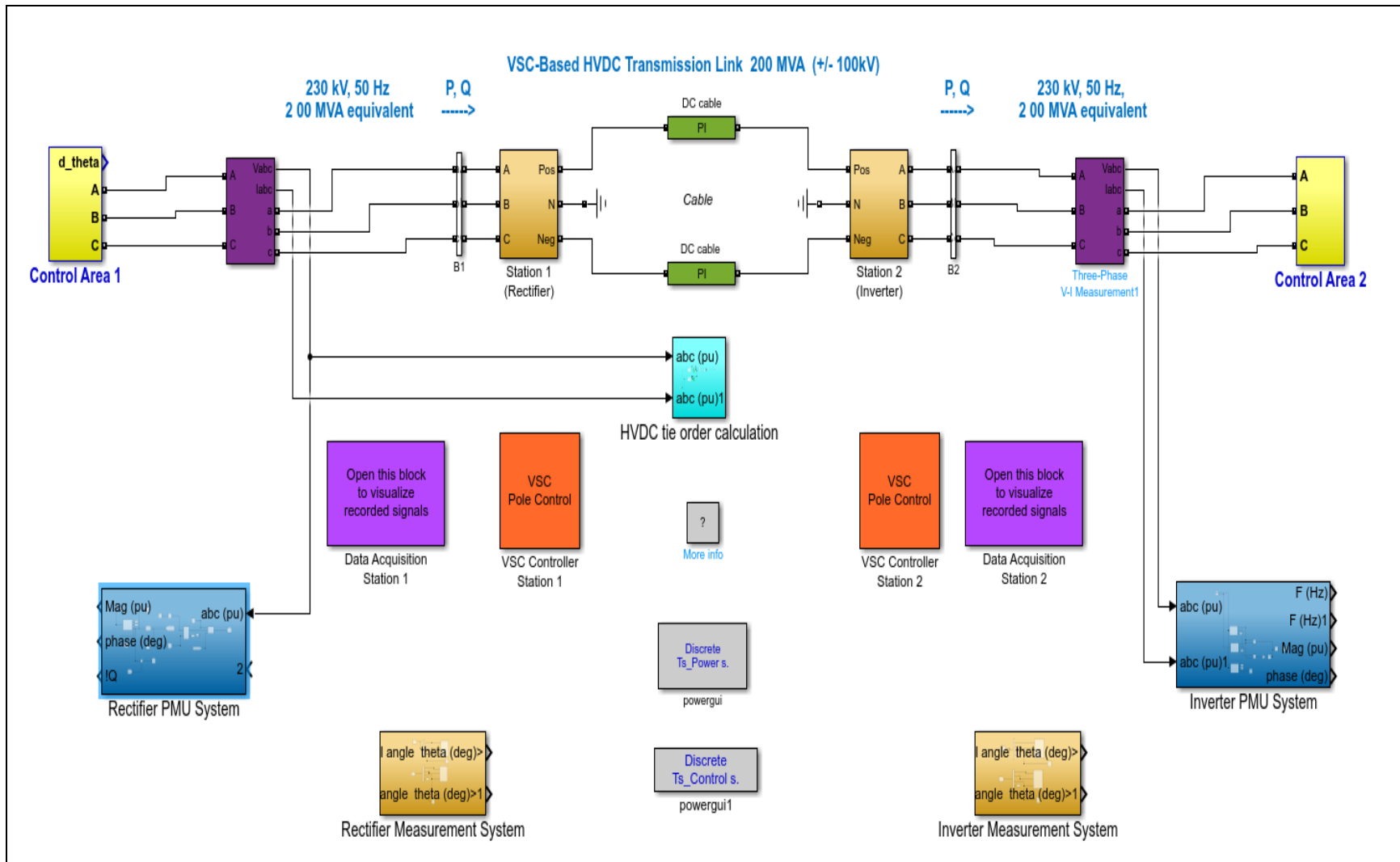


Figure 3.18: The Proposed VSC-HVDC System Design in MATLAB/SIMULINK Software.

3.5 Simulation of Steady State Condition

The steady-state condition was simulated to compare the system response with and without the IAFSC controller as a benchmark for comparison of the system response under transient fault conditions.

3.6 Simulation of Transient Fault

Simulation of transient fault was performed in MATLAB/SIMULINK on control area 2 AC side for two cases, the first case without the IAFSC controller and the second case with the IAFSC controller incorporated in the HVDC controls. A transient fault is performed after 4sec for 100ms and the system response is monitored for the two cases. These are discussed in sections 3.6.1 and 3.6.2.

3.6.1 Simulation Case I

A transient fault simulation was performed in control area 2 after 4 seconds for 100ms which then leads to a 10% loss of generation in this area. This case simulates a transient fault for which control area 1 is capable of providing the required regulating power for control area 2 to recover stability. Given the threshold stability frequency limit of 49.8Hz, a loss of 10% generation in area 2 is assessed mathematically to categorize it as a non-severe fault condition. Equation 3.22 shows the calculation of change in frequency Δf for a total loss of power ΔP_m of 0.1pu. From equation 3.19, the change in frequency is calculated as;

$$\Delta f = - \left(\frac{\Delta P_m}{\beta} \right) \quad (3.22)$$

$$\Delta f = - \left(\frac{0.1}{40} \right) = -2.5e-3 \text{ pu}$$

$$\Delta f = - \left(\frac{0.1}{40} \right) = -2.5e-3 * 50\text{Hz} = -0.125\text{Hz}$$

The final area 2 frequency after the loss of 10% generation is $50\text{Hz} - 0.125\text{Hz} = 49.875\text{Hz}$ which is above the threshold frequency of 49.8Hz and hence is categorized as a non-severe fault condition.

3.6.2 Simulation Case II

A transient fault simulation was performed in control area 2 after 4 seconds for 100ms which then leads to a 25% loss of generation in this area. This case simulates a transient fault for which control area 1 is not capable of providing the required regulating power for control area 2 to recover stability. Given the threshold stability frequency limit of 49.8Hz, a loss of 25% generation in area 2 is assessed mathematically to categorize it as a non-severe fault condition. Equation 3.23 shows the calculation of change in frequency Δf for a total loss of power ΔP_m of 0.25pu. From equation 3.19, the change in frequency is calculated as;

$$\Delta f = - \left(\frac{\Delta P_m}{\beta} \right) \quad (3.23)$$

$$\Delta f = - \left(\frac{0.25}{40} \right) = -6.25e-3 \text{ pu}$$

$$\Delta f = - \left(\frac{0.25}{40} \right) = -6.25e-3 * 50\text{Hz} = -0.3125\text{Hz}$$

The final area 2 frequency after the loss of 25% generation is $50\text{Hz} - 0.3125\text{Hz} = 49.6875\text{Hz}$ which is below the threshold frequency of 49.8Hz and hence is categorized as a severe fault condition.

3.7 Chapter Conclusion

The methodology as discussed was successfully implemented in MATLAB/SIMULINK where simulation of transient faults was performed. The results are discussed in the next chapter for validation of the proposed supplementary controller in improving the transient stability response of interconnected VSC-HVDC systems.

CHAPTER 4

RESULTS AND ANALYSIS

4.1 Introduction

This chapter presents the simulation results done on the Kundur two-area test system interconnected with a VSC-HVDC tie line. The simulations were performed in MATLAB/SIMULINK software as discussed in detail in this chapter. The transient stability responses on the test system with and without the proposed controller are compared to validate the stability improvement of the proposed IAFSC controller.

4.2 Simulation of Steady State Condition

In steady state conditions, the two interconnected areas operate at their nominal frequency of 50Hz. The VSC-HVDC system steady-state condition was simulated to provide the reference system response signals for comparison and validation. Figure 4.1 shows the frequency response of control area one which begins with spikes due to initial switching and finally settles at 50Hz after approximately 2 seconds.

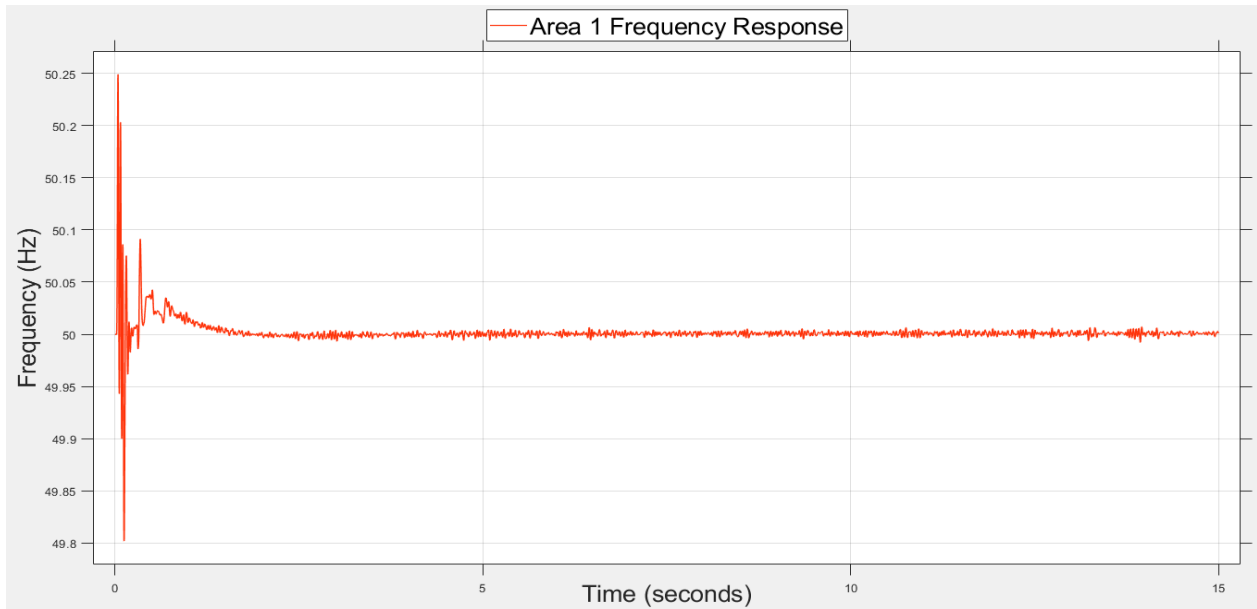


Figure 4.1: Area 1 Frequency Response

Figure 4.2 shows the steady-state frequency response of control area two which begins with spikes due to initial switching and finally settles at 50Hz after approximately 2 seconds.

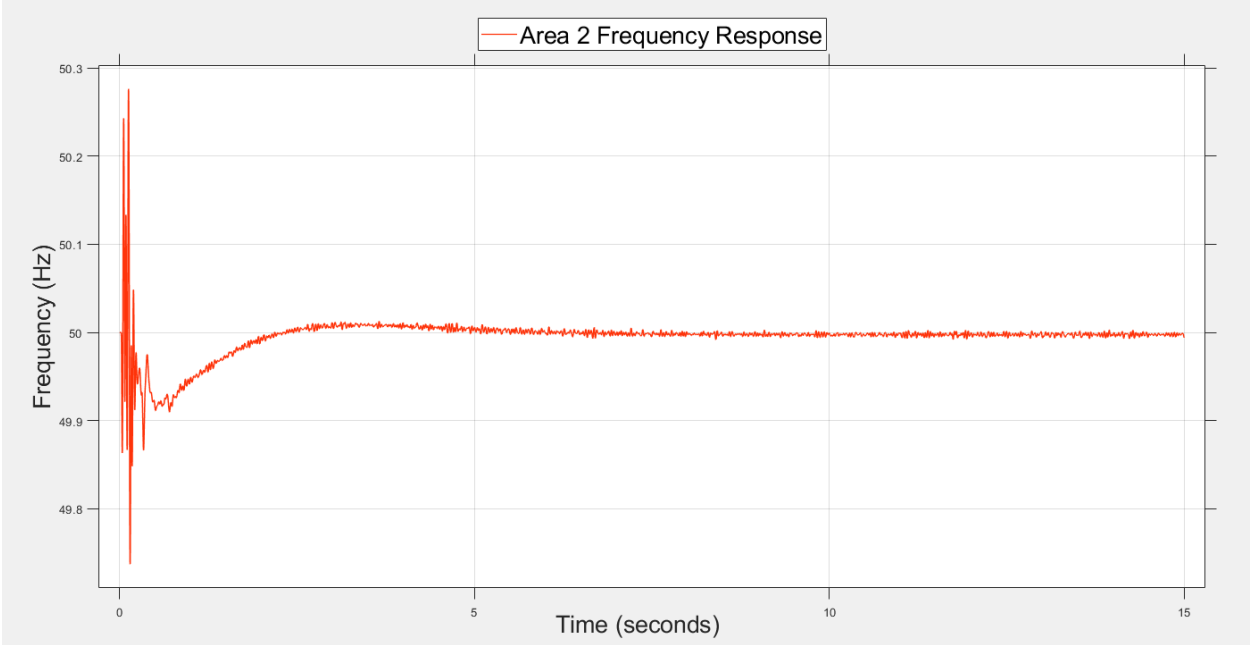


Figure 4.2: Area 2 Frequency Response

Figure 4.3 shows the steady-state rotor speed deviation of control area one which begins with spikes due to initial switching and finally settles at zero (0) per unit.

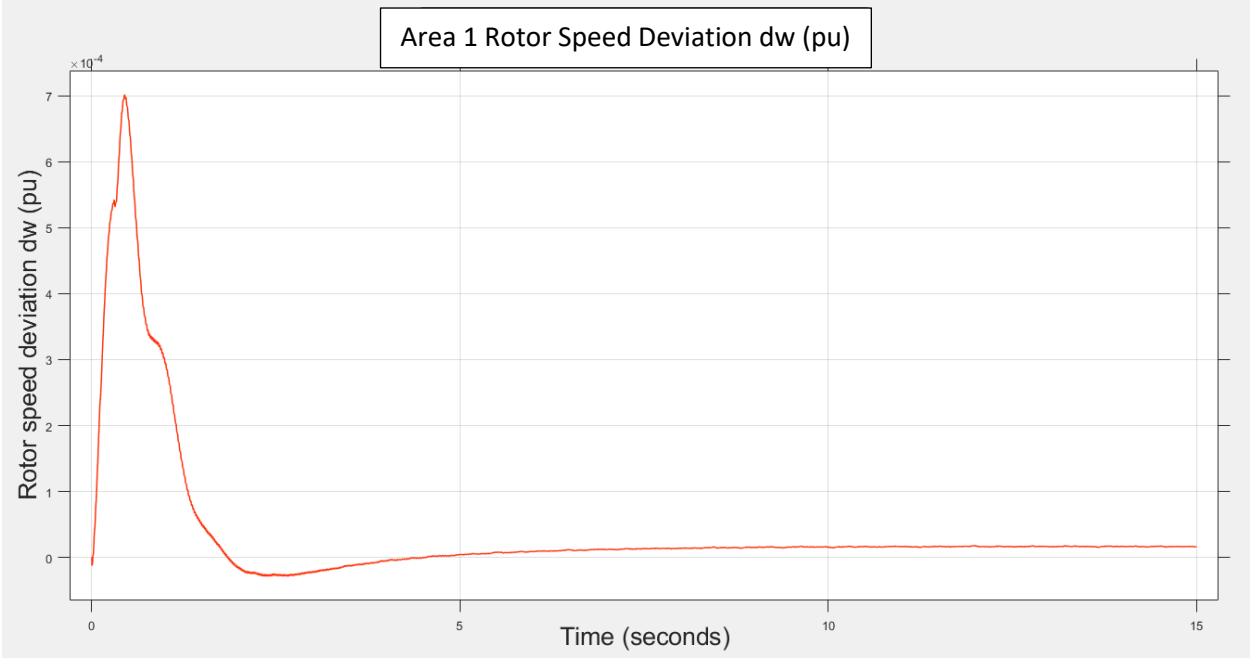


Figure 4.3: Area 1 Rotor Speed Deviation Response

Figure 4.4 shows the steady-state rotor speed deviation of control area two which begins with spikes due to initial switching and finally settles at zero (0) per unit.

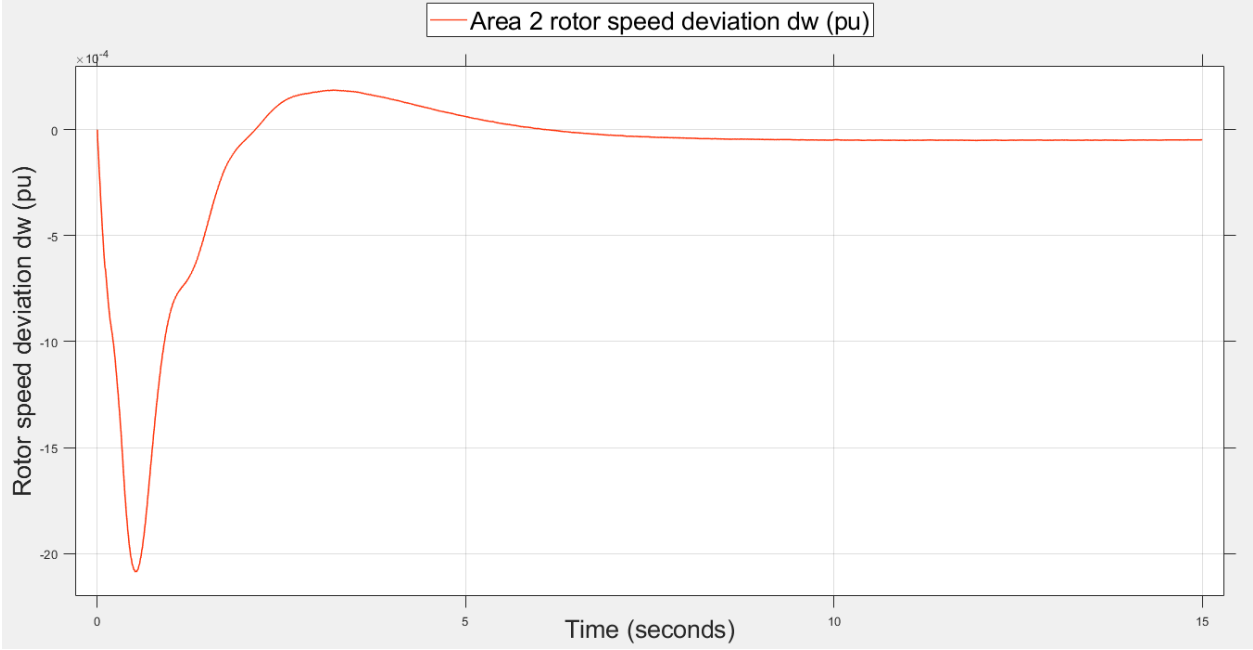


Figure 4.4: Area 2 Rotor Speed Deviation Response

Figure 4.5 shows the steady-state HVDC tie power order from control area one of which also begins with spikes due to initial switching and finally settles.

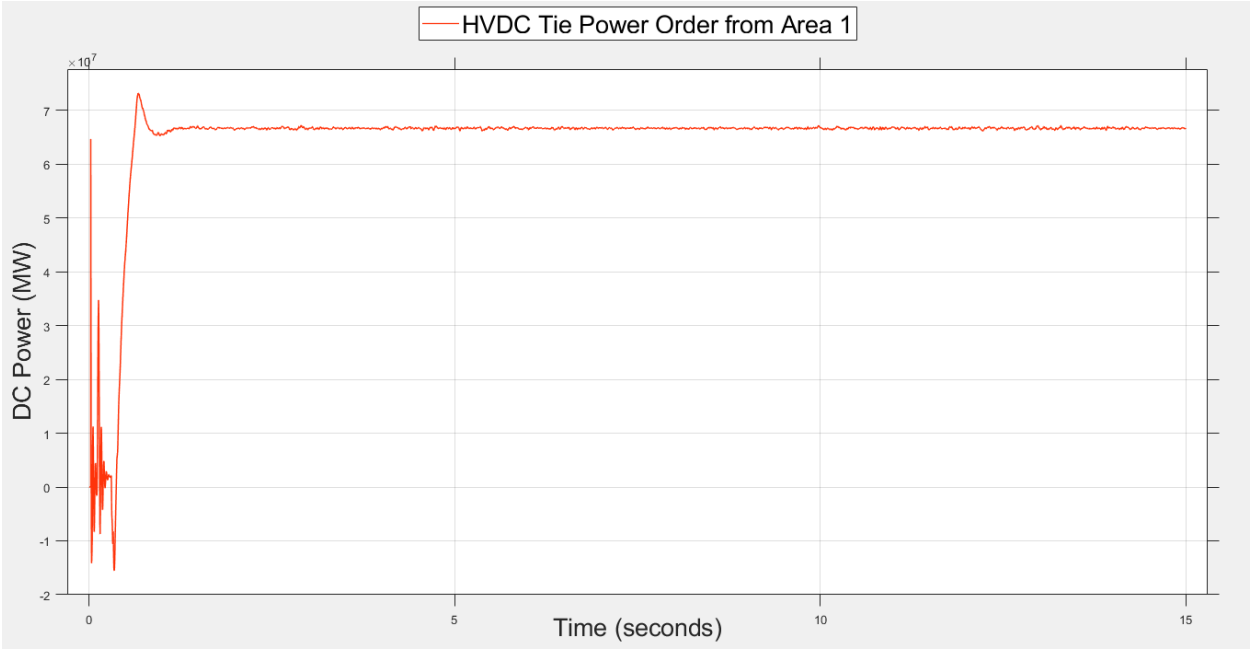


Figure 4.5: HVDC Tie Order Power from Area 1

Figure 4.6 shows control area one generation at steady-state conditions.

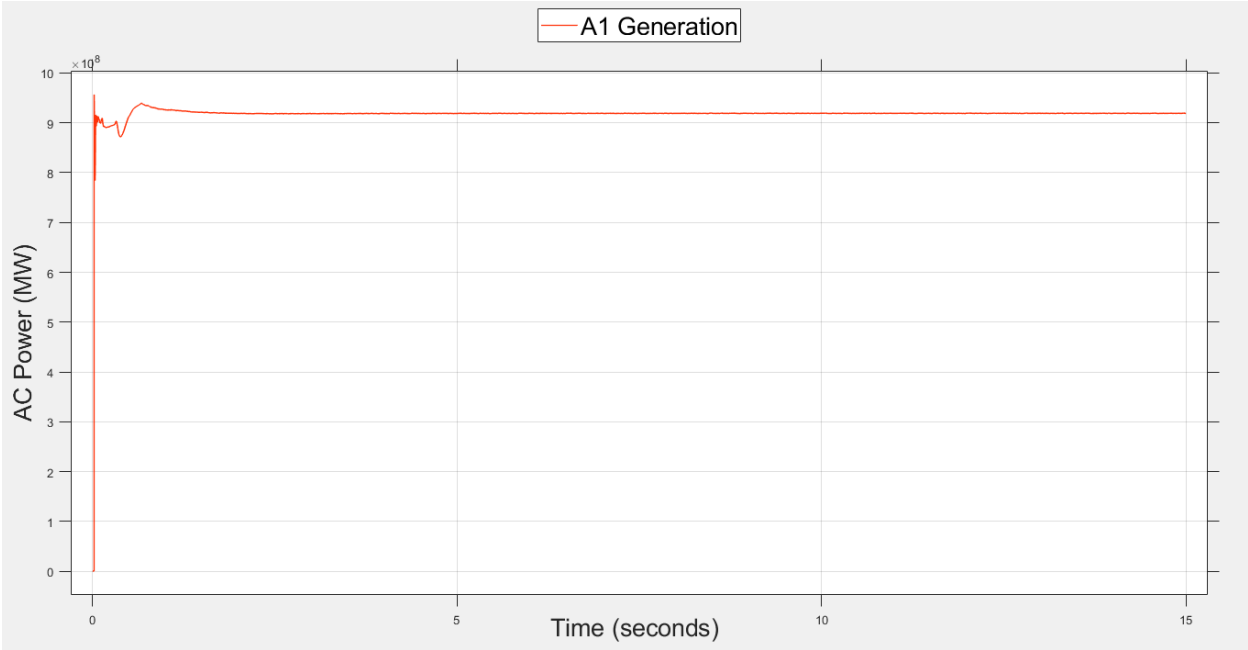


Figure 4.6: Area 1 Generation

Figure 4.7 shows control area two generation at steady-state conditions.

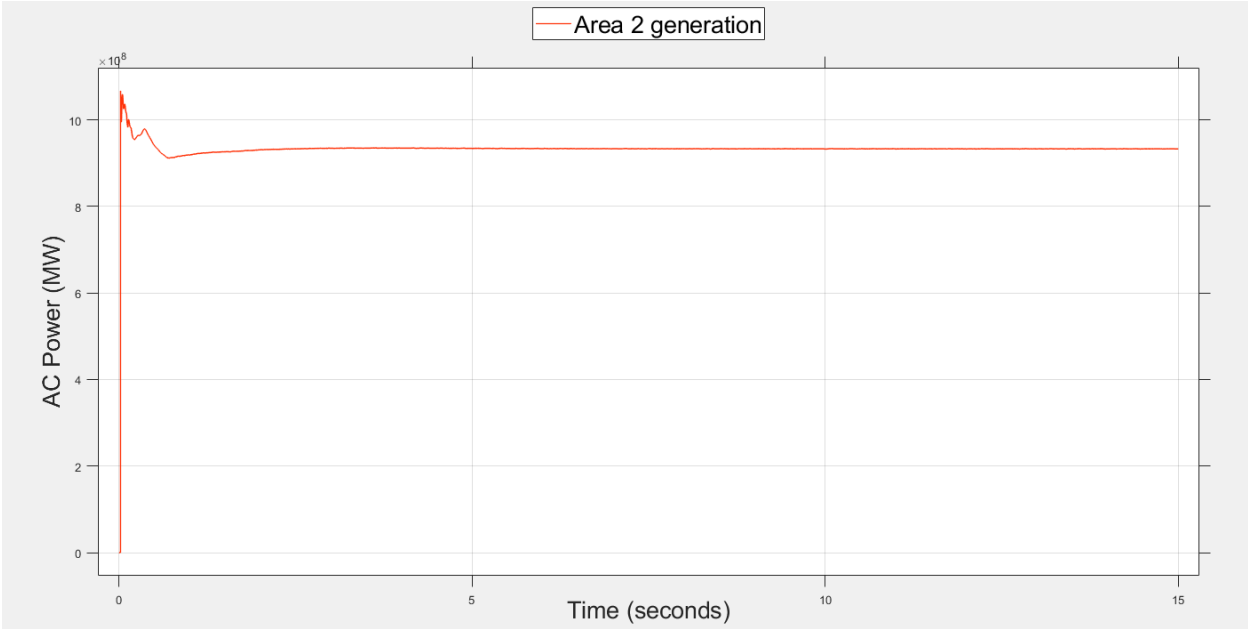


Figure 4.7: Area 2 Generation

4.3 Case I Fault Condition

Case I transient fault condition simulation in control area 2 leads to a 10% loss of generation in this area. This case simulates a transient fault for which control area 1 is capable of providing the required regulating power for control area 2 to recover stable condition.

4.3.1 Case I Fault without IAFSC Controller

Figures 4.8, 4.9, 4.10, 4.11, 4.12, 4.13, and 4.14 show the system responses without the IAFSC controller (typical of the traditional system) following the fault simulation in control area 2. Figure 4.8 shows the control area 1 frequency response which slightly lowers down after the fault (but not below the stability limit) when providing the regulating power to control area 2. Control area 1 is thus capable of providing the required regulating power to control area 2 without deviating much from its nominal state as the fault is not severe. The traditional HVDC controls can thus effectively modulate the active power required by control area 2 without affecting control area 1 stability.

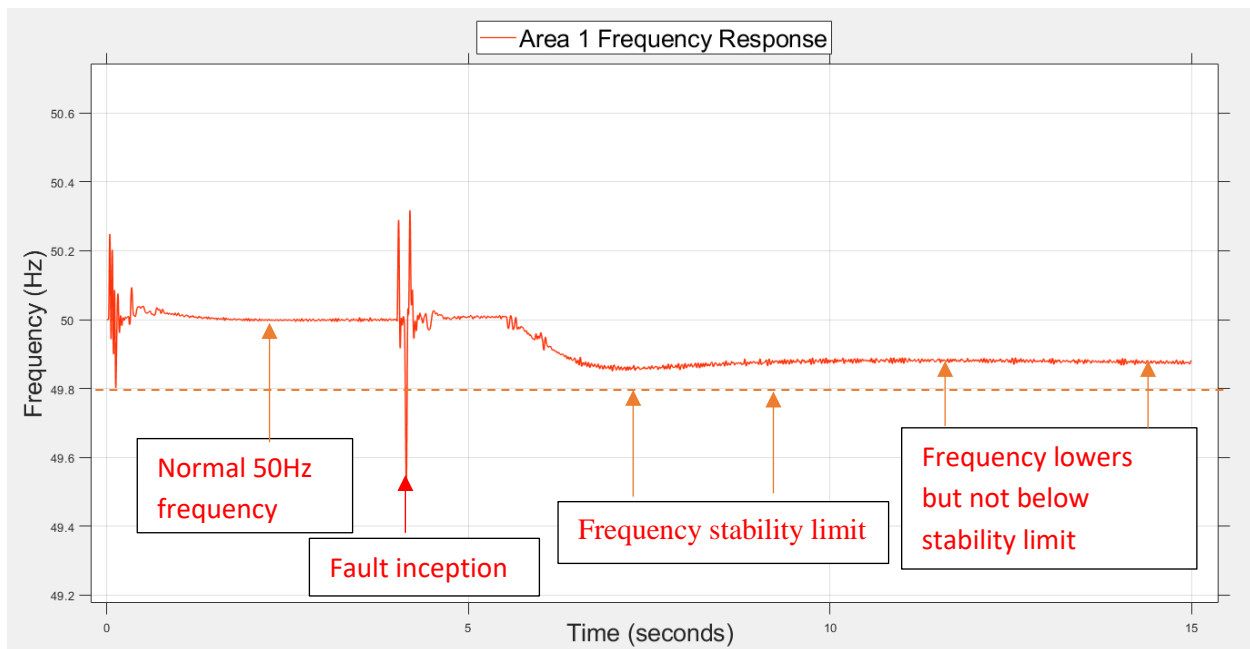


Figure 4.8: Case I Fault Area 1 Frequency Response without IAFSC Controller

Figure 4.9 shows control area 2 frequency response. Immediately after the fault, its frequency starts to lower almost approaching the stability limit line. Then the traditional HVDC controller ramps up DC power to support control area 2. As a result, area 2 recovers stable conditions. The fault is not severe enough to cause unstable conditions in control area 1 hence the action of the traditional controls does not affect control area 1 operating conditions.

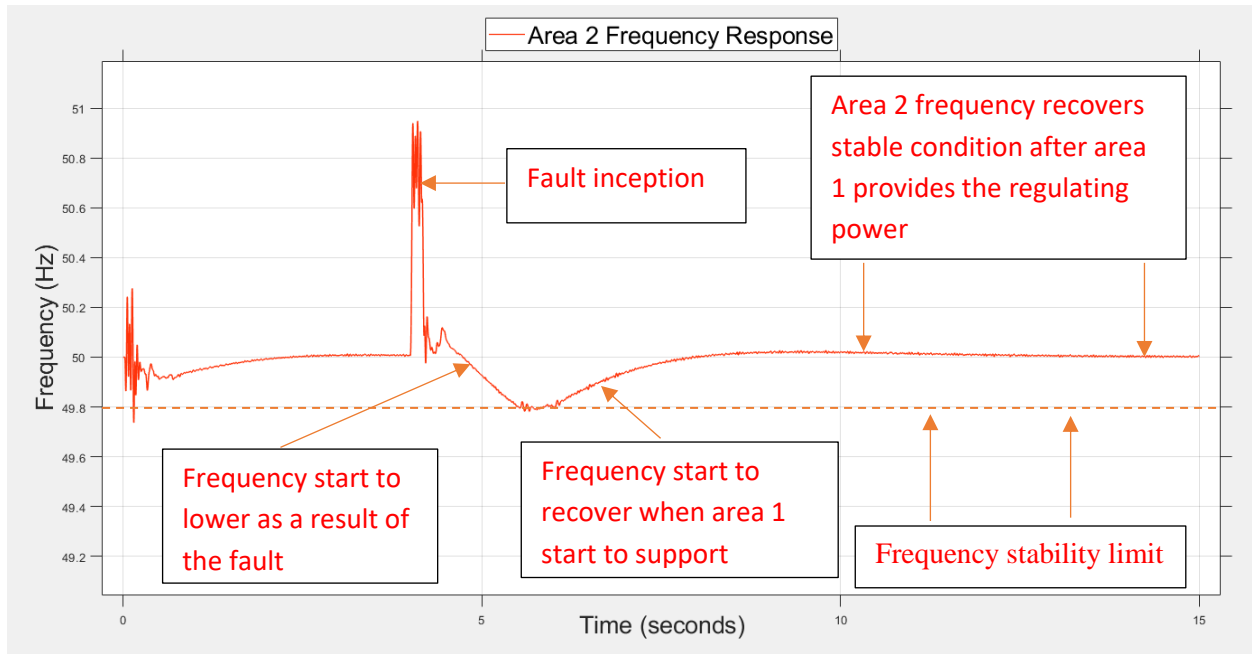


Figure 4.9: Case I Fault Area 2 Frequency Response without IAFSC Controller

Figure 4.10 shows control area 1 rotor speed deviation which reduces by approximately 2.5pu after providing the required regulating power to control area 2. The deviation is not significant to cause unstable conditions since the fault is not severe. This shows that control area 1 was strong enough to support control area 2 following the transient fault and hence the traditional HVDC controls can effectively modulate the active power without affecting control area 1.

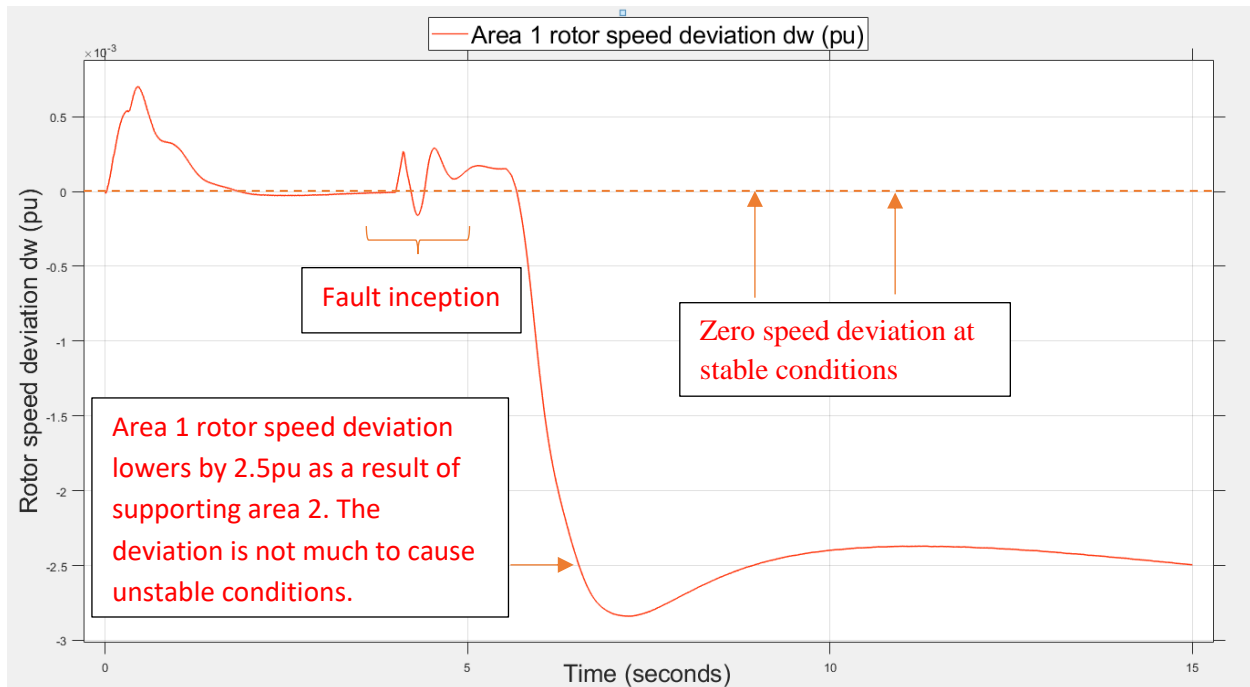


Figure 4.10: Case I Fault Area 1 Rotor Speed Deviation Response without IAFSC Controller

Figure 4.11 shows control area 2 rotor speed deviation which reduces by approximately 4.5pu after the occurrence of the transient fault. However, it recovers stable conditions when control area 1 provides the regulating power by modulating the active power.

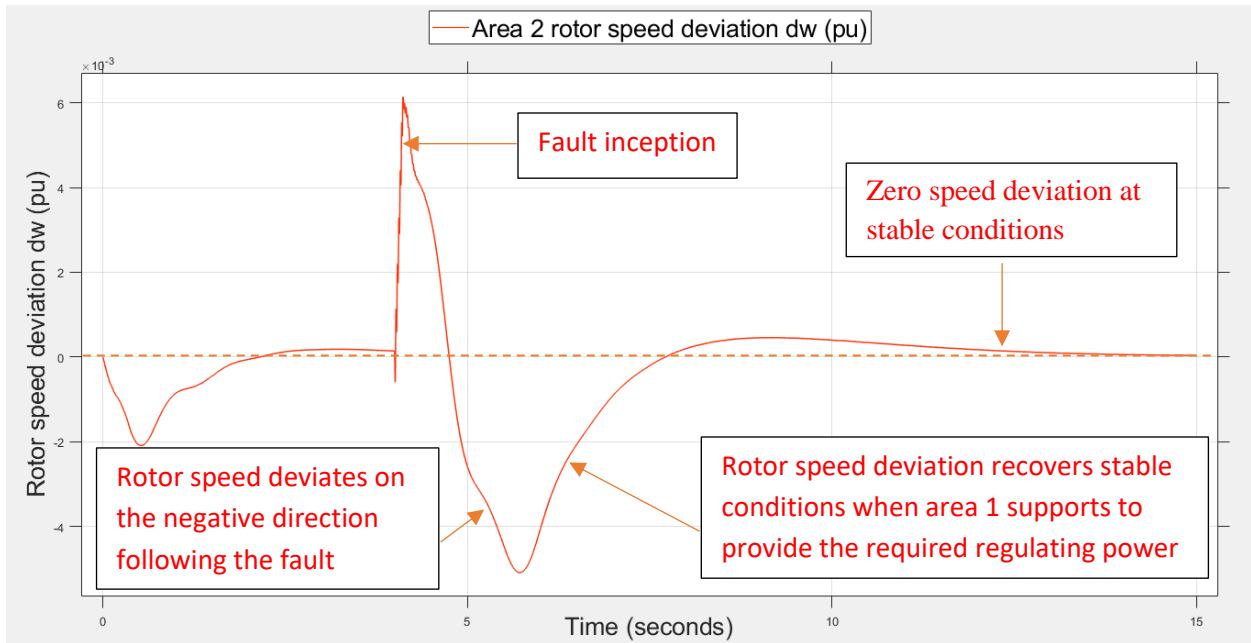


Figure 4.11: Case I Fault Area 2 Rotor Speed Deviation Response without IAFSC Controller

Figure 4.12 shows the HVDC tie power order from control area 1. After the occurrence of the fault, the traditional HVDC controls order control area 1 to ramp up power to provide the regulating power to control area 2 to support its recovery of stable conditions.

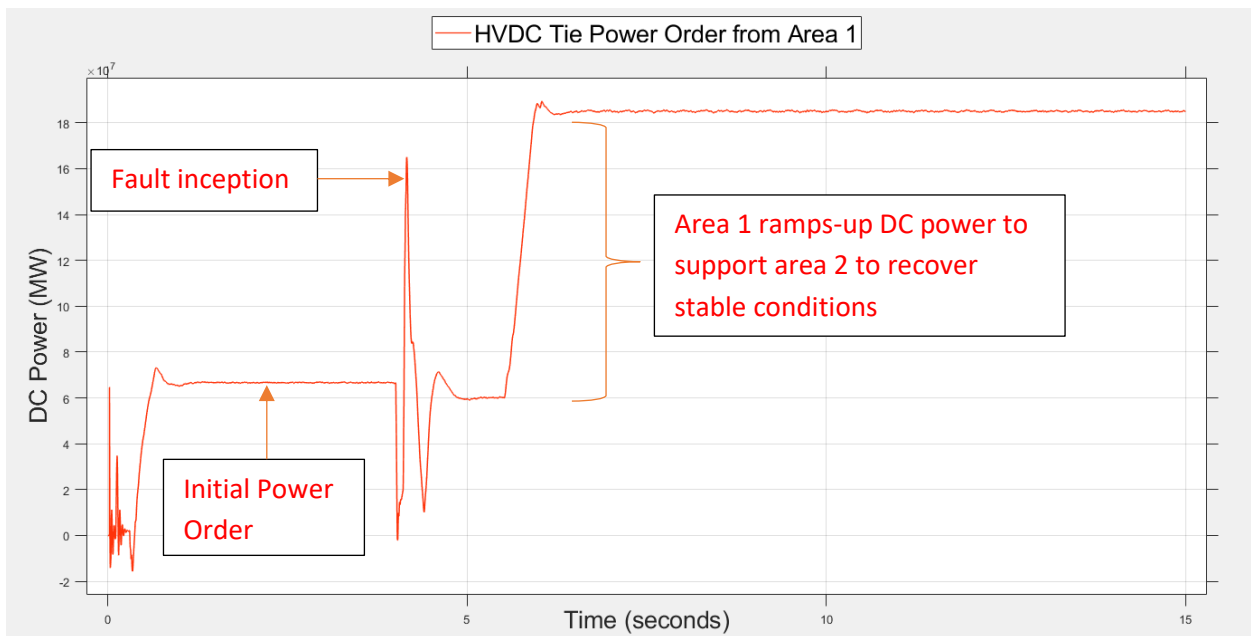


Figure 4.12: Case I Fault HVDC Tie Power Order from Area 1 without IAFSC Controller

Figure 4.13 shows a ramp-up of control area 1 generation as a result of the VSC-HVDC power modulation request by the traditional HVDC controller to support control area 2 that lost generation due to the transient fault.

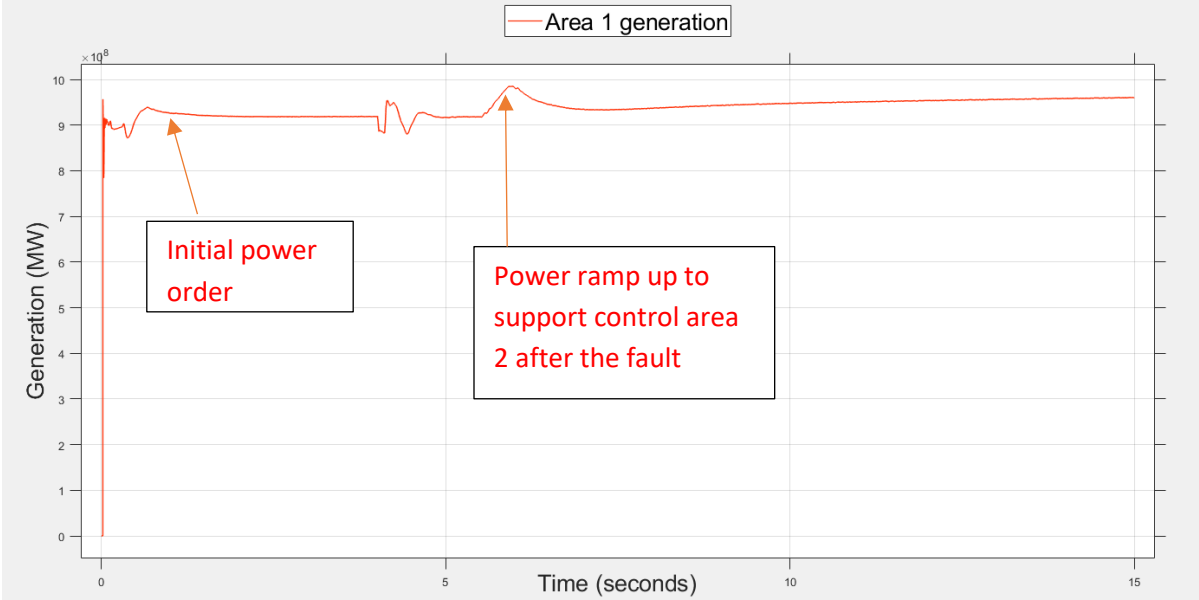


Figure 4.13: Case 1 Fault Area 1 Generation without IAFSC Controller

Figure 4.14 shows control area 2 generation reduction as a result of loss of generation caused by the transient fault. The deficit regulating power was provided by control area 1.

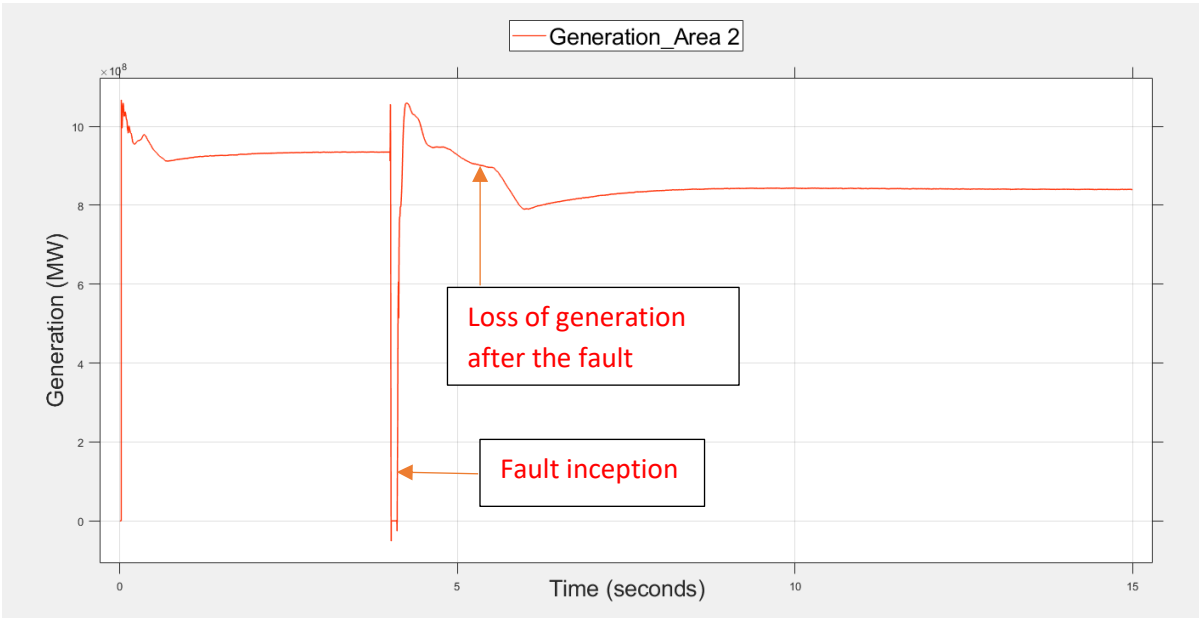


Figure 4.14: Area 2 Generation

Results Interpretation

Since the fault condition in control area 2 was not severe enough to cause unstable conditions in control area 1, the traditional HVDC controller effectively modulated the active power to support control area 2 to recover stable conditions. As long as the operational limits are not violated, the traditional controller will work effectively. However, this will not be the case for severe faults, the very reason for the proposed IAFSC controller in this thesis.

4.3.2 Case I Fault with IAFSC Controller

Figures 4.15, 4.16, 4.17, 4.18, 4.19, 4.20, and 4.21 show the system responses with the IAFSC controller incorporated. As shown in Figure 4.15, control area 1 frequency slightly decreases. From this response, it is noted that control area 1 was capable of providing the regulating power following the fault in control area 2 without violating its frequency stability limit set at 49.8Hz (according to the recommendation of the EAPP interconnection code). Therefore, the IAFSC controller effectively modulated the power order from control area 1 in response to the fault in control area 2 to assist in its recovery of stable conditions.

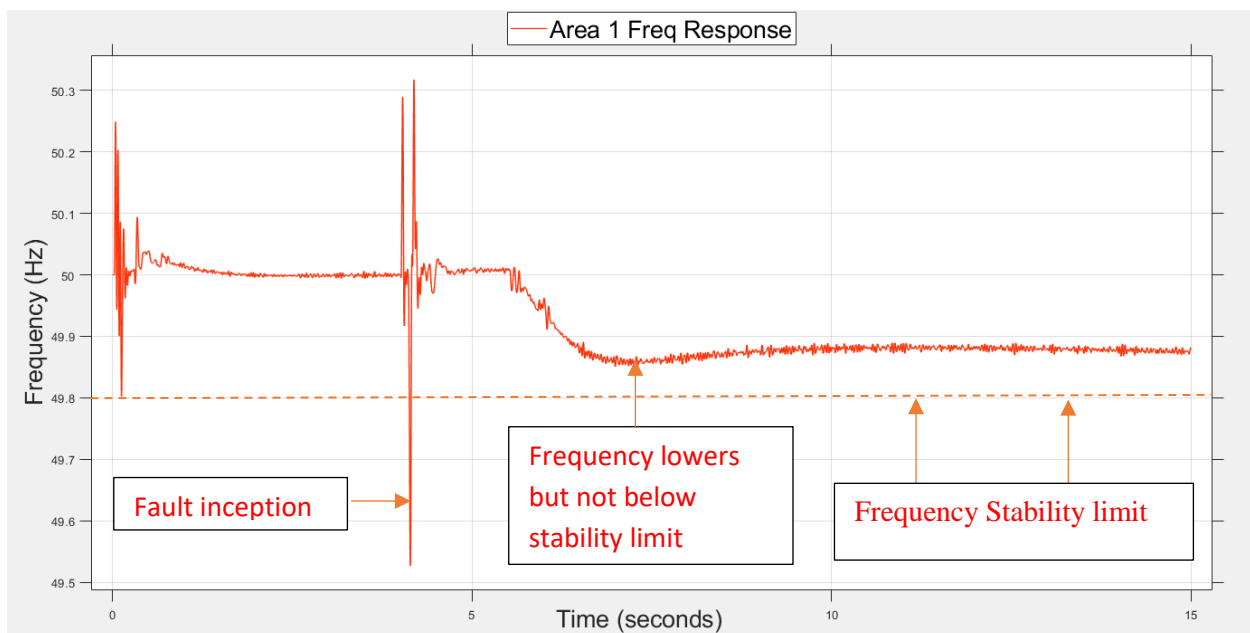


Figure 4.15: Case I Area 1 Frequency Response with IAFSC Controller

Figure 4.16 shows control area 2 frequency response. Immediately after the fault, its frequency lowers almost approaching the stability limit line. The IAFSC controller ramps up DC power to support control area 2. As a result, control area 2 recovers stable conditions.

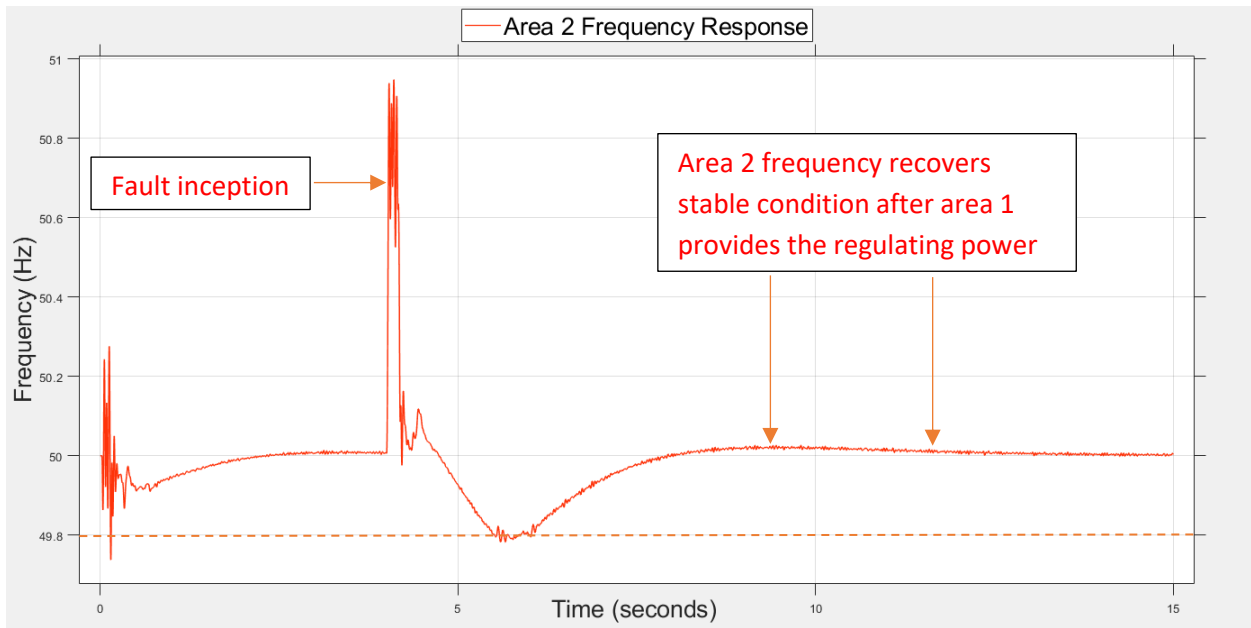


Figure 4.16: Case I Fault Area 2 Frequency Response with IAFSC Controller

Figure 4.17 shows control area 1 rotor speed deviation which reduces by approximately 2.5pu when providing the regulating power to control area 2. The deviation is not significant to cause unstable conditions. This shows that control area 1 was strong enough to support control area 2 following the transient fault.

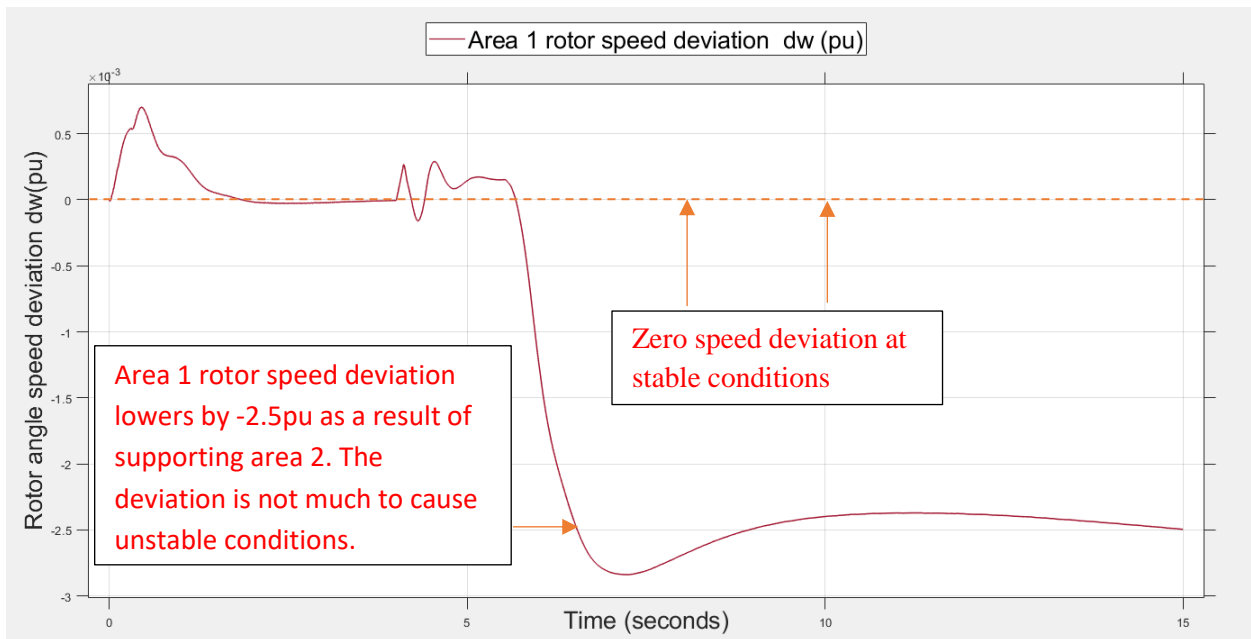


Figure 4.17: Case I Fault Area 1 Rotor Speed Deviation Response with IAFSC Controller

Figure 4.18 shows control area 2 rotor speed deviation which reduces by approximately 4.5pu after the occurrence of the transient fault. However, it recovers stability conditions when area 1 provides the regulating power through the active power modulation by the IAFSC controller.

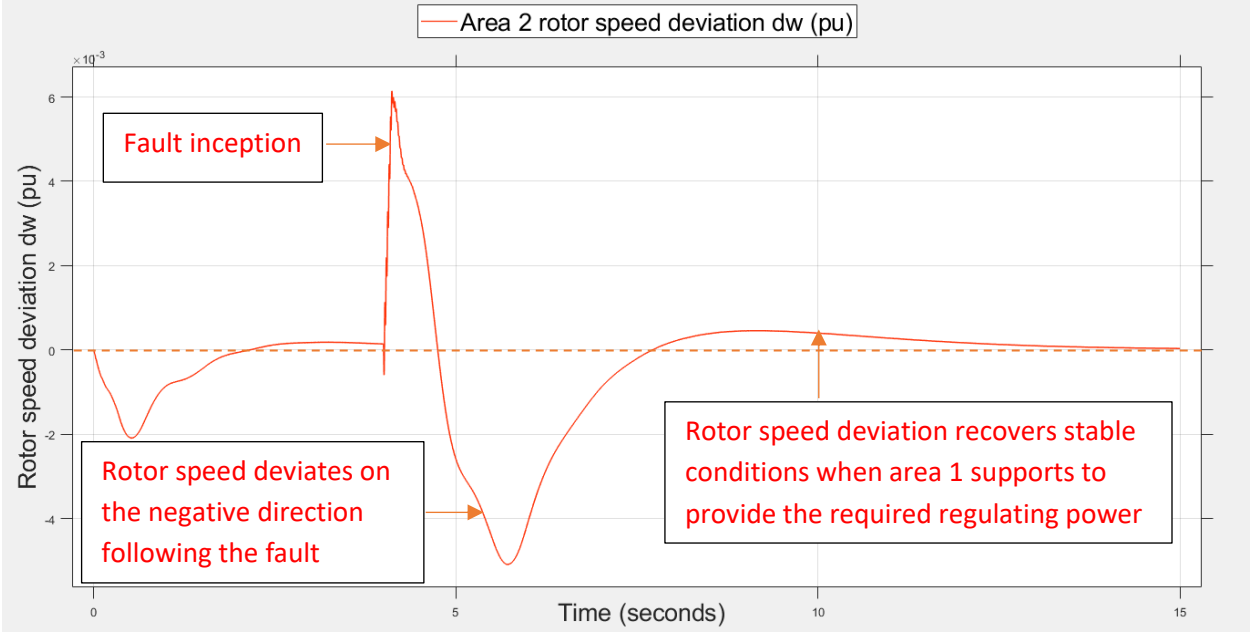


Figure 4.18: Case I Fault Area 2 Rotor Speed Deviation Response with IAFSC Controller

Figure 4.19 shows the HVDC tie power order from control area 1. After the occurrence of the fault, the IAFSC controller orders control area 1 to ramp up power to support control area 2 to recover stable conditions.

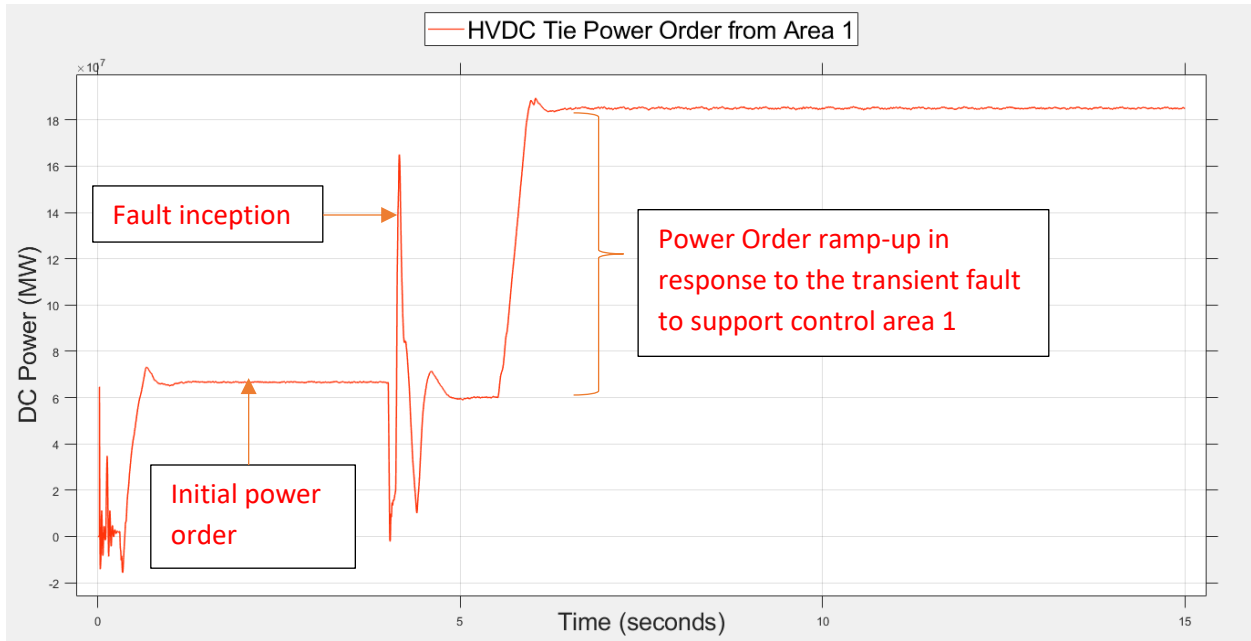


Figure 4.19: Case I Fault HVDC Tie Power Order from Area 1 with IAFSC Controller

Figure 4.20 shows a ramp-up of control area 1 generation as a result of the VSC-HVDC power modulation request by the IAFSC controller to support control area 2 that lost generation due to the transient fault.

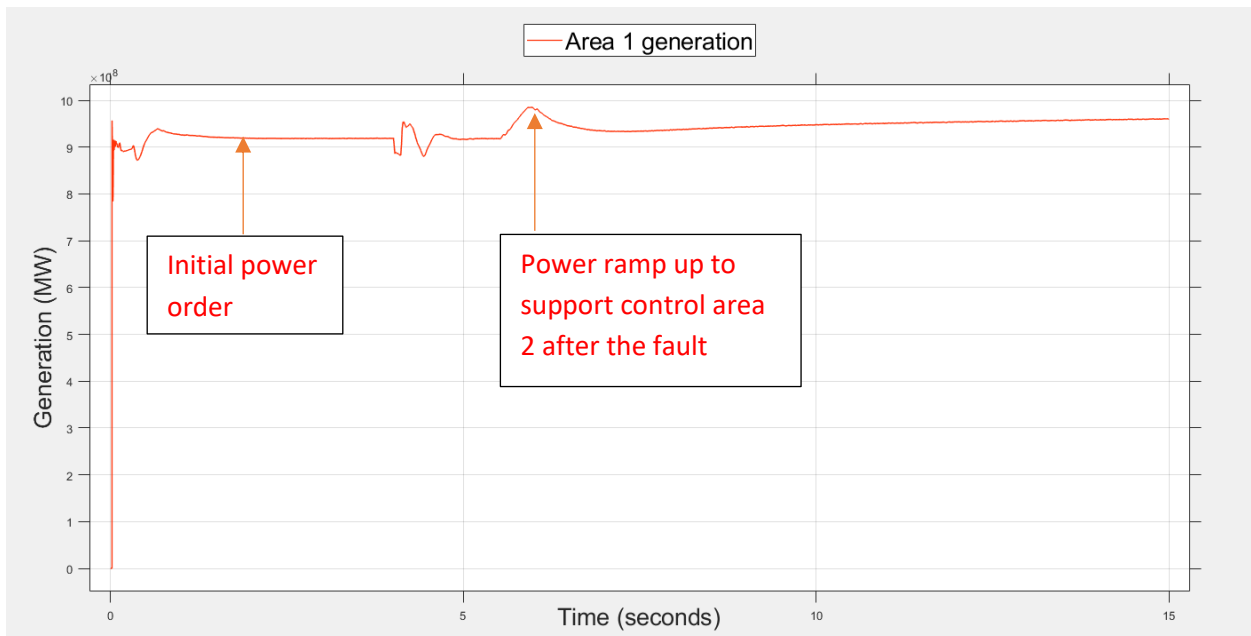


Figure 4.20: Case I Fault Area 1 Generation with IAFSC Controller

Figure 4.21 shows control area 2 generation reduction as a result of loss of generation caused by the transient fault.

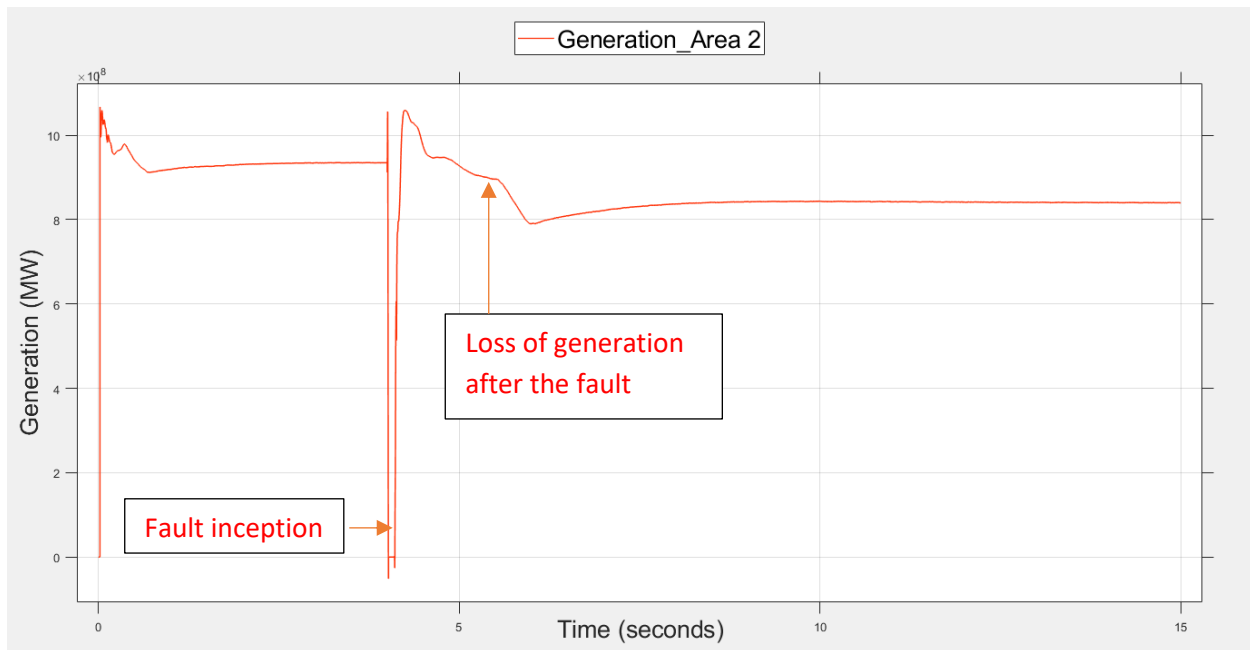


Figure 4.21: Case I Fault Area 2 Generation with IAFSC Controller

Results Interpretation

Since the fault condition in control area 2 was not severe enough to cause unstable conditions in control area 1, the IAFSC controller effectively modulated the active power to support control area 2 to recover stable conditions. As long as the operational limits are not violated, the IAFSC controller will also allow power modulation to assist the faulted control area.

4.4 Case II Fault Condition

Case II transient fault simulation in control area 2 leads to a 25% loss of generation in this area. This case simulates a transient fault for which control area 1 is not capable of providing the required regulating power (considering its stability frequency limit) to assist control area 2 in recovering stability.

4.4.1 Case II Fault without IAFSC Controller

Figures 4.22, 4.23, 4.24, 4.25, 4.26, and 5.27 show the system responses without the IAFSC controller. As shown in Figure 4.22 without the IAFSC controller, the frequency response of area

1 deteriorates significantly, characterized by frequency oscillations. The system response in this case is the typical conventional system that never checks the system strength of the supporting control area. The traditional HVDC control system continues to ramp up HVDC power despite causing unstable conditions in control area 1. As a result, control area 2 as shown in Figure 4.23 recovers stability but at the expense of control area 1 stability. This brings in the essence of the IAFSC controller as proposed and discussed in this thesis for transient stability improvement.

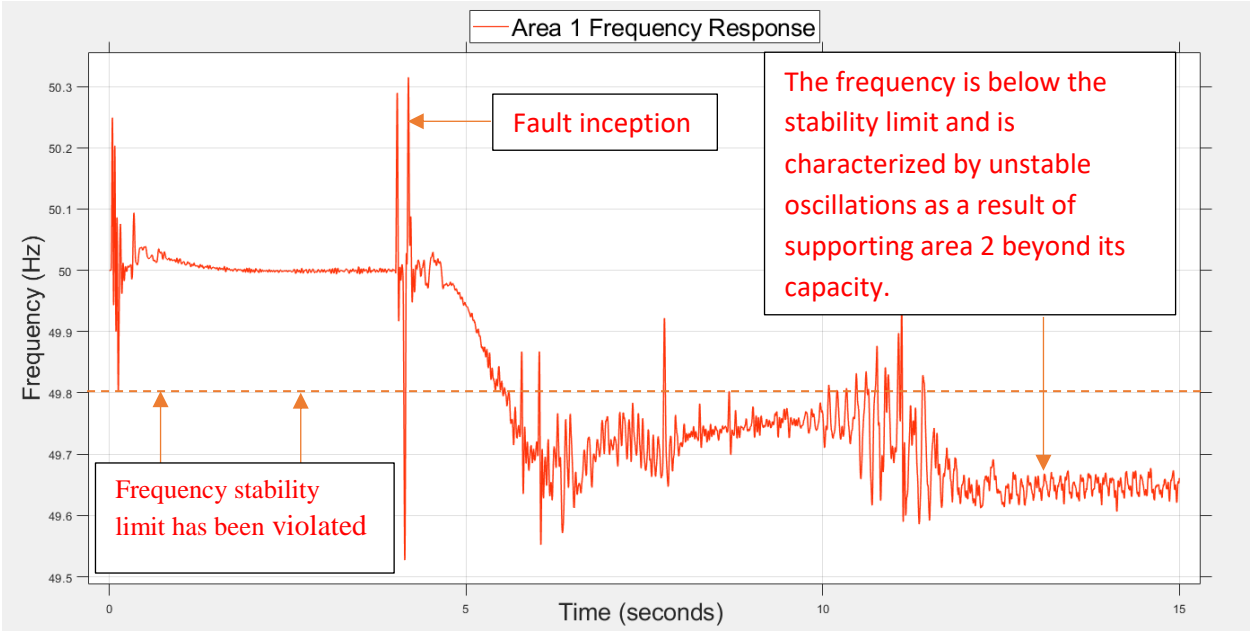


Figure 4.22: Area 1 Frequency Response without IAFSC Controller

Figure 4.23 shows control area 2 frequency response as a result of a severe fault that causes unstable conditions. Without checking the capacity of control area 1 the traditional HVDC ramps up DC power to support control area 2 at the expense of control area 1 stable conditions.

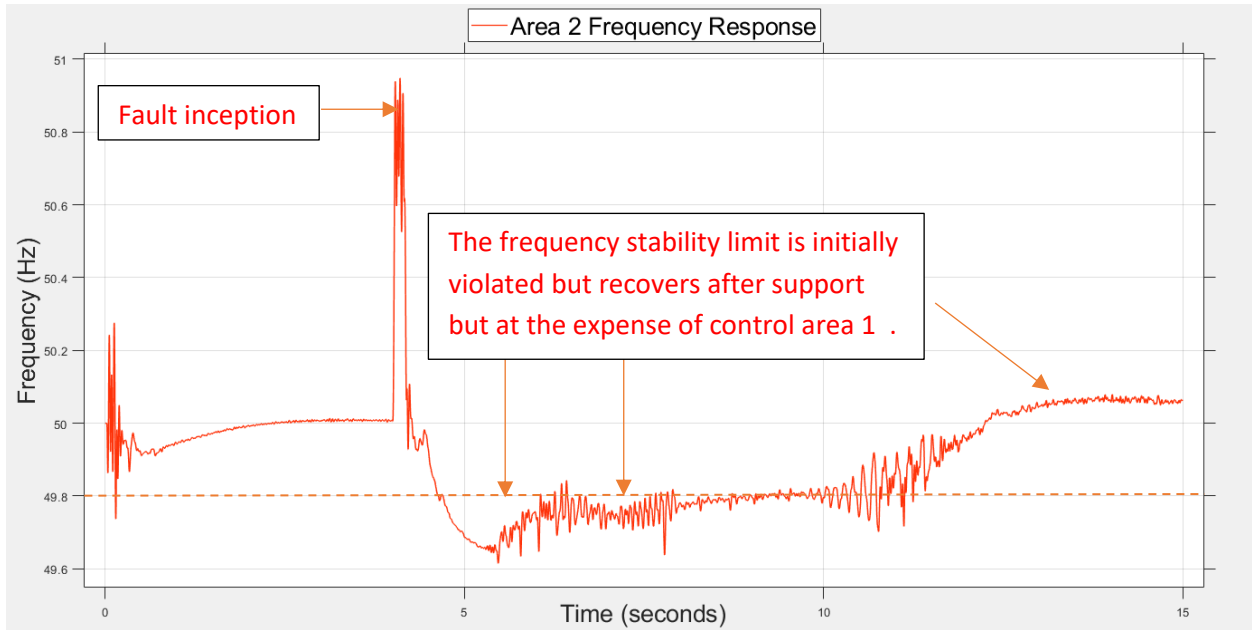


Figure 4.23: Case II Fault Area 2 Frequency Response without IAFSC Controller

Figure 4.24 shows the rotor angle of control area 1 that deviates significantly from its stable condition when supporting control area 2 beyond its support capacity. As shown, without the proposed IAFSC controller the rotor angle deviation deteriorates significantly without recovering stable conditions.

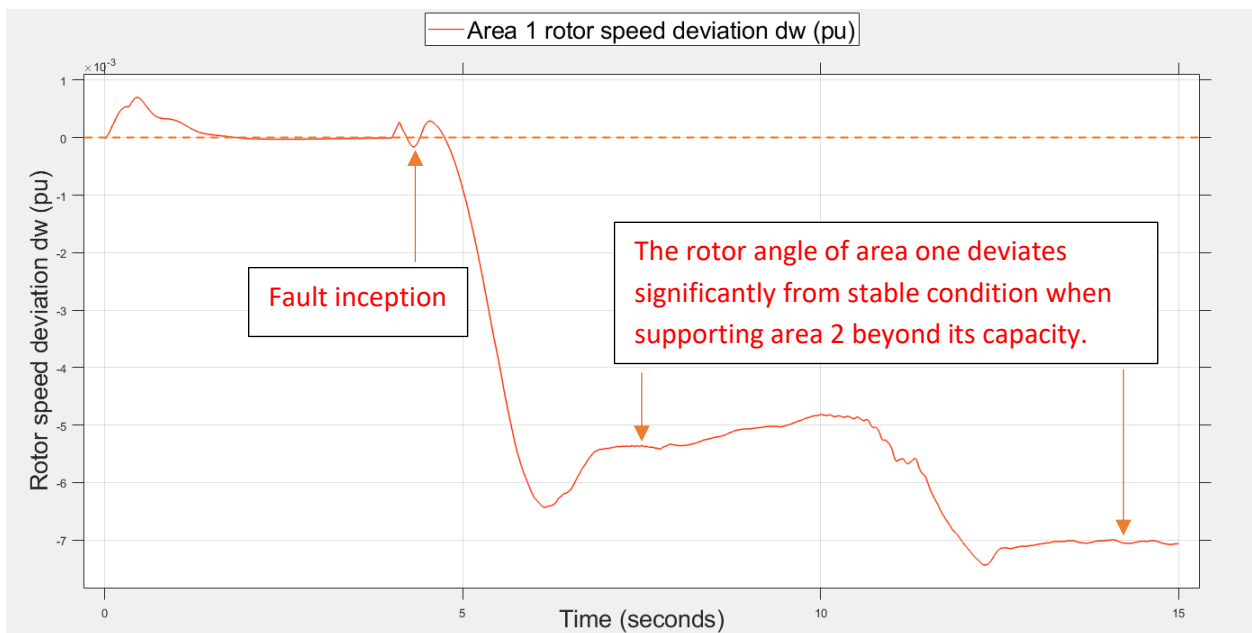


Figure 4.24: Case II Fault Area 1 Rotor Speed Deviation Response without IAFSC Controller

Figure 4.25 shows control area 2 rotor angle deviation which deviates initially but later recovers after support from control area 1, although control area 1 experiences unstable conditions (with the traditional controller).

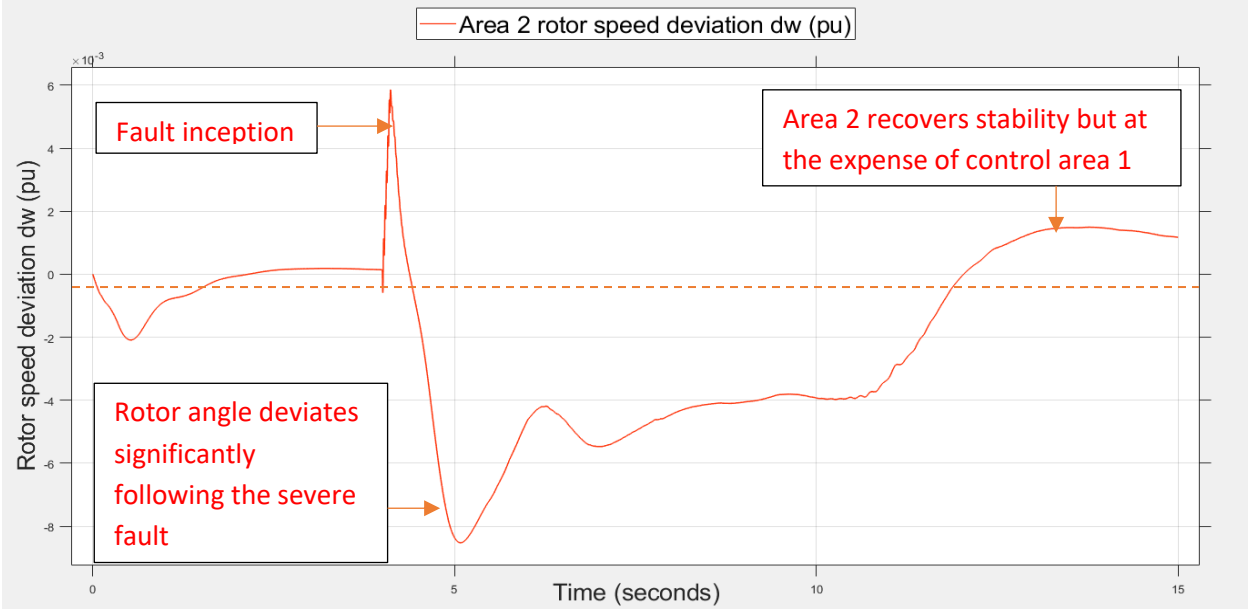


Figure 4.25: Case II Fault Area 2 Rotor Speed Deviation Response without IAFSC Controller

Figure 4.26 shows the HVDC tie power order from control area 1 having unstable oscillations as a result of the severe fault in control area 2. The traditional HVDC controller (without the IAFSC controller) orders control area 1 to ramp up power to support control area 2 but since the fault is severe, control area 1 is not able to provide the regulating power and hence experiences serious unstable power oscillations.

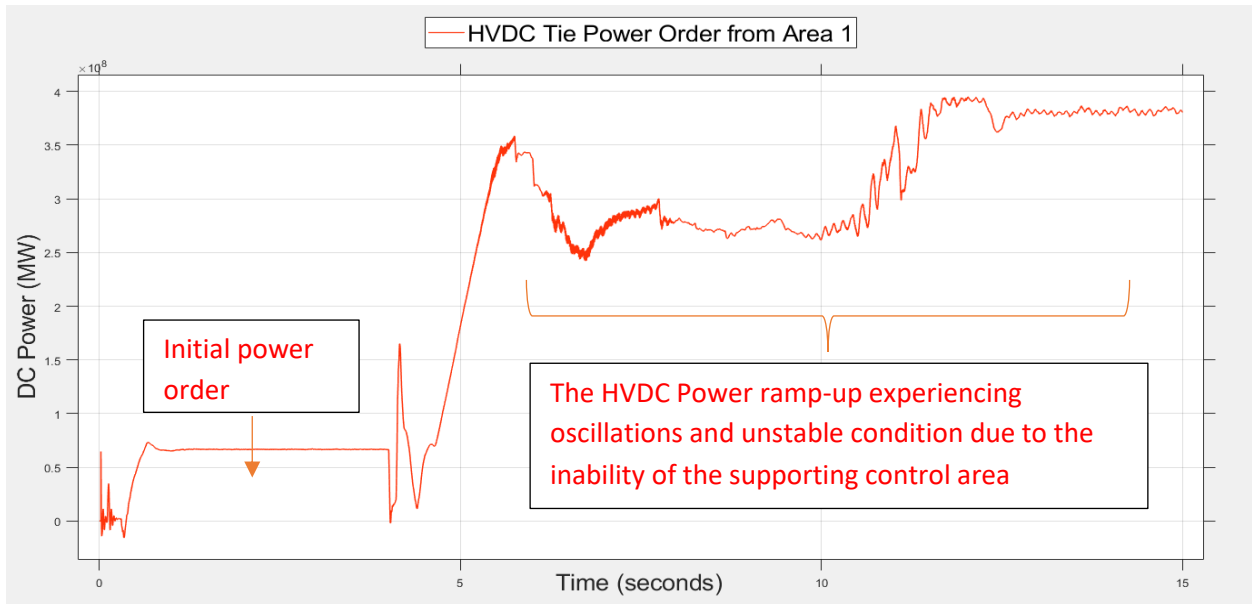


Figure 4.26: Case II Fault HVDC Tie Power Order from Area 1 without IAFSC Controller

Figure 4.27 shows control area 2 generation reducing significantly as a result of loss of generation caused by the severe fault.



Figure 4.27: Case II Fault Area 2 Generation without IAFSC Controller

Results Interpretation

The fault condition in control area 2 was very severe causing unstable conditions in control area 1. Since the traditional HVDC controller does not monitor the system strength of the supporting control area it continued to modulate the active power to support control area 2 but at the expense

of control area 1. Control area 1 stable condition was thus violated hence the experienced unstable system responses as shown in these results. It is concluded that for severe fault conditions, the traditional HVDC controller violates the stable condition of the supporting control area hence the essence of the proposed IAFSC controller.

4.4.2 Case II Fault with IAFSC Controller

Figures 4.28, 4.29, 4.30, 4.31, 4.32, 4.33, and 4.34 give the system responses with the IAFSC controller incorporated. As seen in Figure 4.28, the frequency response of control area 1 recovers its stable condition once the IAFSC controller detects a violation of its stability parameters. The IAFSC controller ramps down the HVDC modulated active power to zero (0) to restore control area 1 system stability. This is because control area 1 was not capable of providing the required regulating power to assist control area 2 during the severe fault. In this way, control area 1 is saved from the danger of system collapse arising from the violation of its stable conditions. The IAFSC controller proposed in this paper comes in handy to assist control area 1 in recovering from the catastrophic unstable conditions.

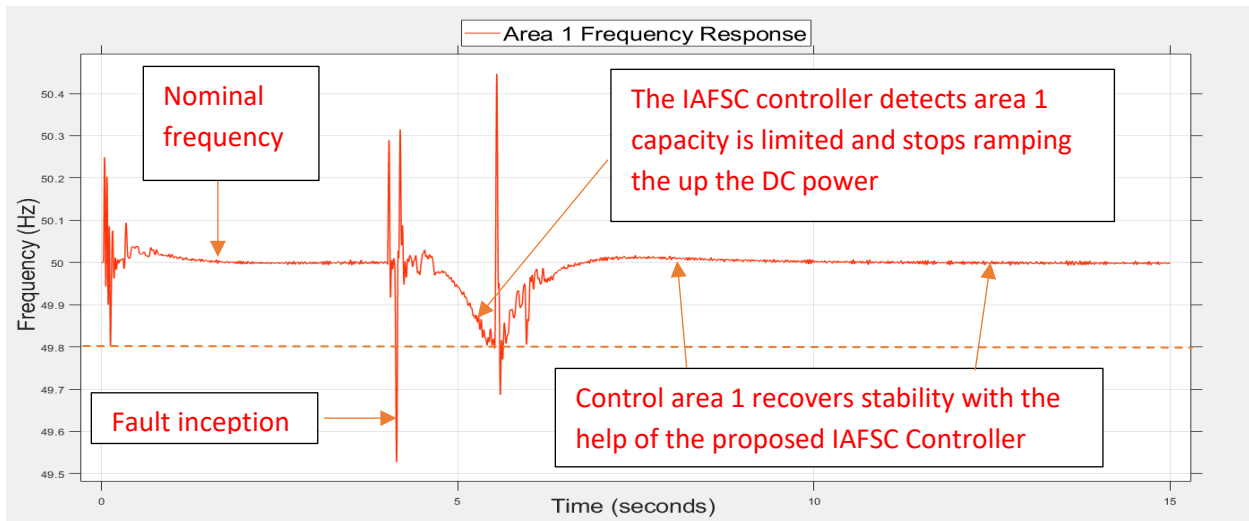


Figure 4.28: Case II Fault Area 1 Frequency Response with IAFSC Controller

Figure 4.29 shows the frequency response of control area 2 that never recovers stable condition as control area 1 capacity is limited and hence IAFSC controller prevented the DC power ramp-up modulation.

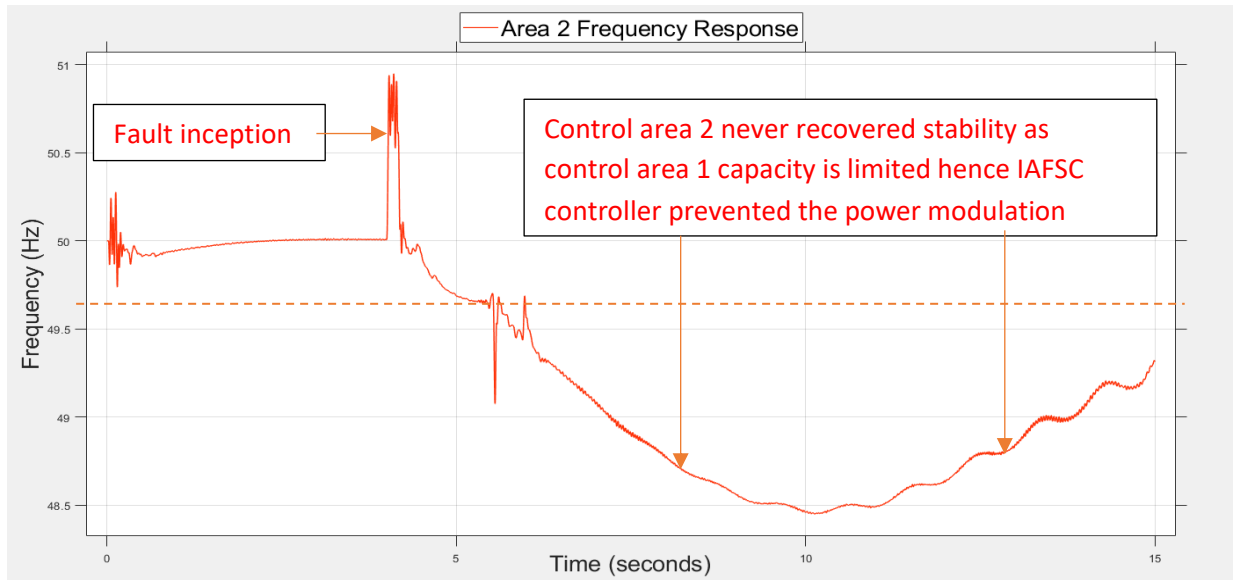


Figure 4.29: Case II Fault Area 2 Frequency Response with IAFSC Controller

Figure 4.30 shows the rotor angle deviation for control area 1. When the IAFSC controller detected a violation of the stability limit, it reset the DC power modulation to zero (0) to mitigate the catastrophic unstable conditions.

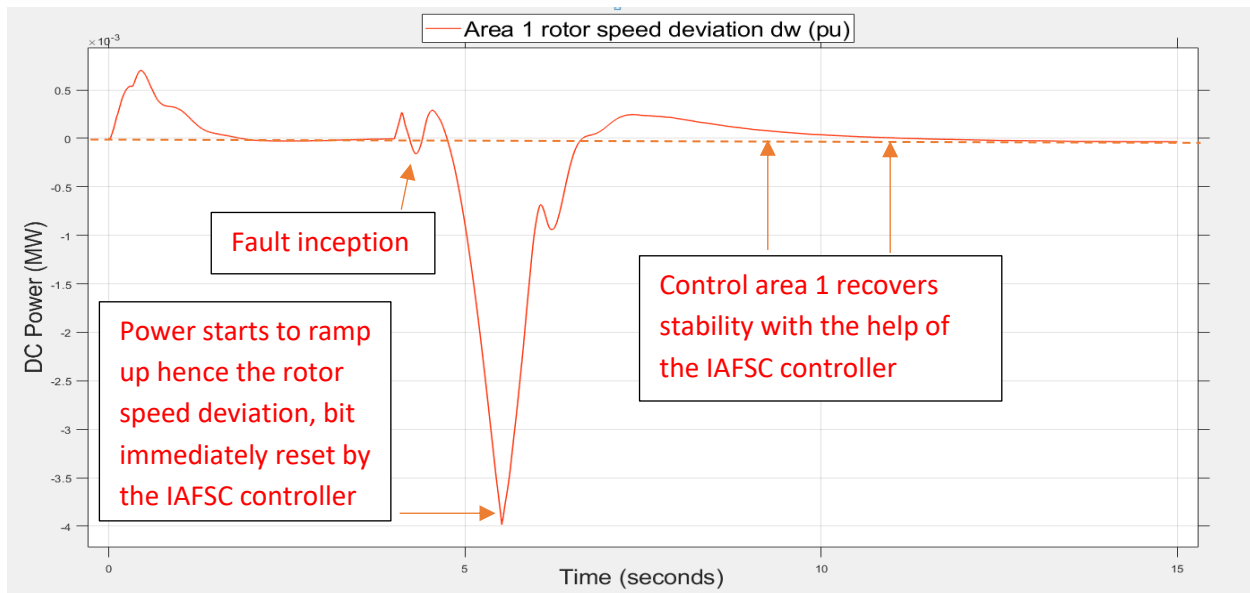


Figure 4.30: Case II Fault Area 1 Rotor Speed Deviation Response with IAFSC Controller

Figure 4.31 shows control area 2 rotor angle deviation response that deviates significantly to the negative as the IAFSC controller prevented DC power ramp-up since control area 1 is limited in its capacity to assist control area 2 in recovering stable conditions.

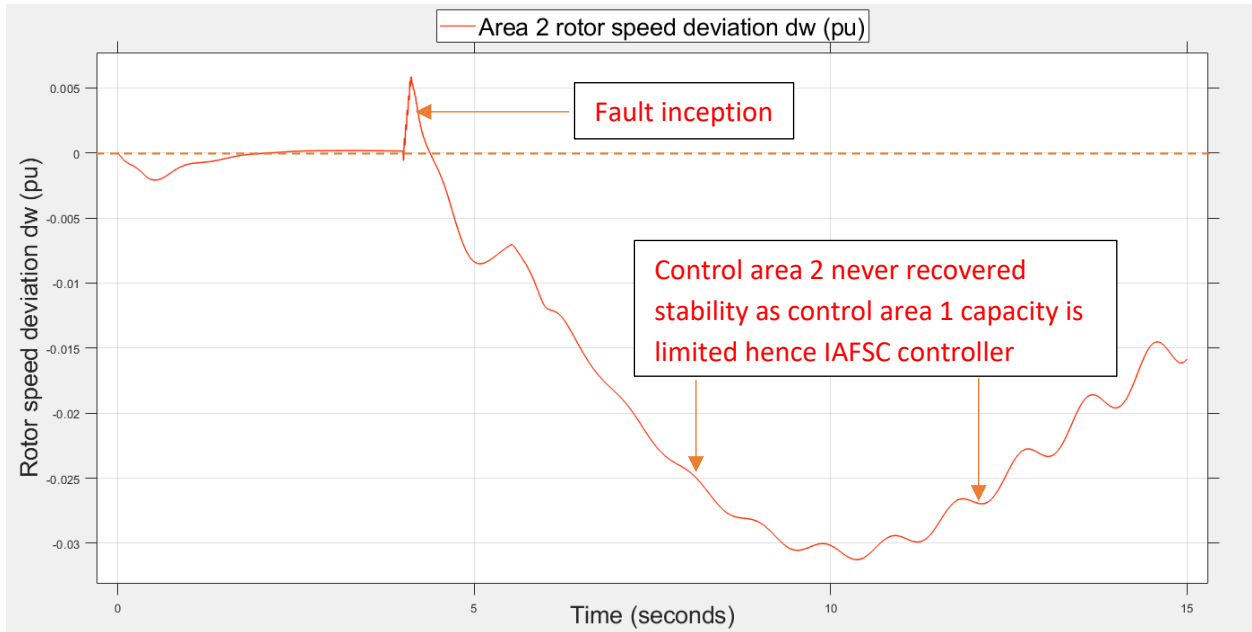


Figure 4.31: Case II Fault Area 2 Rotor Speed Deviation Response with IAFSC Controller

Figure 4.32 shows the HVDC power order ramped down to zero (0) megawatts by the IAFSC controller after detecting the violation of the stability limit in control area 1.

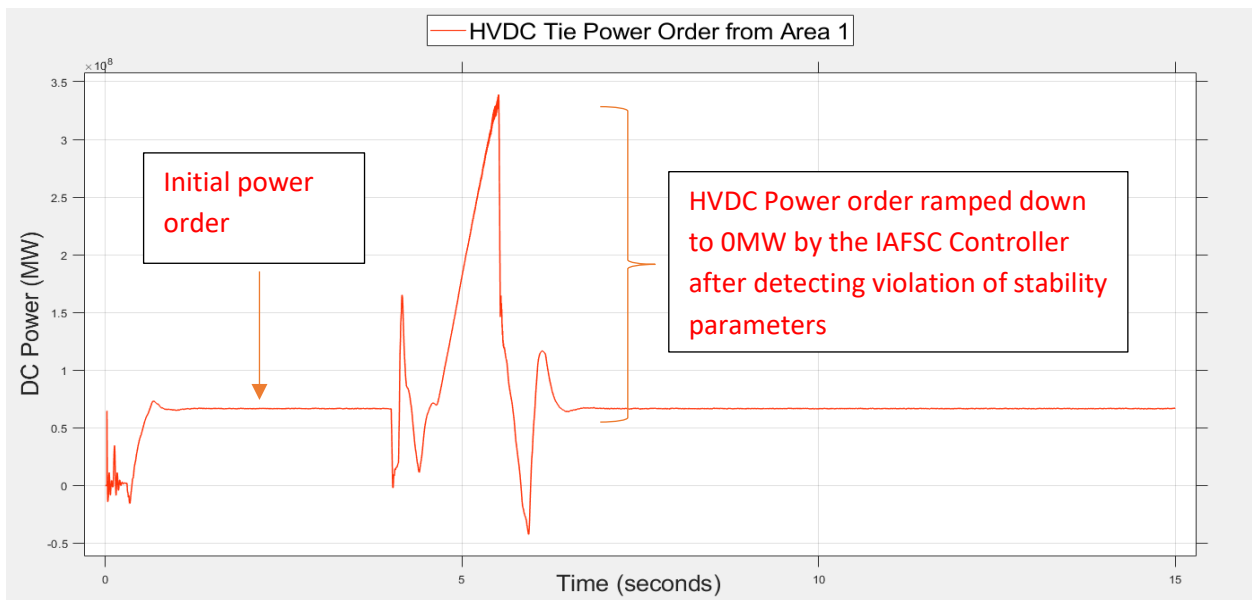


Figure 4.32: Case II Fault HVDC Tie Power Order from Area 1 with IAFSC Controller

Figure 4.33 shows control area 1 generation that initially starts to ramp-up to assist control area 2 but the IAFSC controller prevented further ramp-up of power after the detection of unstable conditions in control area 1.

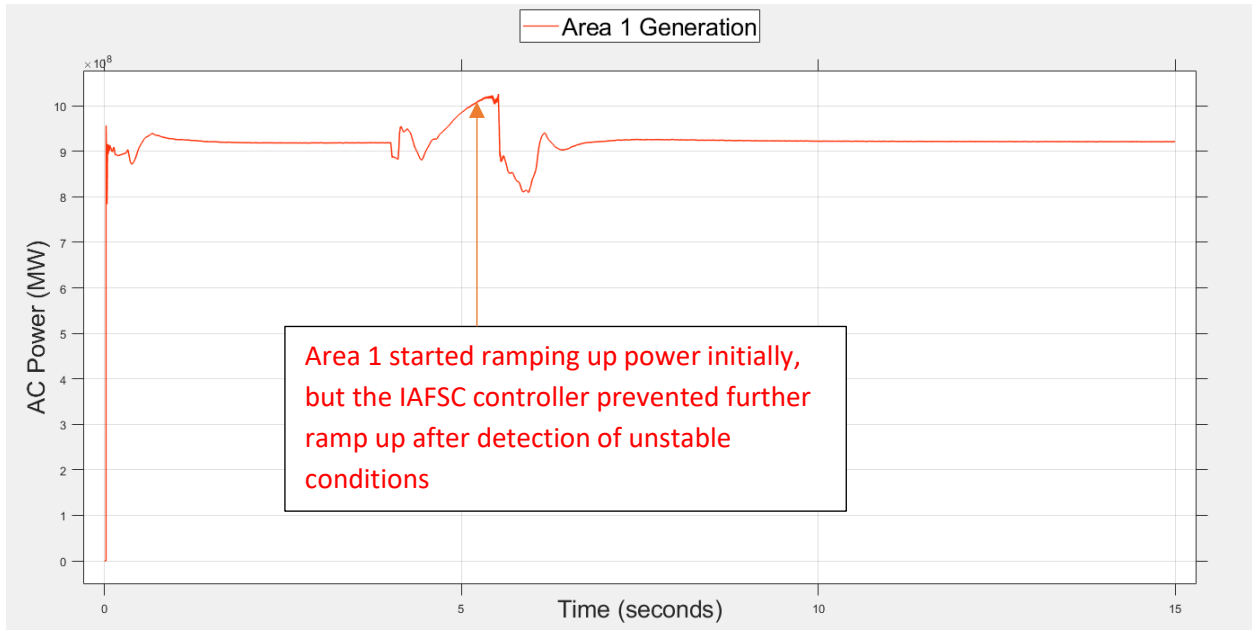


Figure 4.33: Case II Fault Area 1 Generation with IAFSC Controller

Figure 4.34 shows control area 2 generation that reduces as a result of the severe fault. The IAFSC controller prevented the DC power ramp-up to provide the required regulating power as control area 1 is limited in its support capacity.

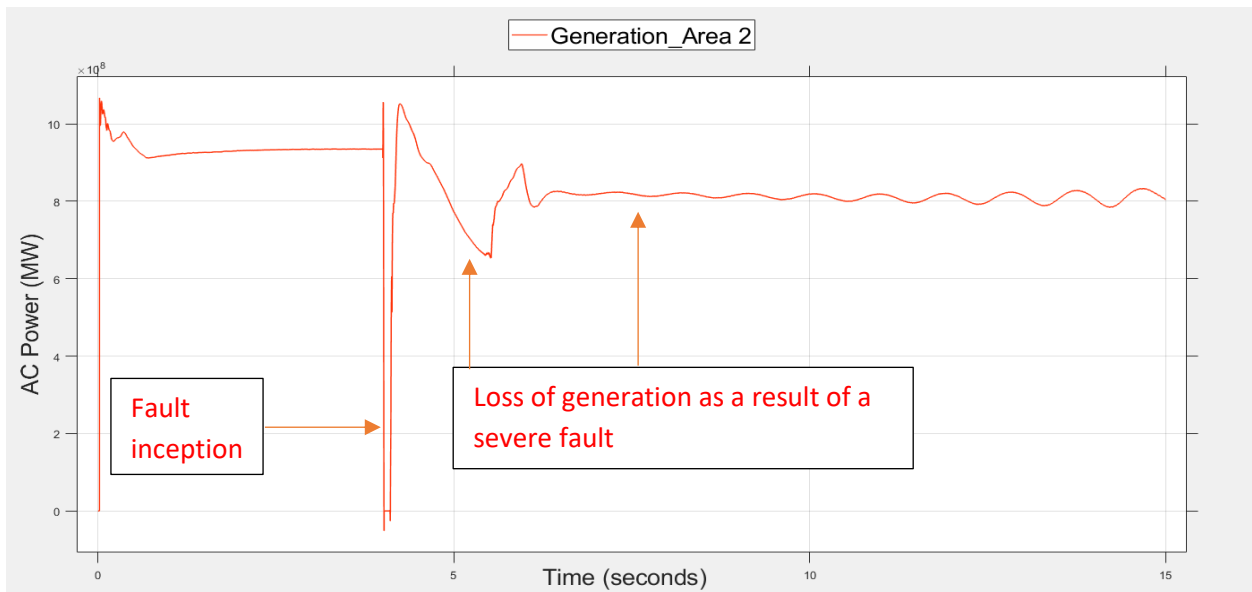


Figure 4.34: Case II Fault Area 2 Generation with IAFSC Controller

Results Interpretation

The fault condition in control area 2 was very severe causing unstable conditions in control area 1. Since the IAFSC controller detected a violation of stable condition in control area 1, the modulated active power was immediately reset to zero (0) to improve its transient stability response during severe fault conditions. Control area 1 stable condition was successfully recovered following the IAFSC controller action proposed in this thesis. This was not the case for the traditional HVDC controller where control area 1 experienced serious unstable conditions. It is therefore concluded that for severe fault conditions, the IAFSC controller improves the transient stability response of the supporting control area.

4.5 Validation of Results

In as much as the VSC-HVDC tie lines are proposed to be handily used for transient stability improvement of interconnected power systems by modulation of DC power order, the simulation results in this thesis have clearly shown that for severe fault conditions, care must be taken to ensure the support capacity of the supporting control area is considered. The supporting control area cannot be considered an infinite system as power systems have operational limits. As simulated, the case I fault scenario simulates a situation where the supporting control area can provide the required regulating power without compromising its system stability. Additionally, the case II fault scenario simulates a situation where the supporting control area cannot provide the required regulating power. Case II fault scenario is where the genesis of this research and thesis originated. A supplementary controller was introduced to monitor the operating capacity of the supporting control area in real-time to mitigate unstable conditions whenever the required regulating power is beyond its support capacity. Case II fault scenario without the IAFSC controller, a typical traditional system, showed a serious deviation from the nominal operating stable conditions in control area 1. The operating frequency decreased below 49.8Hz the recommended lowest operating frequency for stable conditions. This shows that the system disturbance in Control Area 2 was severe and required large regulating power beyond the ability of Control Area 1. With the incorporation of the IAFSC controller, Control Area 1 recovered stable conditions. For example, the frequency recovers to the nominal value of 50.0Hz and mitigates total system collapse. Tables 4.1 shows the system responses of the traditional system. Without the proposed supplementary controller, control area 1 experienced serious unstable conditions without recovering stable conditions when control area 2 was under severe fault conditions. With the proposed IAFSC controller as shown in Tables 4.2, 4.3, and 4.4, Control Area 1 recovers stable

conditions after the severe fault. From the transfer function and the modulation release signal plots, the IAFSC controller responded to the declining frequency and rotor angle of area 1 below the threshold limit and effectively reset the modulated power to assist Control Area 1 in recovering stable conditions. Likewise as shown in Table 4.5, without the IAFSC controller the frequency change violates the stable limit of 0.02 hertz during the post-fault time and never recovers. With the incorporation of the IAFSC controller, the frequency deviation recovers stable conditions with the IAFSC controller action during post-fault time by annulling the power modulation release signal to zero. Table 4.6 shows the rotor angle response of the system with and without the IAFSC controller. The controller action is demonstrated during the severe fault condition to validate its functionality. Without the IAFSC controller, the rotor angle deviation violates the stable limit of 0.003pu during the post-fault time. However, with the IAFSC controller, the rotor angle deviation recovers stable conditions during the post-fault time of the severe fault. Thus the proposed controller was able to assist Control Area 1 in recovering stable condition after the severe fault while the conventional controller could not.

Table 4.1: Control Area 1 Response under Fault Scenario II without The IAFSC Controller

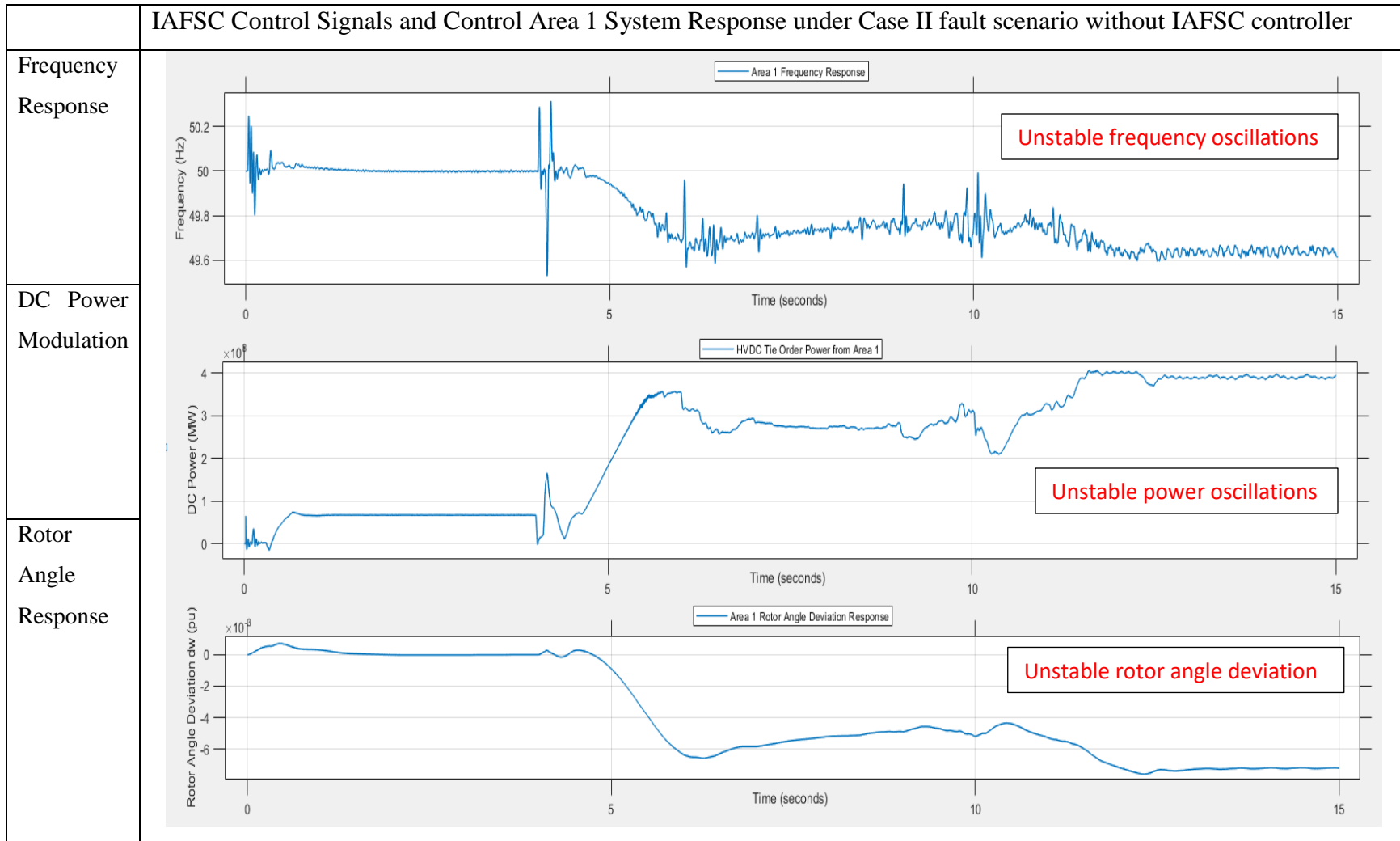


Table 4.2: Control Area 1 Response under Fault Scenario II with The Proposed IAFSC Controller

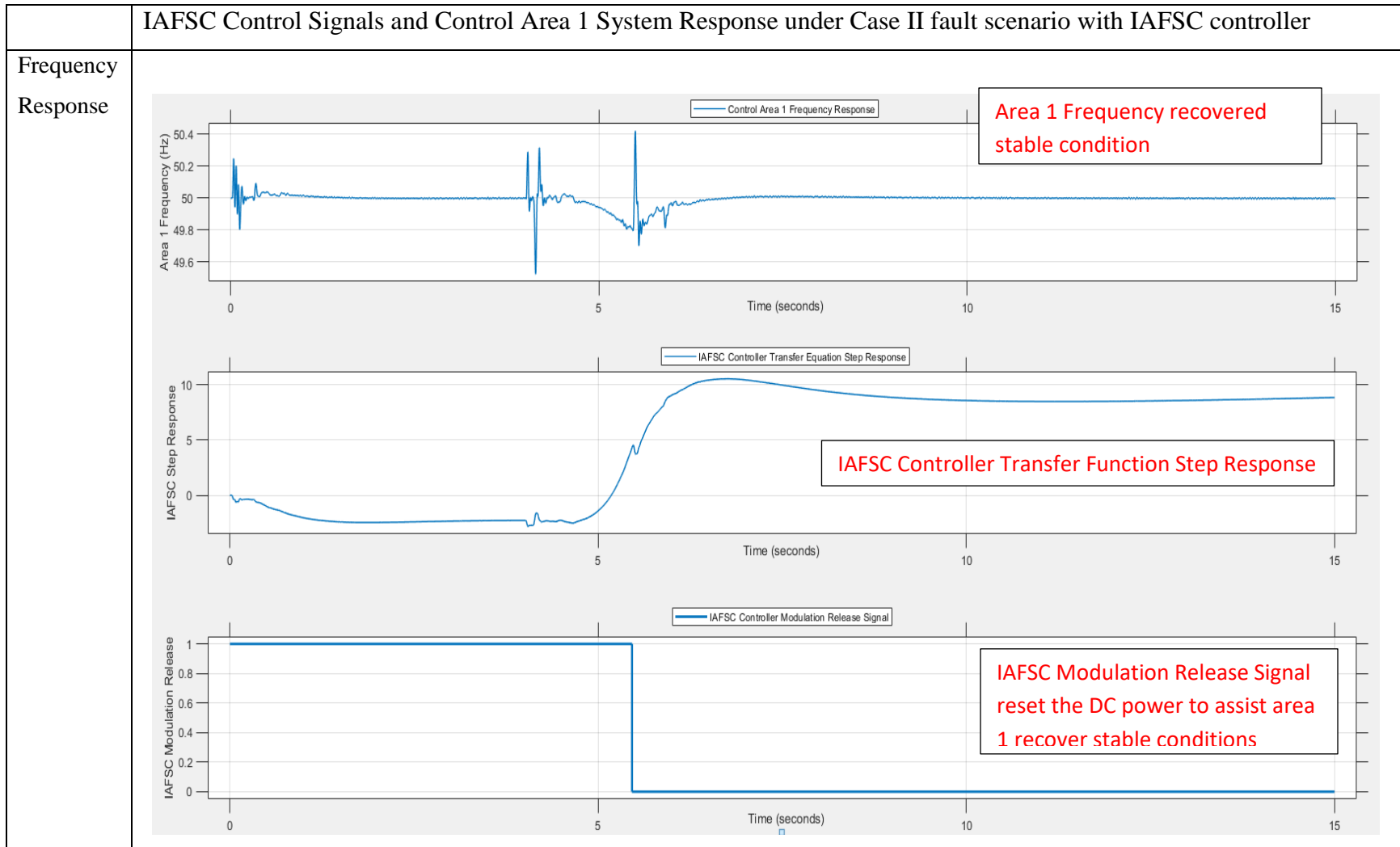


Table 4.3: Control Area 1 Response under Fault Scenario II with The Proposed IAFSC Controller

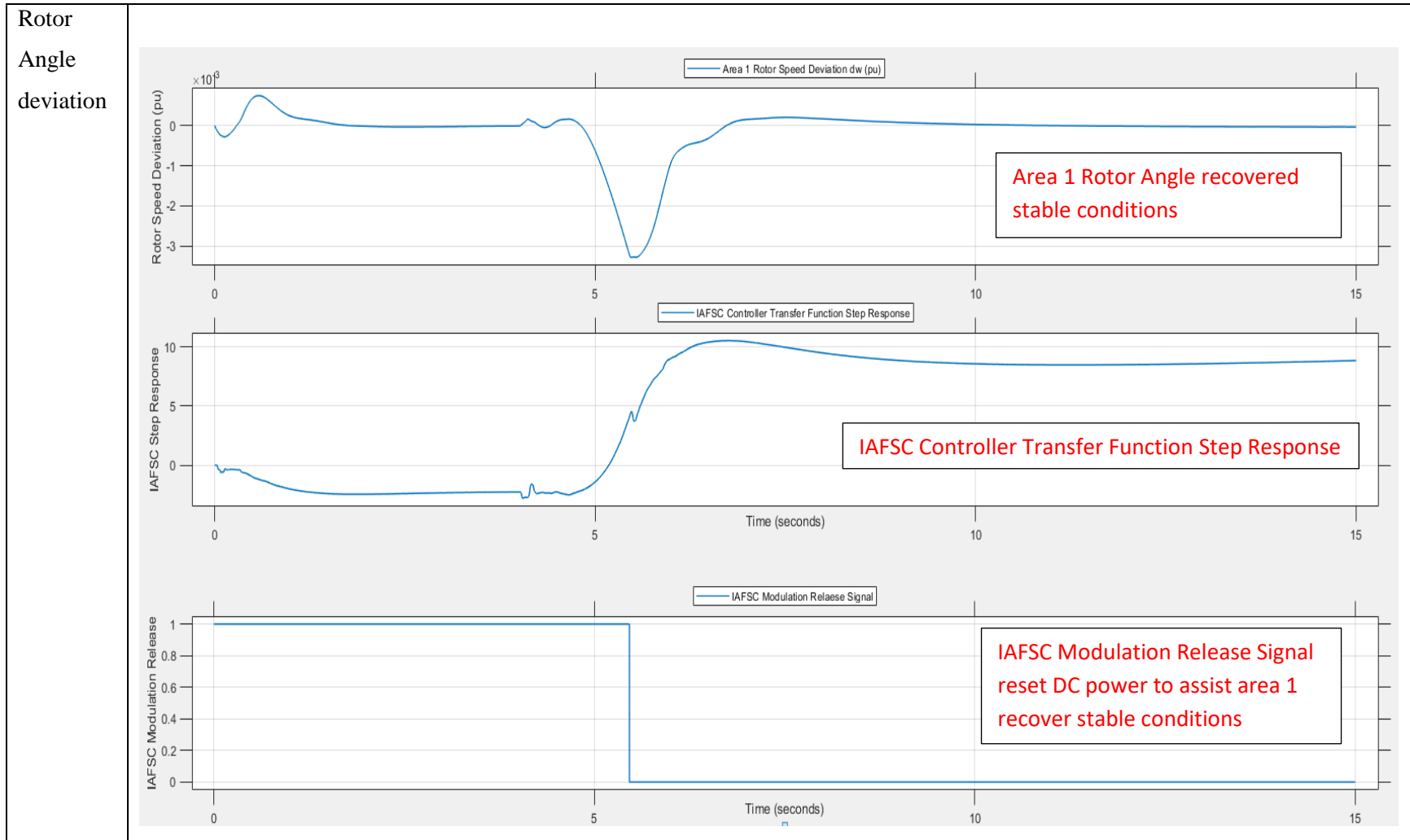


Table 4.4: Control Area 1 Response under Fault Scenario II with The Proposed

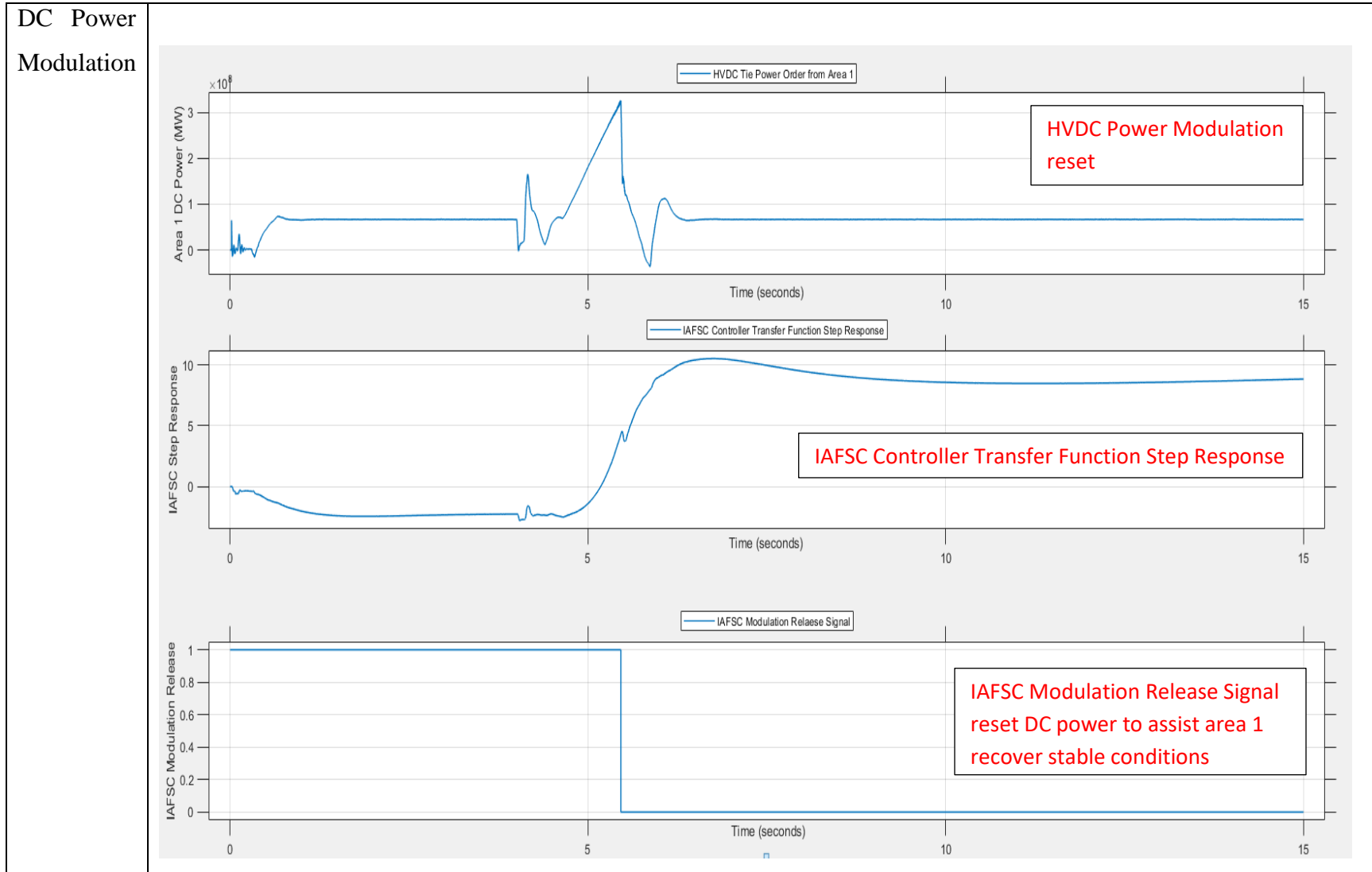


Table 4.5: Validation of the IAFSC Controller with Control Area 1 Frequency Response

Time (Sec)	HVDC without IAFSC					HVDC with IAFSC				
	Parameter: Frequency. Frequency Limit: Frequency Limit: (-0.2/+0.2)					Parameter: Frequency. Frequency Limit: (-0.2/+0.2)				
	System Condition	(f) in Hz	(Δf)	Stability Limit Violation	Conventional Modulation Release Signal	System Condition	(f) in Hz	(Δf)	Stability Limit Violation	IAFSC Modulation Release Signal
1.0	Pre-Fault	50.01	0.01	No	1	Pre-Fault	50.01	0.01	No	1
2.0	Pre-Fault	50.00	0.00	No	1	Pre-Fault	50.00	0.00	No	1
3.0	Pre-Fault	49.99	-0.01	No	1	Pre-Fault	49.99	-0.01	No	1
3.5	Pre-Fault	50.00	0.00	No	1	Pre-Fault	50.00	0.00	No	1
4.0	Fault	49.99	-0.01	No	1	Fault	49.99	-0.01	No	1
5.0	Post-Fault	49.94	-0.06	No	1	Post-Fault	49.94	-0.06	No	1
5.3	Post-Fault	49.84	-0.16	No	1	Post-Fault	49.84	-0.16	No	1
5.5	Post-Fault	49.70	-0.30	Yes	1	Post-Fault	49.70	-0.30	Yes	0
5.7	Post-Fault	49.69	-0.31	Yes	1	Post-Fault	49.89	-0.11	System recovered	0
5.8	Post-Fault	49.65	-0.35	Yes	1	Post-Fault	49.92	-0.08	System recovered	0
6.3	Post-Fault	49.63	-0.37	Yes	1	Post-Fault	49.97	-0.03	System recovered	0
6.6	Post-Fault	49.68	-0.32	Yes	1	Post-Fault	49.99	-0.01	System recovered	0

7.0	Post-Fault	49.70	-0.3	Yes	1	Post-Fault	50.00	0.00	System recovered	0
8.0	Post-Fault	49.73	-0.27	Yes	1	Post-Fault	50.00	0.00	System recovered	0
9.0	Post-Fault	49.74	-0.26	Yes	1	Post-Fault	50.00	0.00	System recovered	0
10.0	Post-Fault	49.74	-0.26	Yes	1	Post-Fault	50.00	0.00	System recovered	0
11	Post-Fault	49.68	-0.34	Yes	1	Post-Fault	50.00	0.00	System recovered	0
12	Post-Fault	49.61	-0.39	Yes	1	Post-Fault	50.00	0.00	System recovered	0

Table 4.6: Validation of the IAFSC Controller with Control Area 1 Rotor Angle Response

Time (Sec)	HVDC without IAFSC				HVDC with IAFSC			
	Parameter: Rotor Angle. Angle Limit: (-0.003/+0.003) pu.				Parameter: Rotor Angle. Angle Limit: (-0.003/+0.003) pu.			
	System Condition	$\Delta\delta$	Stability Limit Violation	Conventional Modulation Release Signal	System Condition	$\Delta\delta$	Stability Limit Violation	IAFSC Modulation Release Signal
1.0	Pre-Fault	0.00	No	1	Pre-Fault	0.00	No	1
2.0	Pre-Fault	0.00	No	1	Pre-Fault	0.00	No	1
3.0	Pre-Fault	0.00	No	1	Pre-Fault	0.00	No	1
3.5	Pre-Fault	0.00	No	1	Pre-Fault	0.00	No	1
3.9	Fault	0.00	No	1	Fault	0.00	No	1
5.0	Post-Fault	-0.0011	No	1	Post-Fault	-0.001	No	1
5.5	Post-Fault	-0.0034	Yes	1	Post-Fault	-0.003	Yes	0
6.0	Post-Fault	-0.0052	Yes	1	Post-Fault	0.00	System recovered	0
6.5	Post-Fault	-0.0056	Yes	1	Post-Fault	0.00	System recovered	0
7.0	Post-Fault	-0.0058	Yes	1	Post-Fault	0.00	System recovered	0
7.5	Post-Fault	-0.0054	Yes	1	Post-Fault	0.00	System recovered	0
8.0	Post-Fault	-0.0052	Yes	1	Post-Fault	0.00	System recovered	0

8.5	Post-Fault	-0.0050	Yes	1	Post-Fault	0.00	System recovered	0
9.0	Post-Fault	-0.0048	Yes	1	Post-Fault	0.00	System recovered	0
9.5	Post-Fault	-0.0047	Yes	1	Post-Fault	0.00	System recovered	0
10.0	Post-Fault	-0.0052	Yes	1	Post-Fault	0.00	System recovered	0
10.5	Post-Fault	-0.0050	Yes	1	Post-Fault	0.00	System recovered	0
11.0	Post-Fault	-0.0055	Yes	1	Post-Fault	0.00	System recovered	0
11.5	Post-Fault	-0.0063	Yes	1	Post-Fault	0.00	System recovered	0
12.0	Post-Fault	-0.0076	Yes	1	Post-Fault	0.00	System recovered	0

4.6 Chapter Conclusion

From the simulation results, it has been demonstrated that power systems have operational limits that must be respected to maintain their system stability. Whenever the VSC-HVDC system is used for transient stability improvement it is critical to monitor the system parameters of the supporting control area to mitigate violation of its stable limits. It has been proved that with the proposed IAFSC controller, the supporting control area system strength is monitored in real-time, and a control decision is made based on its system strength to mitigate violation of its stability limits when providing the regulating power to the faulted control area. The proposed IAFSC controller proposed in this thesis improved the transient stability response of the supporting control area during severe fault conditions which is not the case with the traditional HVDC control system. The objectives of this research were therefore met and effectively demonstrated.

CHAPTER 5

CONCLUSIONS AND RECOMMENDATIONS

5.1 Conclusion

Two cases were simulated in MATLAB/SIMULINK on the Kundur two-area four-machine system and the system responses were compared with and without the proposed IAFSC controller. The first fault case with a 10% generation loss in control area 2 was simulated to demonstrate and prove that as long as the supporting control area can provide the required regulating power, its system parameters are not violated. As seen from the frequency and rotor angle deviation responses, the stability limits are still within the tolerable values and do not compromise stability in control area 1. Consequently, control area 2 recovers its stability without affecting control area 1. For the case of 10% generation loss in control area 2, the responses with and without the IAFSC controller are therefore similar. Control area 1 stability is not violated because the fault is not severe enough to require regulating power beyond its ability.

With more severe fault scenarios where the supporting control area cannot provide the required regulating power, the stability limit of the supporting control area is compromised if the proposed IAFSC controller is not incorporated. As seen with the second fault case of 25% generation loss in control area 2, simulation without the proposed IAFSC controller shows a serious violation of the frequency and rotor angle deviation causing unstable conditions in control area 1. This has proved that it cannot be assumed that the supporting control area is an infinite system. With the incorporation of the IAFSC controller, control area 1 recovers stable conditions thus mitigating catastrophic system collapse. The IAFSC controller is thus a vital supplementary controller that must be incorporated in HVDC controls utilized in power modulation for transient stability improvement. Without the IAFSC controller, the system will collapse for severe system disturbances.

It is thus critical to monitor the system strength of the supporting control area so that its stability limits are not violated. The conventional system lacks the proposed controller thus exposing the supporting control area to the risk of system collapse for severe system disturbances. The power system cannot be assumed as an infinite system. From the simulation results, it has been proved that there is a need for modification of the conventional control system used for HVDC power modulation for transient stability improvement. Continuous real-time monitoring of system

parameters is required to avoid violation of stability limits of the supporting control area during power modulation. The supplementary controller as proposed in this thesis has effectively improved the transient stability response of the supporting control area for severe fault situations.

5.2 Recommendations

5.2.1 Recommendations for Further Work

Further improvements on the IAFSC controller can be done to incorporate a control algorithm for reactive power control to assist in the voltage stability of the interconnected systems. The current IAFSC control algorithm has focussed on the modulation of active power alone and assumes that voltage stability is well maintained.

5.2.2 Adoption of the Results

From the simulation results, it has been proved that the IAFSC supplementary controller is vital in mitigating unstable conditions in the supporting control area. This can be adopted in the Ethiopia – Kenya 500kV HVDC link that is currently operational and has the under-frequency control function to assist in system stability. The IAFSC controller can be incorporated in the under-frequency control function for transient stability improvement where DC power is modulated while considering the system strength in real-time. This will help in mitigating unstable conditions in the supporting control area when the under-frequency function is invoked during severe faults.

5.3 Research Contribution

This research has added to the previous works on VSC-HVDC transient stability improvement a supplementary controller called IAFSC (Inter Area Frequency Controller) that will help mitigate unstable conditions in the supporting control area whenever the required regulating power is beyond its capacity. The IAFSC controller has been proven to improve the transient stability response of the supporting control area during severe system disturbances for which the traditional HVDC controls resulted in the violation of stable conditions.

REFERENCES

- [1] Nikhil Hira, Fred Omondi, Denis Kakembo, ‘The roadmap to a fully and operational East African Power Pool (EAPP)’, Deloitte & Touche, 2015.
- [2] Union for the Coordination of Transmission of Electricity, ‘Feasibility Study-Synchronous Interconnection of the IPS/UPS with the UCTE’, Brussels, November 2008.
- [3] Issarachai Ngamroo, ‘A Stabilization of Frequency Oscillations using a Power Modulation Control of HVDC Link in a Parallel AC-DC Interconnected System’ IEEE PCC, Osaka, 2002.
- [4] Voltage Source Converters, ‘<https://www.entsoe.eu/Technopedia/techsheets/voltage-source-converters>’, accessed 19 May 2022.
- [5] Ulf Hager, Christian Rehtanz, Nikolai Voropai, ‘Monitoring, Control and Protection of Interconnected Power Systems’, Berlin Heidelberg: Springer-Verlag, 2014.
- [6] Teja Bandaru, Ujjwal Dhawa, Dheeman Chatterjee, Tanmoy Bhattacharya, ‘Improving the Transient Stability by Modifying the Power Exchange of the HVDC Transmission’ National Power Systems Conference IEEE, Tiruchirappalli, India, 2019.
- [7] H.F. Latorre, M. Ghandhari and L. Soder, "Active and reactive power control of a VSC HVDC", Electric Power Systems Research, vol. 78, pp. 1756-1763, 2008.
- [8] International Renewable Energy Agency (IRENA), ‘<https://irena.org/cleanenergycorridors/Africa-Clean-Energy-Corridor>’, accessed 4 November 2021.
- [9] D. Povh, D. Retzmann, E. Teltsch, U. Kerin, and R. Mihalic, ‘‘Advantages of large AC/DC system interconnections,’’ CIGRE Session, Paris, France, Tech. Rep. B4-304, 2006.
- [10] H. Wang and M. A. Redfern, ‘‘The advantages and disadvantages of using HVDC to interconnect AC networks,’’ in Proc. IEEE 45th Int. Universities Power Eng. Conf. (UPEC), Aug./Sep. 2010, pp. 1–5.
- [11] P. Kundur, ‘Power system stability and control’, USA: McGraw-Hill; 1994.
- [12] D P Kothari and I J Nagrath, ‘Modern Power Systems Analysis’, New Delhi. Tata McGraw Hill Education Private Ltd. 2011.

- [13] Micea Ereamia, Chen Ching Liu, and Abde Aty Edris. ‘Advanced Solutions in Power Systems: HVDC, FACTS, and Artificial Intelligence’, IEEE Press Series on Power Engineering New Jersey, 2016.
- [14] I. Ngamroo, “A stabilization of frequency oscillations using a power modulation control of HVDC link in a parallel AC-DC interconnected system,” in Proc. Power Conversion Conference (PCC), vol. 1, 2002.
- [15] M. Xiao-ming and Z. Yao, “Application of HVDC modulation in damping electromechanical oscillations,” in Proc. IEEE Power Engineering Society General Meeting, June 2007, pp. 1–6.
- [16] R. Leelaruji, L. Vanfretti, M. Ghandhari, and L. Soder, ‘Coordination of protection and VSC-HVDC system for mitigating cascading failure’ IEEE International Conference on Power System Technology, Zhejiang, China, 2010.
- [17] Sharlene M Builu, ‘Stability Enhancement of HVAC Grids using HVDC Links’, Master Thesis, University of KwaZulu-Natal, Durban, 2016.
- [18] Oluwafemi E. Oni, Innocent E. Davidson, and Kamati N.I. Mbangula, ‘A Review of LCC-HVDC and VSC-HVDC Technologies and Applications’, IEEE 16th International Conference on Environment and Electrical Engineering (EEEIC), Florence, Italy, 2016.
- [19] A.N. Fuchs, S. Mariethoz, M. Larsson, and M. Morari, ‘Constrained optimal control of VSC-HVDC for power system enhancement failure’, ‘IEEE International Conference on Power System Technology, Zhejiang, China, 2010.
- [20] Zhenlin Huang; Yihao Zeng; Lin Guan and Jiandong Cao, ‘Study on a new power modulation strategy of HVDC to improve transient stability in China’, Southern Power Grid International Future Energy Electronics Conference (IFEEC), Tainan, Taiwan, 2013.
- [21] Yu Tao, Zhu Shouzhen, Zhao Yuzhu, and Zhu Weijiang, ‘A Novel Auxiliary Frequency Controller for HVDC Transmission Links’, ‘IEEE Proceedings, International Conference on Power System Technology, Kunming, China, 2002.
- [22] Omid Borazjani, Alireza Rajabi, Mojtaba Saeedimoghadam, and Khodakhast Isapour, ‘Stability Improvement of AC System by Controllability of the HVDC’, IEEE International Conference on Power System Technology, World Academy of Science, Engineering and Technology International Journal of Electrical and Computer Engineering Vol:9, No:3, 2015.

- [23] Lakshmi Sundaresh, Zhiyong Yuan, Kaiqi Sun, Jiuping Pan and Yilu Liu, ‘Improving power grid transient stability and transfer capability using HVDC emergency power controls’, IEEE/PES Transmission and Distribution Conference and Exposition (T&D), Chicago, IL, USA, 2020.
- [24] J. Hazra, Y. Phulpin, and D. Ernst, ‘HVDC Control Strategies to Improve Transient Stability in Interconnected Power Systems’, IEEE Bucharest Power Tech Conference, June 28th - July 2nd, Bucharest, Romania, 2009.
- [25] M. Benasla, T. Allaoui, M. Brahami, M. Denaï, and V. K. Sood, ‘‘HVDC links between North Africa and Europe: Impacts and benefits on the dynamic performance of the European system,’’ *Renew. Sustain. Energy Rev.*, vol. 82, pp. 3981–3991, Feb. 2018.
- [26] A. M. Vural, ‘‘Contribution of high voltage direct current transmission systems to inter-area oscillation damping: A review,’’ *Renew. Sustain. Energy Rev.*, vol. 57, pp. 892–915, May 2016.
- [27] Marwan Rosyadi, Atsushi Umemura, Rion Takahashi and Junji Tamura, ‘Tie line power control of HVDC transmission to damp frequency fluctuation of power system with large scale wind farm integrated’, IEEE Tenth International Conference on Ecological Vehicles and Renewable Energies (EVER), 2015.
- [28] Chan-Ki Kim, Vijay K. Sood, Gil-Soo Jang, Seong-Joo Lim and Seok-Jin Lee, ‘HVDC Transmission Power Conversion Applications in Power Systems’, Asia. John Wiley & Sons Pte Ltd. 2009.
- [29] Alexander Fuchs, Sébastien Mariéthoz, Mats Larsson and Manfred Morari, ‘Grid stabilization through VSC-HVDC using wide-area measurements’, IEEE Trondheim PowerTech, 2011.
- [30] Abdussalam S. Elansari, ‘FACTS and HVDC systems for enhancing tie-line power transfer Capability’, PhD thesis, Department of Electronic and Electrical Engineering, University of Strathclyde, UK. April, 2016
- [31] N Flourentzou, "VSC-Based HVDC power transmission systems: an overview", *IEEE Trans on Power Electron*, vol. 24, pp. 592-602, 2009.
- [32] Sherif Omar Faried, Guosheng Tang. and Saleh Aboreshaid, ‘Power System Stability Enhancement Using a Voltage Source Converter HVDC Back-to-Back Link’, IEEE, The Eleventh International Middle East Power Systems Conference (MEPCON), 2006.
- [33] M. Pavella, D. Ernst, and D. Ruiz-Vega, ‘Transient Stability of power systems’, Kluwer Academic, 2000.

- [34] Imdadullah, Syed Muhammad Amrr, M. S. Jamil Asghar, Imtiaz ashraf, and Mohammad Meraj, 'A Comprehensive Review of Power Flow Controllers in Interconnected Power System Networks', IEEE ACCESS, 2020.
- [35] Nikhil Pathak, Ashu Verma, T. S. Bhatti, and Ibraheem Nasiruddin, 'Modeling of HVDC Tie Links and Their Utilization in AGC/LFC Operations of Multiarea Power Systems', IEEE Transactions on Industrial Electronics, 2018.
- [36] S.Sivanagaraju, G.Sreenivasan, 'Power System Operation and Control', Delhi, Person 2016.
- [37] P. Bapaiah, 'Improvement of Power System Stability Using HVDC Controls of HVDC' International Journal of Emerging Trends in Electrical and Electronics (IJETEE), Vol. 2, Issue. 1, 2013.
- [38] Muhammad Abdul Basit, Rabiah Badar and Farman ullah Jan, 'Intelligent Damping Control for Transient Stability Enhancement using HVDC' IEEE International Conference on Electrical Engineering (ICEE), 2018.
- [39] Lakshmi Sundaresh, Zhiyong Yuan, Kaiqi Sun, Jiuping Pan and Yilu Liu, 'Improving power grid transient stability and transfer capability using HVDC emergency power controls' IEEE/PES Transmission and Distribution Conference and Exposition (T&D), 2020
- [40] A.S. Elansari, S.J. Finney, J. Burr and M.F. Edrah, 'Frequency control capability of VSC-HVDC transmission system' Strathclyde University, Institute of Energy and Environment, Glasgow, UK, 2015
- [41] Dragan Jovcic and Khalid Ahmed, 'High Direct Current Transmission Converter, Systems and DC Grids, School of Engineering University of Aberdeen, United Kingdom 2015.
- [42] Daniel Pérez Dorantes, José Luis Monroy Morales and Máximo Hernández Ángeles, 'A Filter Design Methodology of a VSC-HVDC System' , IEEE International Autumn Meeting on Power Electronics and Computing (ROPEC), Morelia, Mexico, 2013
- [43] Muhammad Abdul Basit, 'Intelligent Damping Control for Transient Stability Enhancement using HVDC', Department of Electrical Engineering, Riphah International University Faisalabad, Pakistan, 2018.
- [44] Lidong Zhang, Lennart Harnfors and Pablo Rey, 'Power System Reliability and Transfer Capability Improvement', Security and Reliability of Electric Power Systems, CIGRÉ Regional Meeting, Tallinn, Estonia, 2007.

- [44] Lorian M. Mbaabu, Keren K. Kaberere and P.K. Hinga ‘Performance Analysis Of The Voltage Source Converter Based High Voltage Direct Current Link On Small Signal Stability’ International Journal of Scientific & Technology Research Volume 8, Issue 10, October 2019.
- [45] M. Klein, G. J. Rogers, and P. Kundur, ‘A Fundamental Study of Inter-Area Oscillations in Power Systems, IEEE Transactions on Power Systems’ vol. 6, no. 3, pp. 914–921, 1991.
- [46] Ying Huang and Zheng Xu, ‘HVDC Supplementary Controller Based on Synchronized Phasor Measurement Units’, IEEE PES Power Systems Conference and Exposition, New York, 2005.
- [47] Alexander Fuchs, Sébastien Mariéthoz, Mats Larsson, and Manfred Morari, ‘Grid stabilization through VSC-HVDC using wide-area measurements’ IEEE Trondheim PowerTech Trondheim, Norway 2011.
- [48] Daniel Pérez Dorantes, José Luis Monroy Morales and Máximo Hernández Ángeles, ‘A Filter Design Methodology of a VSC-HVDC System’, IEEE International Autumn Meeting on Power Electronics and Computing (ROPEC), Morelia, Mexico 2014.

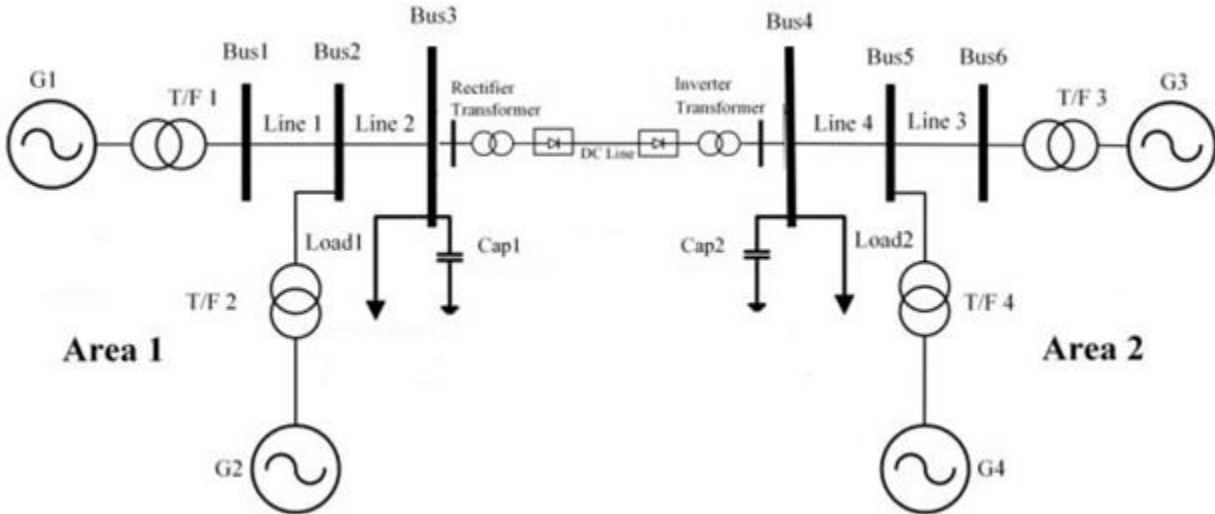
APPENDICES

Appendix I: Kundur Two-Area Test Network Generator Data.

Table A.3 Generator dynamic data for the Kundur two area test network

Generator	Rating (MVA)	X_d (pu)	X'_d (pu)	X''_d (pu)	T'_{d0} (s)	T''_{d0} (s)	X'_q (pu)	X''_q (pu)	T'_{q0} (s)	T''_{q0} (s)	H (s)
G1	900	1.8	0.3	0.25	8	0.03	1.7	0.25	0.4	0.05	6.5
G2	900	1.8	0.3	0.25	8	0.03	1.7	0.25	0.4	0.05	6.5
G3	900	1.8	0.3	0.25	8	0.03	1.7	0.25	0.4	0.05	6.175
G4	900	1.8	0.3	0.25	8	0.03	1.7	0.25	0.4	0.05	6.175

Appendix II: Kundur Two-Area Test Network.



Appendix III: Extract of the EAPP Interconnection code on frequency operational guidelines, page 43.

Further guidance is given in the operational guidelines, its most important criteria are:

- These dedicated control schemes, as well as specific parameters, should be agreed upon on synchronous area level.
- In case of a steady-state frequency deviation outside the permissible frequency range, action must be undertaken to restore frequency and scheduled flows within 15 minutes. The permissible frequency range must be agreed upon between all control area operators in the synchronous zone. (For starting, the range could be specified as 49.75Hz to 50.25Hz)
- Each control area should automatically calculate its ACE, and use it as a guidance to bring the system back to nominal values. If automatic ACE calculation is not available, it should be computed manually at least once per hour.
- In case a control area operator wants to perform its secondary frequency control in a manual way, it should be agreed by all members of the synchronous area.

Mwasaha N. Mwangudza

14-10-2023

TURNITIN SIMILARITY REPORT**Investigation of Constrained VSC-HVDC Tie Lines for Transient Stability Improvement of Interconnected Power Systems**

Handwritten notes:
✓
D.P. MUSAU
15-10-23

ORIGINALITY REPORT

12%

SIMILARITY INDEX

7%

INTERNET SOURCES

9%

PUBLICATIONS

4%

STUDENT PAPERS

PRIMARY SOURCES

1	"Advanced Solutions in Power Systems: HVDC, FACTS, and Artificial Intelligence", Wiley, 2016 Publication	1%
2	stax.strath.ac.uk Internet Source	1%
3	www.mdpi.com Internet Source	1%
4	Mircea Eremia, José Antonio Jardini, Guangfu Tang, Lucian Toma. "VSC-HVDC Transmission", Wiley, 2016 Publication	1%
5	K. R. Padiyar, Anil M. Kulkarni. "Dynamics and Control of Electric Transmission and Microgrids", Wiley, 2019 Publication	<1%
6	Submitted to University of the Highlands and Islands Millennium Institute Student Paper	<1%

7	eprints.usm.my Internet Source	<1 %
8	ijiset.com Internet Source	<1 %
9	upcommons.upc.edu Internet Source	<1 %
10	ljs.academicdirect.org Internet Source	<1 %
11	Lakshmi Sundaresh, Zhiyong Yuan, Kaiqi Sun, Jiuping Pan, Yilu Liu. "Improving power grid transient stability and transfer capability using HVDC emergency power controls", 2020 IEEE/PES Transmission and Distribution Conference and Exposition (T&D), 2020 Publication	<1 %
12	innovexpo.itee.uq.edu.au Internet Source	<1 %
13	www.frontiersin.org Internet Source	<1 %
14	www.researchgate.net Internet Source	<1 %
15	Marija D. Ilić, Shell Liu. "Hierarchical Power Systems Control", Springer Science and Business Media LLC, 1996 Publication	<1 %

UNIVERSITY OF NAIROBI

DIGITAL REPOSITORY DEPOSIT AGREEMENT

To efficiently administer the University of Nairobi Digital Repository and preserve its contents for long-term use, the University requires certain permissions and warrants from a depositor or copyright owner. By accepting this agreement, a copyright owner still retains copyright to their work and does not give up the right to submit the work to publishers or other repositories. If one is not a copyright owner, they represent that the copyright owner has given them permission to deposit the work.

By accepting this agreement, a depositor/copyright owner grants to the University the non-exclusive right to reproduce, translate and distribute the submission, including the descriptive information (metadata) and abstract, in any format or medium worldwide and royalty free, including, but not limited to, publication over the internet except as provided for by an addendum to this agreement.

By depositing my/our work in the University of Nairobi Digital Repository, I/we agree to the following:

1. This submission does not, to the best of my/our knowledge, infringe on anyone's copyright or other intellectual property rights.
2. If the submission contains material for which I/we do not hold copyright and that exceeds fair use, I/we have obtained the unrestricted permission of the copyright owner to grant the University the rights required by this agreement and that such third-party owned material is clearly identified and acknowledged within the text or content of the submission.
3. The submitted material does not contain any confidential information, proprietary information of others or export controlled information
4. There are no restrictions or required publication delays on the distribution of the submitted material by the University.
5. Once the submission is deposited in the repository, it remains there in perpetuity.
6. The information I/we provide about the submitted material is accurate.
7. That if copyright terms for, or ownership of, the submitted material changes, it is my/our responsibility to notify the University of these changes.

I/we understand that the University of Nairobi Digital Repository:


1. May make copies of the submitted work available world-wide, in electronic format via any medium for the lifetime of the repository, or as negotiated with the repository administrator, for the purpose of open access.
2. May electronically store, translate, copy or re-arrange the submitted works to ensure its future preservation and accessibility within the lifetime of the repository unless notified by the depositor that specific restrictions apply.
3. May incorporate metadata or documentation into public access catalogues for the submitted works. A citation/s to the work will always remain visible in the repository during its lifetime.
4. Shall not be under any obligation to take legal action on behalf of the depositor or other rights holders in the event of breach of intellectual property rights or any other right in the material deposited.
5. Shall not be under any obligation to reproduce, transmit, broadcast, or display the submitted works in the same format or software as that in which it was originally created.
6. May share usage statistics giving details of numbers of downloads and other statistics with University of Nairobi staff.

While every care will be taken to preserve the submitted work, the University of Nairobi is not liable for loss or damage to the work(s) or associated data while it is stored within the digital repository.

Work(s) to be deposited:

Author: Mwasaha Nyemi Mwangudza
Title: Investigation of Constrained VSC-HVDC Tie Lines for Transient Stability Improvement of Interconnected Power Systems

Depositor's Declaration

I/we Mwasaha Nyemi Mwangudza hereby grant to the University of Nairobi Digital Repository, a non-exclusive license on the terms outlined above.
Name Mwasaha Nyemi Mwangudza
College UON Main Campus Faculty of Engineering
Sign 
Date 18-10-2023

STUDENT ID



University of Nairobi

1

A world-class university committed to scholarly excellence

Portal Home

Student Fees

Timetables

Course Registration

Results

Enquiries

Book Room

Logout

Change Password

My profile

Year 1 Registration

Student ID

Inter Faculty

Clearance Status

Caution Refund

Academic Tracking

F56/38456/2020 MWASAH NYEMI MWANGUDZA (Regular/Integrated)

DOWNLOAD PROVISIONAL STUDENT ID

ID/PP No. Type:

Previous Requests

Request Date	Status	Receipt No.	Validity	Remarks	
1. 06-OCT-2020	PENDING			Photo Missing; Signature Missing;	1.

Procedure for getting the new generation Student ID Card

1. Ensure that your fees (including that of Student ID) is paid and receipted before making the ID card request.
2. Fees for Re-Issue of lost ID card must be paid and receipted separately.
3. Place your request for the Student ID through the Student Portal.
4. Request for renewal of expired ID card should be made **NOT MORE THAN ONE MONTH BEFORE EXPIRY OF THE CURRENT ONE**.
5. Ensure that your photo has been taken and uploaded into the System at your Faculty.
6. Allow at least two working days for the processing of your ID card.
7. Keep checking the status of your ID request through the Student Portal.
8. Collect your printed Student ID from your Faculty / School / Institute Office once the STATUS of your request is reflected as PRINTED.

Note:

1. Validity for Re-Issued ID Card will be the same as that of previously Issued (Lost) ID.
2. Validity for Replacement / ID Re-New will start after expiry of current Issued ID.